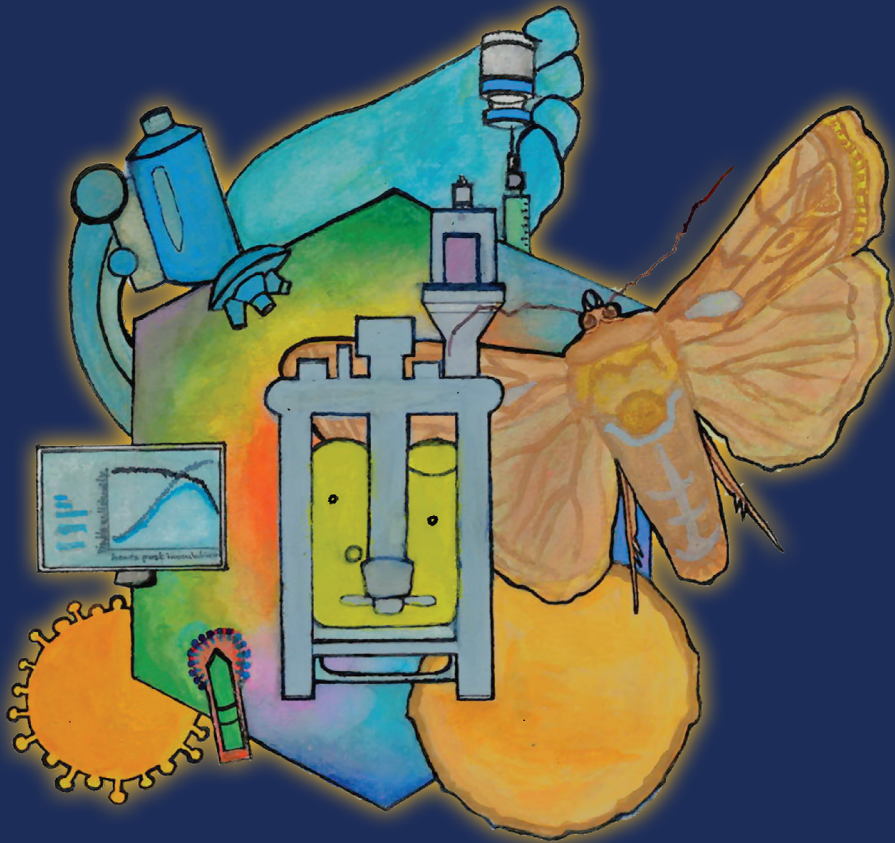


# PROCESS OPTIMIZATION OF THE BACULOVIRUS EXPRESSION VECTOR SYSTEM FOR VACCINE PRODUCTION



**Jort J. Altenburg**

# Propositions

1. The lack of adequate virus quantification methods is the major bottleneck during process development for the baculovirus expression vector system. (this thesis)
2. Without good process understanding, online monitoring is only useful when things go wrong. (this thesis)
3. The COVID-19 pandemic proved that single-use technologies lack flexibility when flexibility is needed.
4. Artificial intelligence enhances quantity more than quality.
5. Striving for the optimal solution is suboptimal.
6. Neglecting probabilities leads to emotional decision making.
7. Social factors, rather than technical limitations, cause the main obstacles for innovation.
8. Football is a universal language that is easy to understand but difficult to master.

Propositions belonging to the thesis, entitled

Process optimization of the baculovirus expression vector system for vaccine production

Jort J. Altenburg  
Wageningen, 3 November  
2023

# Process optimization of the baculovirus expression vector system for vaccine production

Jort J. Altenburg

## **Thesis Committee**

### **Promotors**

Prof. Dr R.H. Wijffels  
Professor of Bioprocess Engineering  
Wageningen University & Research

Dr G.P. Pijlman  
Associate Professor at the Laboratory of Virology  
Wageningen University & Research

### **Co-promotor**

Dr D.E. Martens  
Associate Professor, Bioprocess Engineering  
Wageningen University & Research

### **Other members**

Prof. Dr D.Z. Machado de Sousa, Wageningen University & Research  
Dr M.E. Klijn, TU Delft  
Dr A.S. Coroadinha, iBET, Oeiras, Portugal  
Dr M. Streefland, uniQure N.V., Amsterdam

This research was conducted under the auspices of the Graduate School for Biobased, Biomolecular, Food and Nutritional Sciences (VLAG).

# Process optimization of the baculovirus expression vector system for vaccine production

**Jort J. Altenburg**

## **Thesis**

submitted in fulfilment of the requirements of the degree of doctor  
at Wageningen University  
by the authority of the Rector Magnificus,  
Prof. Dr A. P. J. Mol,  
in the presence of the  
Thesis Committee appointed by the Academic Board  
to be defended in public  
on Friday 3 November 2023  
at 1.30 p.m. in the Omnia Auditorium.

Jort J. Altenburg

Process optimization of the baculovirus expression vector system for vaccine production,

146 pages.

PhD thesis, Wageningen University, Wageningen, the Netherlands (2023).

With references, with summary in English

ISBN 978-94-6447-905-8

DOI <https://doi.org/10.18174/639258>

## Table of Contents

<b>Chapter 1</b> - Introduction and thesis outline	7
<b>Chapter 2</b> - Two-component nanoparticle vaccine displaying glycosylated spike S1 domain induces neutralizing antibody response against SARS-CoV-2 variants	17
<b>Chapter 3</b> - Real-time online monitoring of insect cell proliferation and baculovirus infection using digital differential holographic microscopy and machine learning	45
<b>Chapter 4</b> - Novel temperature-sensitive baculovirus expression vector system with upstream reduction of baculovirus contaminants (BacFree)	65
<b>Chapter 5</b> - Process intensification of the baculovirus expression vector system by high cell density infection at low multiplicity of infection using acoustic perfusion	91
<b>Chapter 6</b> - General discussion	113
<b>References</b>	128
<b>Summary</b>	149
<b>Samenvatting</b>	155
<b>About the author</b>	161
<b>Overview of completed training activities</b>	163
<b>Acknowledgments</b>	165

1

# **Chapter 1**

---

**Introduction and thesis outline**

### 1.1 The Baculovirus Expression Vector System (BEVS)

The demand for vaccines is increasing due to the emergence of new diseases, existing diseases that are spreading to new regions because of trade, travel and climate change, and existing pathogens that are increasingly becoming resistant to antibiotics. In addition, partly due to population aging, new medicines must be developed against diseases like cancer and autoimmune diseases. At the same time, our increased understanding of the mechanisms behind these diseases leads to an increasing number of new medicines (Taylor et al., 2009). Many of these new vaccines and medicines are complex proteins, such as capsid proteins of a virus or membrane proteins of bacteria in the case of vaccines, and monoclonal antibodies in the case of medicines (Zhao et al., 2012).

To ensure proper immunogenic properties (vaccines) and functioning (medicines) of the protein and avoid side effects, post-translational modifications (PTMs) of the synthesized protein are often needed. Proper glycosylation is an important example of such a PTM. Several host organisms and techniques are available for recombinant protein expression including mammalian, insect, yeast, bacterial, algal, and even cell-free systems (Gomes et al., 2016). However, until now, only animal cells can perform the extent of PTMs on proteins that are needed to achieve the desired functionality and absence of side effects.

The baculovirus expression vector system (BEVS) is a eukaryotic expression system based on insect cell lines derived from for example *Spodoptera frugiperda* and a baculovirus, which commonly is *Autographica californica* Multiple Nucleopolyhedrovirus (AcMNPV) (Van Oers et al., 2015). If a wild-type budded baculovirus particle infects an insect cell, cell division stops, and cells start producing new budded virus (BV) particles after about 8 hours. After about 18 hours the cells start producing so-called occlusion-derived virus (ODV) particles and a large amount of polyhedrin protein. These ODVs are packaged in the polyhedrin protein matrix forming so-called polyhedra. Finally, the cell dies and falls apart releasing the polyhedra in the medium. The polyhedrin protein is expressed up to high levels in the cell. In the BEVS, the polyhedrin gene within the baculovirus genome is replaced by a gene of interest. In a cell culture process, the infection starts by adding recombinant baculovirus to the culture medium. Upon infection of the insect cells with these genetically modified baculoviruses carrying the gene of interest, the cells start to synthesize the target protein (Figure 1).

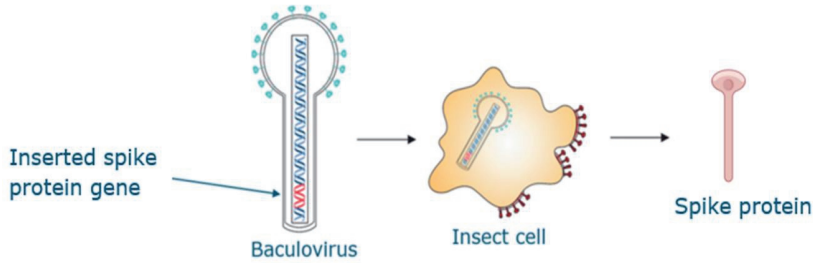


**Figure 1.** Schematic representation of protein expression using the baculovirus insect expression system with the spike protein as an example (adapted from Sedova et al., 2012).

The strength of the BEVS lies in the speed of development to express new recombinant proteins, which takes about one week (Figure 2). This is due to the transient nature of the BEVS allowing a single, well-characterized cell line to be used to produce different therapeutic protein candidates. This eliminates the time-consuming process of preparing and qualifying a new cell line for each new protein as is often the case, for instance for Chinese Hamster Ovary (CHO) cell lines. This means that the BEVS has the potential to develop new vaccines quickly when a fast response is needed, for instance during disease outbreaks such as Zika fever and Ebola, and more recently COVID-19 (Azali et al., 2022; M. M. J. Cox & Hashimoto, 2011; Schrauf et al., 2020).

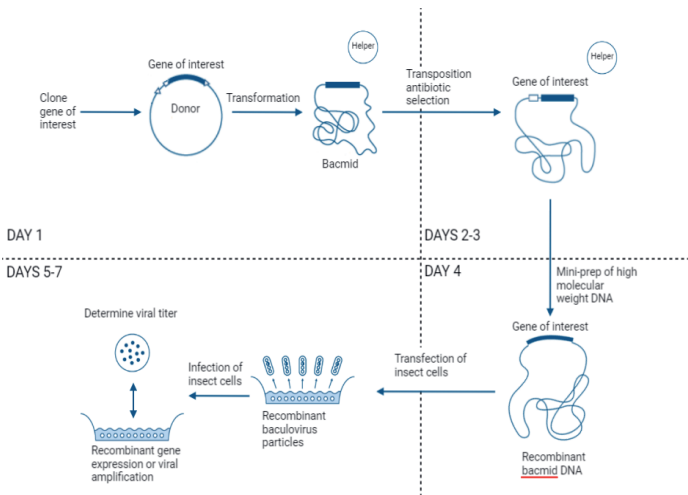


**Figure 2.** Example of the Bac-to-Bac system workflow for recombinant protein expression in insect cells (Thermo Fisher).

## 1.2 Large-scale manufacturing of therapeutic proteins using the BEVS

The large-scale production of therapeutic proteins with the BEVS is complex. In principle first cells are grown to a certain concentration, the cell concentration at infection (CCI) at which the virus is added. Two distinct strategies can be discerned: (1) using high cell density of infection in combination with a high multiplicity of infection (MOI), where MOI is the number of infective BVs added per cell, (2) using a low MOI and a lower cell density of infection. Using a high MOI all cells are infected at once and no cell growth occurs anymore. This approach requires a large number of BVs for infection of all the cells. In the second approach, first only a small part of the cells is infected. These cells stop growing and after a certain time produce new BVs that infect the rest of the cells in the reactor. In the meantime, cells that are initially not infected keep growing, which is why a lower cell density of infection is used. In this approach, the amount of virus needed for infection is much lower. The volumetric productivity and final product concentration reached in the final production reactor depend on the cell concentration that is reached, the amount of product made per cell, and the duration of the process. The cell concentration is influenced by the medium conditions and process type (i.e., batch, fed-batch, perfusion). The cell-specific production is dependent on the infection kinetics and nutrient availability during infection. Notably nutrient requirements during infection are probably different from those during cell growth (Palomares et al., 2001a).

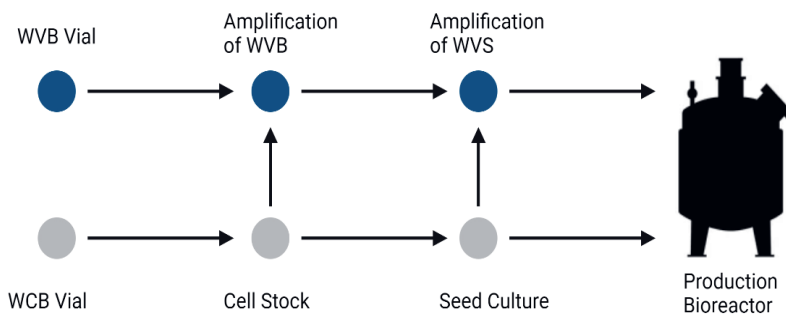


**Figure 3.** Schematic of a typical vaccine production process involving a working virus bank (WVB) generating the working virus stock (WVS) and a working cell bank (WCB) generating the seed culture, before both stock and seed come together in the production reactor.

Since the infection results in the arrest of growth and eventually cell lysis, the insect cells and virus seed for the production reactor have to be obtained separately. This means two separate scale-up trains are needed, one to grow the insect cells and one to generate the virus particles for infection. These come together in the production reactor where the insect cells are infected with baculovirus to produce the final product (Figure 2).

### 1.3 Challenges in BEVS manufacturing

The primary focus of large-scale manufacturing using the BEVS lies in the production of virus-like particles (VLPs) for vaccine applications and adeno-associated virus (AAV) particles for gene therapy applications. VLPs are particles that closely resemble virus particles, but do not contain genetic material. These two properties make them very suitable molecules for vaccination since the VLPs cause an immune response but do not have the infectious properties of the virus they resemble (Pijlman, 2015). During VLP production with the BEVS also BVs are formed (Van Oers et al., 2015). These BVs may be taken up by mammalian cells and some baculovirus promoters might show activity, triggering an undesired immune response (Ono et al., 2014). Therefore, BVs are considered contaminants and must be removed from the final product. For several products, especially for VLPs, the BVs have similar characteristics as the product. This makes separation of VLPs from BVs difficult and costly, often resulting in considerable loss of valuable product during downstream processing (DSP).

Instead of separating VLPs from BVs during DSP, prevention of the formation of contaminating BVs during upstream processing (USP) could be an alternative strategy to reduce BV contamination. For such a strategy, an inducible system would be highly advantageous, as it permits the use of the same cell line and baculovirus construct throughout seed expansion and production stages.

A temperature-sensitive baculovirus mutant, tsB1074, was described to affect BV secretion, while polyhedrin was still produced in the very late phase of infection (Lee & Miller, 1979). Complementation analyses of tsB1074 revealed a point mutation in *ac80*, the gene encoding baculovirus GP41 (Olszewski & Miller, 1997). GP41 is a *Baculoviridae* core protein of 45 kDa that is involved in the nuclear export of nucleocapsids on their way to the plasma membrane, where BVs leave the cell by budding. GP41 is essential for BV secretion but is dispensable for viral DNA replication or very-late gene expression (Li et al., 2018; Olszewski & Miller, 1997). BV production appeared normal at 23.5°C but a single-cell infection phenotype was observed at 32.5°C (Lee & Miller, 1979; Olszewski & Miller, 1997). This ts mutant may be useful to engineer a temperature inducible BEVS. However, it is still unknown how this would function in a larger-scale production process.

Furthermore, BEVS production processes still seem underdeveloped compared to their more industrial-established counterparts. Although the BEVS has been used for over thirty years by researchers to express recombinant proteins, it has mostly been used for research purposes (Van Oers et al., 2015). Such lab-scale protein expression and production processes are batch cultivations, often using large virus stocks to infect at a high multiplicity of infection (MOI). The complex culture conditions required for baculovirus-infected insect cell cultures hinder process intensification efforts to further optimize large-scale manufacturing. Optimizing parameters such as CCI, MOI, and time of harvest (TOH) is crucial for efficient protein production. Modifying these conditions to intensify

the process can be difficult without adversely affecting viral replication or protein quality. For instance, high cell densities might be detrimental to the overall infection kinetics (Bernal et al., 2009), and using a low MOI is challenging due to the increased variability and unpredictability of the production process.

Despite this, fifteen BEVS-derived products have been approved for use, including five human vaccines, the first ever gene therapy product, and seven veterinary vaccines (Table 1) (Hong et al., 2022). Further improvements are essential to establish the BEVS as a strong platform technology to timely tackle future pandemics and allow novel biologicals to enter the market.

**Table 1.** BEVS-derived products approved till date (Hong et al., 2022; Pidre et al., 2023).

<i>Category</i>	<i>Commercial Name</i>	<i>Manufacturer</i>	<i>Product Type</i>	<i>Target</i>
<i>Human vaccines</i>	Cervarix®	GSK	VLP	HPV
	FluBlok®	Sanofi	subunit	Influenza virus
	Nuvaxoid™	Novavax	subunit	SARS-CoV-2
	FluBlok®	Sanofi	VLP	Influenza virus
	Quadrivalent VidPrevtyn™ Beta	Sanofi	subunit	SARS-CoV-2
<i>Veterinary products</i>	Porcilis pesti®	MSD Animal Health	subunit	Classical swine fever
	Porcilis PCV®	MSD Animal Health	VLP	Porcine circovirus 2
	CircoFLEX®	Boehringer Ingelheim	VLP	Porcine circovirus 2
	Circumvent® PCV	Merck Animal Health	VLP	Porcine circovirus 2
	Bayovac® E2	CSF- Bayer / Pfizer Animal Health	subunit	Classical swine fever
	Virbagen® Omega	Virbac	interferon	FeLV/FIV <sup>1</sup>
	INTERDOG™	TORAY Industries	interferon	Atopic dermatitis
<i>Gene therapy</i>	Glybera®	UniQure	rAAV-based gene therapy	Lipoprotein lipase deficiency
	HEMGENIX®	CSL Behring / UniQure	rAAV-based gene therapy	Haemophilia B
<i>Personalized immunotherapy</i>	Provenge®	Dendreon	fusion protein	Prostate cancer

## Aim

This thesis aims to explore effective strategies to characterize, develop and improve the BEVS production process that can be used for large-scale baculovirus-free manufacturing of therapeutic proteins, such as VLPs and AAVs, while simultaneously improving its volumetric productivity. To achieve this, a novel temperature sensitive BEVS with upstream reduction of baculovirus contaminants (BacFree) is proposed. To achieve higher volumetric productivity for the BEVS, a low MOI perfusion strategy is explored that could be compatible with the BacFree system.

## Thesis outline

During this thesis, the outbreak of the COVID-19 pandemic led to a significant development as research teams worldwide rapidly initiated the development of potential COVID-19 vaccine candidates. In **Chapter 2** the development, production, and pre-clinical testing of a nanoparticle vaccine against SARS-CoV-2 is reported. Using the BEVS, we demonstrated insect cell-mediated production and purification of (1) the full-length spike protein, (2) a secreted form of a prefusion-stabilized spike, and (3) a secreted form of the SARS-CoV-2 S1 domain. We formulated the secreted S as an adjuvanted subunit vaccine and tested the protection of K18-hACE2 mice from a SARS-CoV-2 challenge. We also fused the S1 domain to the split-protein tag and displayed this on AP205 VLPs. Mice vaccinated with the S1-VLP vaccine had strong immune responses and neutralizing antibodies against both the Wuhan SARS-CoV-2 and the UK/B.1.1.7 variant (VOC-202012/01) that was predominant in Europe in the early stage of the pandemic.

Obtaining real-time monitoring of cell culture status during bioreactor cultivation and production yields significant advantages in enhancing the understanding of the BEVS and timely control of the production process. For instance, an accurate online monitoring tool could play a crucial role in determining the precise moment of temperature shift when implementing a low MOI in the proposed BacFree strategy. **Chapter 3** focuses on evaluating the performance of online double-differential digital holographic microscopy (D<sup>3</sup>HM) and machine learning to monitor insect cell proliferation and baculovirus infection in bioreactors. We found that with a limited training set the microscope and machine learning algorithm could predict cell numbers, viability, and infection percentage for different viral constructs, MOIs, and process conditions. The high resolution of the online measurements enabled the detection of small events or process deviations, such as the growth arrest of the cells due to the addition of butyrate to the culture, which would have otherwise been missed by manual sampling.

A baculovirus-free expression system would minimize downstream processing requirements and associated product loss during purification. In **Chapter 4**, we reported the development and characterization of a novel temperature-sensitive baculovirus expression system with upstream reduction of baculovirus contaminants (BacFree). We investigated if the temperature-sensitive point mutation in GP41 could result in a BEVS with an inducible shutdown of BV production to aid the

production of chikungunya virus (CHIKV) enveloped VLPs. For this, the I317T mutation in GP41 was implemented in a baculovirus bacmid vector at the polyhedrin locus and under the p10 promoter. Using a micro-bioreactor screening system, it was found that increasing temperatures to 34°C shortly after baculovirus infection significantly decreased BV titers while VLP production and insect cell viability were maintained. This strategy was successfully scaled up to stirred-tank bioreactors and a 100-fold reduction in final BV titers was achieved for both high and low MOI infection strategies. For the low MOI strategy, online monitoring of cell diameter was an effective tool for determining the optimal timing of the temperature shift.

**Chapter 5** focuses on process intensification to improve product yield and volumetric productivity for the BEVS. Bioreactor perfusion was implemented to allow high-cell density infection of insect cells at low MOI. The recombinant protein yield per cell was maintained at high cell densities and bioreactor volumetric productivity was up to 4.8-fold higher compared to batch processes. Implementing this perfusion strategy for the BEVS allows for production on a smaller scale, which would also reduce the time needed for scale-up to the production reactor or could increase the production capacity of existing production facilities. Process optimization to reduce total cultivation time or reach even higher cell densities may further increase volumetric productivity while combined with the BacFree strategy has the potential to simultaneously reduce final BV titers.

In **Chapter 6**, we present a systematic overview of the reported results and discuss various aspects that we consider important or potentially advantageous for the continued development and improvement of the BEVS for large-scale manufacturing of therapeutic proteins:

- An improved BacFree strategy combined with a perfusion strategy to further reduce final BV titers and simultaneously improve volumetric productivity.
- Oxygen sparging with microbubbles (microsparging), to improve oxygen transfer and reduce gas flows into the reactor. This could be especially beneficial for perfusion processes.
- Addition of short-chain fatty acids to the cell culture, of which butyrate and 2-hydroxybutyrate showed to be promising candidates to improve protein yield and virus production.
- High-throughput, rapid, and label-free baculovirus quantification, either through D3HM technology or by using electrical parameters such as capacitance. This would be highly beneficial for BEVS process development, in particular for low MOI processes.

Altogether, these measures are expected to strengthen the position of the BEVS as a robust platform technology to meet current and future demand for vaccines and new medicines.



2

# Chapter 2

---

## Two-component nanoparticle vaccine displaying glycosylated spike 2 S1 domain induces neutralizing antibody response against SARS- CoV-2 variants

---

Linda van Oosten<sup>1</sup>, Jort J Altenburg<sup>2</sup>, Cyrielle Fougeroux<sup>3</sup>, Corinne Geertsema<sup>1</sup>, Fred van den End<sup>2</sup>, Wendy AC Evers<sup>2</sup>, Adrie H Westphal<sup>4</sup>, Simon Lindhoud<sup>4</sup>, Willy van den Berg<sup>4</sup>, Daan C Swarts<sup>4</sup>, Laurens Deurhof<sup>5</sup>, Andreas Suhrbier<sup>6</sup>, Thuy T Le<sup>6</sup>, Shessy Torres Morales<sup>7</sup>, Sebenzile K Myeni<sup>7</sup>, Marjolein Kikkert<sup>7</sup>, Adam F Sander<sup>3,8</sup>, Willem Adriaan de Jongh<sup>3,8</sup>, Robert Dagit<sup>8</sup>, Morten A Nielsen<sup>8</sup>, Ali Salanti<sup>8</sup>, Max Søgaaard<sup>9</sup>, Timo MP Keijzer<sup>10</sup>, Dolf Weijers<sup>4</sup>, Michel HM Eppink<sup>2</sup>, René H Wijffels<sup>2</sup>, Monique M van Oers<sup>1</sup>, Dirk E Martens<sup>2</sup>, Gorben P Pijlman<sup>1</sup>

<sup>1</sup>Laboratory of Virology, Wageningen University, Droevendaalsesteeg 1, 6708PB Wageningen, The Netherlands.

<sup>2</sup>Bioprocess Engineering, Wageningen University, Droevendaalsesteeg 1, 6708PB Wageningen, The Netherlands.

<sup>3</sup>AdaptVac Aps, 2970 Horsholm, Denmark.

<sup>4</sup>Laboratory of Biochemistry, Wageningen University, Stippeneng 4, 6708WE, Wageningen, the Netherlands.

<sup>5</sup>Laboratory of Phytopathology, Wageningen University, Droevendaalsesteeg 1, 6708PB Wageningen, The Netherlands

<sup>6</sup>QIMR Berghofer Medical Research Institute, Brisbane 4006, QLD, Australia.

<sup>7</sup>Department of Medical Microbiology, Leiden University Medical Center, 2333ZA Leiden, Netherlands.

<sup>8</sup>Centre for Medical Parasitology at Department of Immunology and Microbiology, Faculty of Health and Medical Sciences, University of Copenhagen, 220 Copenhagen, Denmark.

<sup>9</sup>ExpreS2ion Biotechnologies Aps, 2970 Horsholm, Denmark.

<sup>10</sup>Applikon Biotechnology BV, Heertjeslaan 2, 2629 JG Delft, The Netherlands.

*This chapter has been published in mBio (2021)*

### Abstract

Vaccines pave the way out of the SARS-CoV-2 pandemic. Besides mRNA and adenoviral vector vaccines, effective protein-based vaccines are needed for immunization against current and emerging variants. We have developed a virus-like particle (VLP)-based vaccine using the baculovirus-insect cell expression system, a robust production platform known for its scalability, low cost, and safety. Baculoviruses were constructed encoding SARS-CoV-2 spike proteins: full-length S, stabilized secreted S, or the S1 domain. Since subunit S only partially protected mice from SARS-CoV-2 challenge, we produced S1 for conjugation to bacteriophage AP205 VLP nanoparticles using tag/catcher technology. The S1 yield in an insect-cell bioreactor was ~11 mg/liter, and authentic protein folding, efficient glycosylation, partial trimerization, and ACE2 receptor binding was confirmed. Prime-boost immunization of mice with 0.5 µg S1-VLPs showed potent neutralizing antibody responses against Wuhan and UK/B.1.1.7 SARS-CoV-2 variants. This two-component nanoparticle vaccine can now be further developed to help alleviate the burden of COVID-19.

## Introduction

Vaccination has become a key instrument in the fight against the severe acute respiratory syndrome coronavirus 2 (SARS-CoV-2) outbreak, which was declared a pandemic by the World Health Organization in March 2020. Within 6 months, the coronavirus disease 19 (COVID-19) had claimed the lives of one million people (<https://covid19.who.int>). Despite global efforts to restrict the viral spread through economic and social interventions, the virus continues to put a substantial strain on economies and health care systems around the world. Large-scale vaccination programs have proven to be critical in reducing the viral spread and preventing severe disease (Carvalho et al., 2021).

The envelope of the SARS-CoV-2 virion contains membrane and spike (S) proteins. The S protein is a trimeric glycoprotein involved in virion attachment and entry into host cells. S is divided into two domains, S1 and S2, by a furin protease cleavage site (Coutard et al., 2020; Walls, Park, et al., 2020). S1 contains the receptor-binding domain (RBD) that binds the human angiotensin 2 (hACE2) receptor, whereas the fusion peptide (FP) is found in S2 (Hoffmann et al., 2020; P. Zhou et al., 2020). Since S is indispensable for virus entry and is highly immunogenic, it is the main target in vaccine design to induce antibody-mediated virus neutralization in immunized individuals (Addetia et al., 2020; Yu et al., 2020). In many vaccine development studies, S is stabilized in its prefusion state by eliminating the furin cleavage site and inserting a stabilizing diproline mutation in S2 (Kirchdoerfer et al., 2018; Pallesen et al., 2017; Walls, Park, et al., 2020; Wrapp et al., 2020).

At unprecedented speed, multiple COVID-19 vaccines have entered the market via emergency approvals from, among others, the European Medicines Agency and the U.S. Food and Drug Administration. These early vaccines, which are based on mRNA or adenoviral vectors, have been shown to be effective in preventing COVID-19 infection (Baden et al., 2021; Polack et al., 2020; Sadoff et al., 2021). Recombinant subunit vaccines based on recombinant S protein are currently in late-stage clinical trials and have been shown to induce potent neutralizing antibody (nAb) responses in nonhuman primates (Guebre-Xabier et al., 2020; Liang et al., 2021; Tian et al., 2021) and humans in phase II and III clinical trials (Keech et al., 2020).

The recent emergence of SARS-CoV-2 variants (<https://nextstrain.org/sars-cov-2>) highlights the importance of a robust vaccine production platform with good scalability and modularity for rapid adaptation to novel variants. For the production of recombinant proteins, the insect cell-baculovirus expression vector system (IC-BEVS) is a well-established platform. It is used for (commercial)

producing virus-like particles (VLPs; human papillomavirus; Cervarix, GlaxoSmithKline), proteins with complex posttranslational modifications, including glycoproteins (influenza A virus hemagglutinin; FluBlok; Sanofi), and difficult-to-produce protein complexes (Felberbaum, 2015; Van Oers et al., 2015). IC-BEVS has been used to produce coronavirus spike proteins of SARS-CoV (Z. Zhou et al., 2006) and Middle East respiratory syndrome-coronavirus (MERS-CoV) (Chun et al., 2019; Kato et al., 2019; Pallesen et al., 2017) as well as SARS-CoV-2 spikes in structural studies (Fan et al., 2020; Lan et al., 2020; Shang, Wan, et al., 2020; Shang, Ye, et al., 2020; Q. Wang et al., 2020) and as subunit vaccines (J. Li et al., 2013; T. Li et al., 2020). The IC-BEVS is rapidly scalable up to a million doses using insect cell bioreactors with working volumes of a few thousand liters in animal component-free medium (Buckland et al., 2014; Cox et al., 2015; Felberbaum, 2015). Furthermore, protein-based vaccines offer a very high safety profile, since millions of people have been vaccinated with IC-BEVS-produced proteins (Cervarix, FluBlok) without experiencing any severe adverse effects (Angelo et al., 2014; Cox et al., 2015). Therefore, IC-BEVS would be well-suited for producing SARS-CoV-2 vaccines.

A potential shortcoming for such subunit vaccines is their relatively low immunogenicity that can be compensated for by the addition of adjuvants and/or sequential immunizations (boosters). This has also been demonstrated in the case of SARS-CoV-2 RBD immunization (Fougeroux et al., 2021; Y. Wang et al., 2020) and prefusion stabilized S (Goepfert et al., 2021). The immunogenicity of subunit vaccines can be improved by the presentation of antigens on nanoparticles or VLPs. The unidirectional display of antigens and the size of the particles more closely resemble that of a virus and result in increased B-cell responses by cross-presentation of epitopes, resulting in enhanced processing by antigen-presenting cells (APC) and B-cell receptors (Bachmann & Jennings, 2010; Hua & Hou, 2013; López-Sagaseta et al., 2016). Moreover, VLPs are replication-deficient because they do not contain genetic material from the originating virus and, thus, are considered safe (Mohsen et al., 2018). The licensed human papillomavirus vaccine (Cervarix; GSK) is a VLP made with the IC-BEVS that provides long-lived protective immunity after just one dose (De Vincenzo et al., 2014; Schiller & Lowy, 2018). Experimental SARS-CoV-2 VLP and nanoparticle vaccines have also been developed and have demonstrated their potential to induce protection against disease with low doses (Arunachalam et al., 2021; Tian et al., 2021; Walls, Fiala, et al., 2020; Zhang et al., 2020).

In this study, we use the AP205 VLP and tag/catcher system to construct a baculovirus-derived SARS-CoV-2 vaccine based on the S1 subunit. Covalent conjugation of antigens on the VLP surface can be

achieved by the Spytag/Spycatcher platform (L. Li et al., 2014; Thrane et al., 2016). This plug-and-display technology is based on a bacterial adhesin that has been split genetically into a tag and catcher peptide, which forms a covalent bond upon mixing (Zakeri et al., 2012). Even without adjuvant, AP205 VLPs decorated with antigens have been found to induce robust immune responses at a single dose (Brune et al., 2016; Fredsgaard et al., 2021). Recently, the RBD domain of SARS-COV-2 was coupled to these VLPs using a proprietary split-protein tag/catcher technology, resulting in robust neutralizing antibody production in mice (Fougeroux et al., 2021), and has been further developed into a phase I/II clinical study.

Using the IC-BEVS, we demonstrate insect cell-mediated production and purification of (i) the full-length spike protein, (ii) a secreted form of a prefusion-stabilized spike, and (iii) a secreted form of the SARS-CoV-2 S1 domain. We formulated the secreted S as an adjuvanted subunit vaccine and tested protection of K18-hACE2 mice from SARS-CoV-2 challenge. We also fused the S1 domain to the split-protein tag and displayed this on AP205 VLPs. Mice vaccinated with the S1-VLP vaccine had strong immune responses and neutralizing antibodies against both the Wuhan SARS-CoV-2 and the UK/B.1.1.7 variant (VOC-202012/01) that was predominant in Europe.

### Materials and Methods

#### Insect cells

*Spodoptera frugiperda* Sf9 insect cells were cultured in Sf900II serum-free media (Gibco, Thermo Fisher) with 50 mg/mL gentamycin. ExpiSf9 cells were cultured in ExpiSf Chemically Defined medium (CDM) (Thermo Fisher). Both cell lines were cultured in suspension in shaker flasks at 27 °C and 110 rpm in an orbital shaker.

#### Plasmid design and construction

All constructs are based on the SARS-CoV-2 Wuhan isolate (Accession QIA20044.1) spike gene that was codon-optimized for production in *Drosophila melanogaster* (Fougeroux et al., 2021, PMID: 33436573). For ER translocation and secretion, the native N-terminal signal sequence was substituted with either the Honeybee Melittin (HBM) or AcMNPV GP64 signal sequence. PCR was performed on either the wildtype spike sequence or the prefusion-stabilized sequence with primers found in supplementary Table 1 (Q5 High-Fidelity 2X Master Mix, New England BioLabs). All PCR products were flanked by Gateway™ AttB sites. The PCR products were gel-purified with the Illustra GFX Gel band purification kit (GE-Healthcare), which were then gateway cloned into the pDONR207 (Thermo Fisher), pDest8 (Thermo Fisher), and/or the pOET1 Gateway vectors (Oxford Expression Technologies) according to the protocol of Gateway™ cloning (Invitrogen).

Multiple constructs were designed based on the full-length spike (S-full length), the prefusion stabilized secreted spike (S), and the S1 domain (see also Figure a). First, the S-full length spike constructs contain the wildtype spike coding sequence (residue 16-1237) with an N-terminal HBM signal sequence (Sp1) or GP64 signal sequence (Sp2). Second, the S spike construct encodes an N-terminal HBM signal sequence, the prefusion stabilized ectodomain (residue 16-1208), a C-terminal T4 fibrin trimerization signal (T4 foldon), and an 8x histidine tag (His) (Sp9). Third, the S1 domain (residue 16-679) was PCR amplified and cloned into the pDONR207 vector. At the C-terminus of the S1 gene in pDONR207, a synthetic DNA fragment (IDT DNA) was inserted by SapI restriction cloning (New England BioLabs). The resulting construct (Sp53) encodes the S1 domain with a C-terminal GSGSGS-linker, the proprietary split-protein tag, Tobacco Etch Virus (TEV) protease cleavage site (ENLYFQS), and triple strep-tag (WSHPQFEKGGGSGGGSGGSAWSHPQFEKGGGSGGGSGGS-AWSHPQFEK).

### Recombinant baculoviruses

Recombinant baculoviruses of *Autographa californica* multicapsid nucleopolyhedrovirus (AcMNPV) were generated in two ways. First, pDest8 plasmids were transposed into *E.coli* cells containing bacmid AcBACe56 ( $\Delta$ cc) (Pijlman et al., 2020), PMID: 33339324) with the bac-to-bac baculovirus expression system (Invitrogen, Thermo Fisher), followed by transfection of the bacmid into insect cells with Expres2TR transfection reagent (Expres2ion Biotechnologies). Second, pOET1 plasmids were transfected into insect cells with the baculovirus genome AcOET ( $\Delta$ cc  $\Delta$ p10  $\Delta$ p74  $\Delta$ p26) with the *flashBAC* Ultra kit (Oxford Expression Technologies). Baculovirus stocks were amplified in ExpiSf9 cells and viral titers were determined by endpoint dilution assay on Sf9-easy titer cells (Hopkins & Esposito, 2009). Viral titers are defined as tissue culture infectious dose 50% (TCID<sub>50</sub>) units per mL.

### Immuno Alkaline Phosphatase Monolayer Assay

Production of S full-length in insect cells was assessed by IAPMA. Sf9 cells were infected with recombinant baculovirus at a multiplicity of infection (MOI) of one TCID<sub>50</sub> per cell. At 3 days post-infection, cells were washed once with phosphate-buffered saline (PBS) and fixed in acetone:ethanol (1:1) fixative, followed by another wash step. Cells were incubated for 30 minutes at 37 °C with one of the following primary antibodies: rabbit-anti-S1 (Sino Biological cat#40591-T62, binds the SARS-CoV-2 S1 domain), rabbit-anti-S2 (Abcam, cat# ab272504, binds the cytoplasmic tail (CT) of S2), or human convalescent sera (Isala Ziekenhuis, Zwolle; Erasmus Medical Centre, Rotterdam, obtained from Covid-19 patients). All primary antisera were diluted in PBS with 0.05% Tween-20 (Merck) and 5% skim milk powder (Campina, The Netherlands). Wells were washed once with PBS and incubated with Alkaline Phosphatase (AP)-conjugated Goat-anti-Rabbit or Goat-anti-human secondary antibodies (Sigma). Proteins were detected by NBT/BCIP staining (Roche Diagnostics GmbH, Basel, Switzerland) and cells were visualized by using a Zeiss Axio Observer Z1m inverted microscope.

### Protein production in shake flasks

Recombinant proteins were produced with the ExpiSf<sup>TM</sup> Expression System (Thermo Scientific). ExpiSf9 cells were grown in 1 L shake flasks with 250 mL cell culture volume and were diluted to a density of  $5 \times 10^6$  cells/mL in medium supplemented with ExpiSf<sup>TM</sup> Enhancer. At 18-24 h after dilution, the cells were infected with recombinant baculovirus at an MOI of 4-5 TCID<sub>50</sub> units per cell. The flasks were incubated for 2-4 days until the viability was reduced to 70%. Then, PMSF protease

inhibitor (Roche) was added at a final concentration of 170 mg/mL. Cells were removed by centrifugation and the pH of the resulting supernatant was increased to pH 7.8 by adding 0.1 M NaOH. The clarified supernatant was immediately used for purification or was stored at -80 °C after the addition of glycerol (final concentration 20%).

### Protein production in insect-cell bioreactor

A 3 L bioreactor (Applikon Biotechnology) with a 2 L working volume was inoculated at  $0.5 \times 10^6$  ExpiSf9 cells/mL at 99% viability. Cells were grown in CDM at 27 °C with an agitation speed of 266 rpm. The dissolved oxygen (DO) was controlled at 30% air saturation by adding pure oxygen through a macroporous L-sparger. In addition, a constant headspace flow of 0.01 vvm air was applied. Cells were infected at MOI 0.01 at 3 days post-inoculation at a viable cell density (VCD) between  $2.0$ - $4.0 \times 10^6$  cells/mL. The reactor was harvested at 5 days post-infection (dpi) at a cell viability around 70% as described above. The reactor was monitored online continuously and was sampled daily for offline measurements. 60 mL of cell culture was transferred to a shake flask during harvesting and was sampled for another 6 days. The viable cell density (VCD), viability, and the fraction of infected cells were measured online by Differential Digital Holographic Microscopy (DDHM) with the iLine F holographic microscope (OVIZIO). The bioreactor samples were analyzed offline for VCD and viability by trypan blue exclusion by using a TC20 automatic cell counter (Bio-Rad). The SARS-CoV-2 spike S1 concentration in the medium was determined by protein ELISA (AssayGenie cat.# CBK4154).

### Protein Purification

His-tagged S spike protein was purified from the clarified medium by using immobilized metal ion affinity chromatography (IMAC). The expression medium was clarified by centrifugation ( $12,000 \times g$ , 4 °C). The clarified medium was loaded onto a Ni Sepharose excel (Cytiva) column that was equilibrated in equilibration buffer (20 mM Tris/Cl, 400 mM NaCl, pH 7.8). Non- and weakly bound contaminants were removed by washing with equilibration buffer. The bound proteins were eluted from the column by a 0 - 360 mM imidazole gradient in equilibration buffer. Eluted fractions were pooled and concentrated by using an Amicon Ultra-15 centrifugal filter unit (30 kDa, Merck). The concentrate was further purified by size exclusion chromatography (SEC) with a Superdex S200 (Cytiva) column equilibrated with PBS buffer at pH 7.4. Eluted fractions were analyzed on SDS-PAGE. The fractions containing the S protein were pooled, concentrated, flash-frozen, and stored at -20 °C.

Strep-tagged S1 spike protein was purified on a Strep-TactinXT superflow 5 mL cartridge (IBA GmbH). The clarified medium was treated with 15 mL/mL BioLock Biotin Blocking Solution (IBA) to remove free biotin. It was then loaded onto the Strep-Tactin column equilibrated in 100 mM Tris/HCl, 150 mM NaCl and 1 mM EDTA, pH 8.0 buffer (buffer W). The column was washed with buffer W and proteins were eluted from the column in buffer W containing 50 mM biotin. To remove the triple-strep tag, we pooled the eluted fractions and incubated them overnight at 4 °C with Tobacco Etch Virus (TEV) protease at a 10:1 ratio (w/w) in 50 mM Tris/Cl, 0.5 mM EDTA, and 1 mM DTT, pH 8.0. The protein was concentrated and further purified by using SEC as described above. Eluted fractions were analyzed with SDS-PAGE. The fractions containing S1 were pooled, flash-frozen, and stored at -20 °C. Removal of the strep-tag by TEV-cleavage was confirmed on western blot immunodetection by Strep-Tactin AP-conjugated antibody (IBA Lifesciences).

#### SDS-PAGE and western blot immunodetection

Protein samples were incubated in Laemmli buffer containing 5% b-mercaptoethanol for 10 min at 95 °C and were separated on a 7.5% SDS-PAGE gel (Bio-Rad), or a 4-20% or 4-15% stain-free SDS-PAGE gel (containing photoactivatable trihalo compound, Bio-Rad). Proteins were visualized by 2.5 min UV-activated stain-free imaging (Bio-Rad GelDoc). Then, the proteins in the gel were blotted on a PVDF or nitrocellulose membrane (Thermo Scientific, Bio-Rad). The membranes were blocked in PBS with 0.1% Tween-20 (PBST) supplemented with 3% skim milk powder (Campina, The Netherlands) and recombinant spike proteins were detected by immunodetection. As primary antibodies, we used rabbit-anti-S1 polyclonal serum diluted 1:3000-1:5000 (Sino Biological cat#40591-T62) or human covid-19 convalescence sera diluted 1:500 (Isala Ziekenhuis, Zwolle) or 1:1000 (Erasmus Medical Centre, Rotterdam).

Detection was performed with either Alkaline Phosphatase (AP)-conjugated secondary antibody or Horseradish Peroxidase (HRP)-conjugated secondary antibody diluted 1:2500 in PBST. The AP-conjugated goat-anti-rabbit (Aligent) and AP-conjugated goat-anti-human (Sigma-Aldrich) were detected by conversion of NBT-BCIP staining (Roche Diagnostics GmbH, Basel, Switzerland). HRP conjugated goat-anti-rabbit (Sanbio) was visualized by Clarity Western ECL substrate (BioRad) by using a Chemidoc MP (Bio-Rad). The strep-tag was detected by immunodetection with Strep-Tactin AP according to the manufacturer's protocol (IBA Lifesciences cat#2-1503-001).

### PNGase treatment and PAS stain

The glycosylation status of recombinant spike proteins was analyzed by a PNGase treatment and PAS staining. Protein samples were incubated with PNGase-F (New England Biolabs cat#P0704) for 1 hour at 37 °C under denaturing conditions as described by the manufacturer. PNGase-F treated and non-treated samples were analyzed on SDS-PAGE and western blot. Next, protein glycosylation was confirmed by Periodic acid-Schiff (PAS) staining of the western blot membrane. The PVDF membrane was soaked in PAS solution (1% periodium acid in 3% acetic acid) for 15 min. The membrane was washed twice with water and incubated for 15 min with Schiff's Reagent (Sigma Aldrich). The membrane was washed once in 0.5% w/v sodium bisulfite for 5 min and rinsed with demi water before imaging.

### Far-UV circular dichroism (CD) spectroscopy

The structural features of the insect cell-produced S1 were assessed by far-UV circular dichroism (CD). Purified S1 was diluted to 1.3  $\mu\text{M}$  in PBS. The far-UV CD was measured by using a Jasco J715 spectropolarimeter at 20 °C with 1-mm quartz cuvettes. Spectra were obtained by averaging 30 scans and were background corrected by subtracting the far-UV CD spectrum of 30 scans of PBS acquired under identical conditions. We used the CD-data as input for the BeStSel webserver (Micsonai et al., 2015, 2018) to acquire the secondary structure content of S1. This was compared to the structural data of the S1-domain (derived from the wildtype spike protein structure) we obtained by the program STRIDE (Frishman & Argos, 1995). In both algorithms, it was assumed that glycosylation and other protein modifications do not influence the amount of estimated secondary structures.

### Size-exclusion chromatography coupled with multi-angle light scattering (SEC-MALS)

The molar mass, oligomerization state, and degree of glycosylation of S1 were determined by SEC-MALS. The S1 protein from the scaled-up production run was purified by Strep-Tactin purification followed by removal of the strep-tag by TEV protease incubation and SEC. After SEC, the second peak on the chromatogram (Supplementary figure 2, elution 99-117 mL) was selected for SEC-MALS analyses to exclude large aggregates. An Infinity 1260 II HPLC system (Agilent) was coupled to an Optilab dRI detector and miniDawn MALS detector (Wyatt Technologies, USA). The column thermostat and autosampler were both set to 20 °C. The protein was diluted to 0.83 mg/mL in PBS (Sigma-Aldrich) and was then resolved in duplicate experiments on a Superdex 200 increase 10/30 GL column (GE Life Sciences) equilibrated in PBS. With ASTRA software (Wyatt Technologies),

the absorption at 280 nm, light scattering, and refractive index properties of the eluates were collected and analyzed. The contribution of protein and glycosylation in the eluting species was determined by the conjugate analysis method in ASTRA using  $dn/dc$  values of 0.185 mL/g and 0.14 mL/g for protein and glycans, respectively, and an extinction coefficient for the protein at 280 nm of 1.2 mL/(mg.cm). The  $dn/dc$  value obtained for the conjugate was used for further molecular weight determination.

#### Ace2 binding kinetics

Interactions of S1 antigens to hACE2 protein were performed with a QCM Attana A200 Biosensor (Attana AB) as described elsewhere (Fougeroux et al., 2021) (PMID: 33436573). Briefly, ExpreS<sup>2</sup> expressed hACE2 at 50 mg/mL (Expre2ion Biotechnologies) was immobilized on an LNB carboxyl chip. The binding of S1 proteins to the chip was measured in a two-fold serial dilution series (200 nM to 6.25 nM) in PBS pH 7.4.

#### Vaccinations Queensland Institute of Medical Research Berghofer

Cytokeratin-18 promoter (K18)-hACE2 mice were housed at QIMRB. K18 mice (n=4) received two intramuscular administrations of 50 ml vaccine, containing 25 ml purified S and 25 ml AS01 adjuvant. Blood was collected and tested for neutralizing antibodies against SARS-CoV-2 in a VN assay. The sera were diluted 1:10, and then 2-fold serial dilutions were incubated with 100 CCID<sub>50</sub> of SARS-CoV-2 (strain hCoV-19/Australia/QLD02/2020) for 2 h. Samples were added to Vero E6 cells in 96-well plates and viral cytopathic effect (CPE) was quantified on day 4 by crystal violet staining. Mice vaccinated with UV-inactivated SARS-CoV-2 provided positive control sera and naive mice provided negative control sera. At 18 weeks post-prime, the mice were challenged intranasally with  $5 \times 10^4$  TCID<sub>50</sub> SARS-CoV-2 per mouse (hCoV-19/Australia/QLD02/2020). Weight change was monitored for five days, and viral titers were determined in the lungs, brain, and nasal turbinates.

#### Coupling S1 antigen to virus-like particles

Catcher-VLPs based on the AP205 coat protein (Gene ID: 956335) fused to the proprietary catcher sequence were produced in *E.coli* (Thrane et al., 2016) (PMID: 27117585). The purified S1 was coupled to the catcher-VLPs and formulated as an adjuvanted vaccine as previously described (Fougeroux et al., 2021) (PMID: 33436573). In short, S1 and catcher-VLPs were mixed in a 1:1 molar ratio in PBS overnight at room temperature. A part of the mix was spun down at 16000  $\times g$  for 2 minutes to assess the stability of the coupled protein. Equal amounts of pre- and post-spin samples were mixed with DTT and were heated prior to analyses by SDS-PAGE. The coupling

efficiency was calculated as the percentage of AP205 capsids that had been conjugated to an S1 domain via Tag/Catcher interactions (Janitzek et al., 2016). The protein bands on the SDS-PAGE gel were analyzed by Imagequant<sup>TL</sup> software to determine the band intensity. The band intensity of the VLP subunit before the coupling reaction was divided with the equivalent protein band after coupling and was multiplied by 100. After the coupling reaction, the S1-VLP was purified from the remaining coupling mixture. This was loaded onto an Optiprep<sup>TM</sup> step gradient (23%, 29%, and 35%) (Sigma-Aldrich) and was centrifuged at 47800 rpm for 3.30 h. Buffer exchange was then performed by dialysis in PBS.

### Transmission Electron Microscopy of the S1-VLP vaccine

The quality of the VLPs after coupling, purification, and buffer exchange was assessed by Transmission Electron Microscopy (TEM). For this, 1 ml VLP mixture was added to a carbon-coated copper grid and was incubated for 2 minutes at room temperature. The grid was washed once with milli-Q water and was negatively stained for 30 seconds in 2% uranyl acetate and air-dried before observation with a JEOL 1400 plus transmission electron microscope.

### Vaccinations University of Copenhagen

Experiments were authorized by the Danish National Animal Experiments Inspectorate (Dyreforsøgstilsynet, license no. 2018-15-0201-01541) and performed according to national guidelines. Female BALB/c AnNRj mice were vaccinated with 0.5 mg S1 (n=4) or 0.5 mg S1-VLP (n=4) formulated in Addavax<sup>TM</sup> (Invivogen). Blood was collected two weeks post each immunization. The serum was isolated by two centrifugation steps at 800 *x g* for 8 minutes at 8 °C. Specific IgG titers in serum samples were measured by enzyme-linked immune-sorbent assay (ELISA). For this, the plates were coated with 0.1 mg/well recombinant Expres<sup>S2</sup> produced Spike protein or RBD (Expres2ion Biotechnologies). Serum samples were added at a starting dilution of 1:50 and added in 3-fold dilutions. IgG titers were determined by OD measurements after incubation with Horseradish peroxidase (HRP) conjugated goat anti-mouse IgG (Life Technologies, A16072). Plates were developed by using TMB X-tra substrate (Kem-En-Tec, 4800A) and absorbance measurements at 450 nM. Virus-neutralizing antibody titers in the mice sera were determined on Vero E6 cells as described elsewhere (Fougeroux et al., 2021) (PMID: 33436573) with SARS-CoV-2 Wuhan (L008) or SARS-CoV-2 UK/B.1.1.7 (VOC-202012/01) strain at 120 TCID<sub>50</sub>/well.

## Results

### Baculovirus expression and localization of SARS-CoV-2 spikes in Sf9 insect cells.

To determine the most suitable recombinant baculovirus system to produce SARS-CoV-2 spike variants and to determine the most suitable secretion signal sequence, Sf9 cells were infected with AcBACe56 and AcOET recombinant baculoviruses encoding the SARS-CoV-2 spike (Figure a). The spike proteins were similarly expressed in the cells with either the N-terminal HBM signal sequence or the baculovirus GP64 signal sequence (Figure b, compare Sp1 with Sp2). Furthermore, the AcBACe56 and AcOET recombinant baculoviruses induced expression of S proteins that were recognized by convalescent-phase sera from COVID-19 patients (Figure b). Baculovirus encoding GFP (AcGFP) and mock-infected Sf9 cells were included as controls and were not detected by the same sera. As expected, removal of the C-terminal transmembrane (CT) domain from the spike protein lowered the detection signal, since S was now excreted from the cells (Figure b, AcOET-Sp9). Compared to AcOET, our in-house AcBACe56 produced similar yields of secreted S (Supplementary figure 1). Generation of recombinant AcOET baculovirus stocks demands less hands-on time than AcBACe56. Therefore, AcOET-Sp9 was used for further production and purification of secreted S.

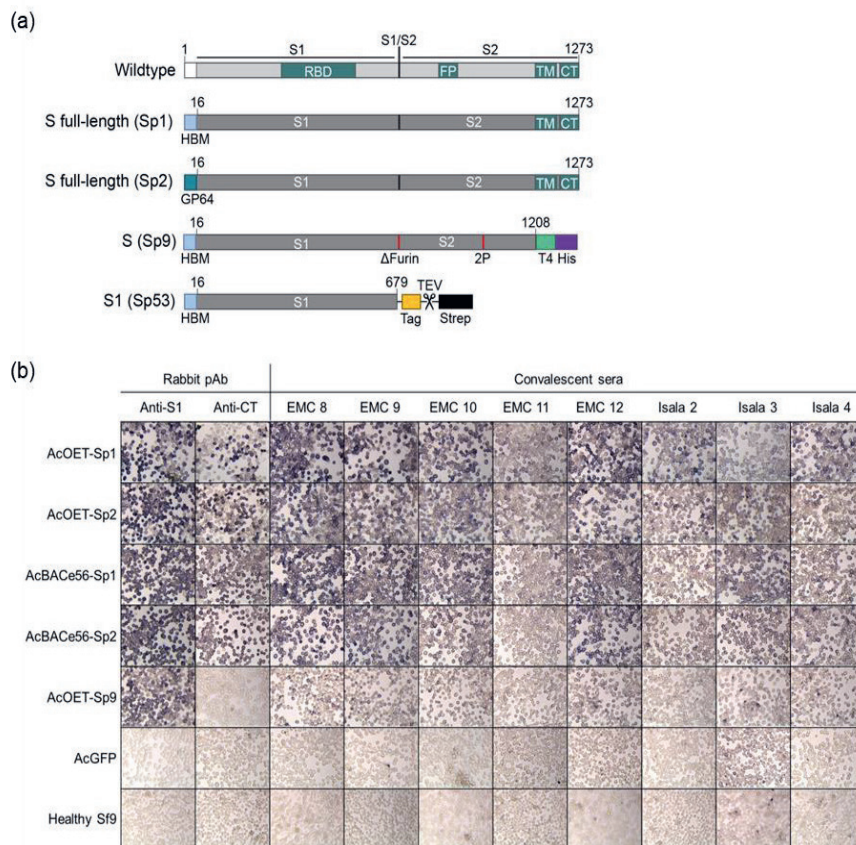


**Figure 1.** Expression of recombinant SARS-CoV-2 spike protein in insect cells. (a) In this study, recombinant baculoviruses were constructed containing spike proteins as schematically represented. (b) S full-length and S (delta TM) were detected inside Sf9 cells after staining with rabbit polyclonal sera against S1 (anti-S1) or cytoplasmic tail in S2 (anti-CT) or with human convalescent-phase sera obtained from two hospitals (EMC and Isala). pAb, polyclonal antibody.

### Immunogenicity of a SARS-COV-2 subunit vaccine from insect cells.

The prefusion-stabilized S was produced with AcOET-Sp9 baculoviruses in ExpiSf9 cells cultured in shake flasks in chemically defined medium. After purification, the recombinant protein yield was estimated to be 180 µg S protein per liter of culture fluid with relatively low purity (Figure a). The insect cell proteins in the culture fluid contaminated the S protein and could not be removed with a single purification step. We subsequently used this S with AS01 adjuvant in a vaccination challenge study in four K18-hACE2 transgenic mice (Figure b). After two intramuscular immunizations with 5 µg adjuvanted S, we measured virus-neutralizing activity in sera of the vaccinated mice. Two mice (M3 and M4) had detectable neutralizing antibody responses, both with a reciprocal serum dilution

titer of 15. There were no measurable amounts of neutralizing antibodies in the other two animals (M1 and M2) or in the sera obtained after the first immunization. Mice were challenged with an intranasal sublethal dose of SARS-CoV-2 at 18 weeks post-prime. Two mice, M1 and M2, developed disease symptoms and showed a loss of body weight, in contrast to the exposed-immune control group (Figure c). At 5 days post-challenge, SARS-CoV-2 virus was found in their lungs, nasal turbinate, and brains (Figure d). This demonstrates SARS-CoV-2 infection and replication in the vaccinated K18-hACE2 mice (Kumari et al., 2021; Moreau et al., 2020), similar to the nonvaccinated controls (Figure d). M3 and M4 were protected from clinical COVID-19 disease and weight loss similar to the exposed-immune control group (Figure c). Although no SARS-CoV-2 was detected in the lungs, virus was measured in the nasal turbinate of M3 and in the brains of both M3 and M4 (Figure d). As a result, two intramuscular doses of adjuvanted S could provide partial protection against SARS-CoV-2 in hACE2 mice.

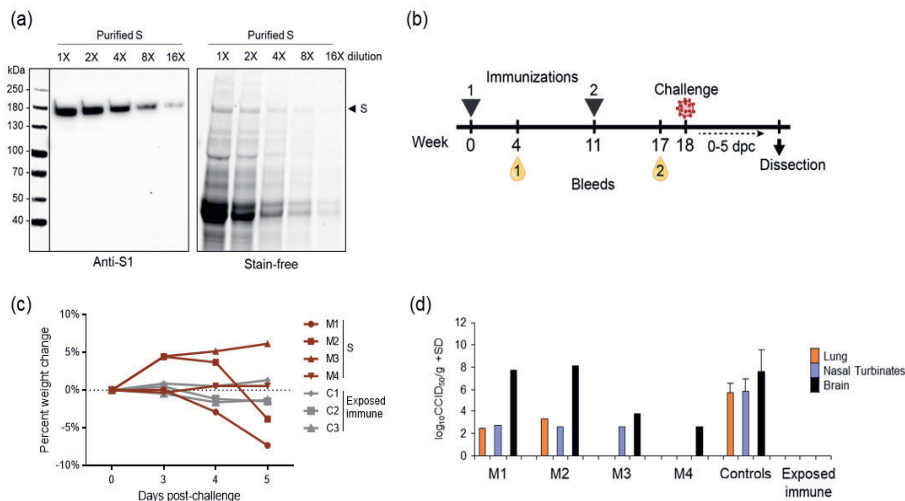


**Figure 2.** Production of S and immunization of K18-hACE2 mice with two doses of adjuvanted S induce limited nAb responses and result in partial protection from SARS-CoV-2 challenge. (a) S was produced with the ExpiSf expression system and purified from medium. The elution fractions were pooled and analyzed on SDS-PAGE (stain-free) and Western blotting (anti-S1) in a serial dilution. (b) K18-hACE2 mice (n = 4, M1 to M4) were immunized with two doses of 5  $\mu\text{g}$  S and AS01 adjuvant, where blood was collected after each vaccination. At 18 weeks postprime, the mice were challenged intranasally with SARS-CoV-2. (c) From 0 to 5 days postchallenge (dpc), body weight change was monitored. (d) At 5 dpc, the viremia in lungs, nasal turbinates, and brain were measured. Mice vaccinated with UV-inactivated SARS-CoV-2 served as an exposed immune control (n = 3, C1-C3), and nonvaccinated controls (n = 12) were included in viremia titrations.

### Production of strep-tagged S1 subunit increases yield and purity.

We next aimed to produce the S1 subdomain to improve protein yield and purity after purification. Moreover, the adjuvanted spike subunit vaccine did not completely inhibit viral infection in K18-hACE2 transgenic mice. To improve the immunogenicity of the S1 antigen, the nanoparticle-based AP205 VLP display system was used. The secreted S1 (Figure a, Sp53) was produced with AcOET-Sp53 baculoviruses in ExpiSf9 cells in shake flasks. SDS-PAGE and Western blot analyses showed that S1 was successfully expressed and secreted into the culture fluid (Figure a) and could be purified efficiently using strep-tag affinity chromatography (Figure b). The strep-tag affinity column had a higher specificity than the His-tag nickel affinity column and resulted in a relatively pure S1 protein compared to the purity of S after immobilized-metal affinity chromatography. The C-terminal strep-tag was removed by tobacco etch virus (TEV) protease cleavage, resulting in TEV-cleaved S1 (60%) and an S1 aggregate (30%) (Supplementary figure 2). Removal of the strep-tag was demonstrated by a shift in protein size on SDS-PAGE and a loss of signal from StrepTactin-alkaline phosphatase (AP) antibody on Western blotting (Figure c). Both S1 and the S1 aggregate fractions show a band with the same mass on denaturing SDS-PAGE and binding on Western blotting to rabbit-anti-S1 and several human COVID-19 convalescent-phase sera (Figure d). Moreover, S1 has a high binding affinity to immobilized ACE2, with a dissociation constant ( $K_D$ ) of 16.7 nM (Figure e), which is in a similar range as previously reported (Fougeroux et al., 2021; Ke et al., 2020; Wrapp et al., 2020). This indicates that the receptor-binding site within S1 is exposed and available to interact with ACE2.

The secreted S1 production was further scaled up from shake flasks to a 3-liter bioreactor system infected at low multiplicity of infection (MOI). Cells were grown for 3 days before infection with baculovirus. The reactor was monitored continuously online using a holographic microscope and was sampled daily for offline measurements. The maximum viable cell density (VCD) was monitored both online and offline and peaked at 3 dpi (Figure f). At 4 dpi, all detected cells showed signs of baculovirus infection (Figure g). The bioreactor was harvested at 5 dpi when viability dropped below 70%. The culture fluid then contained 7 mg/liter S1, which further increased to 11 mg/liter during subsequent shake flask cultivation (Figure g). This is a substantial increase in protein yield compared to the 0.18 mg/liter that was obtained for the S protein.

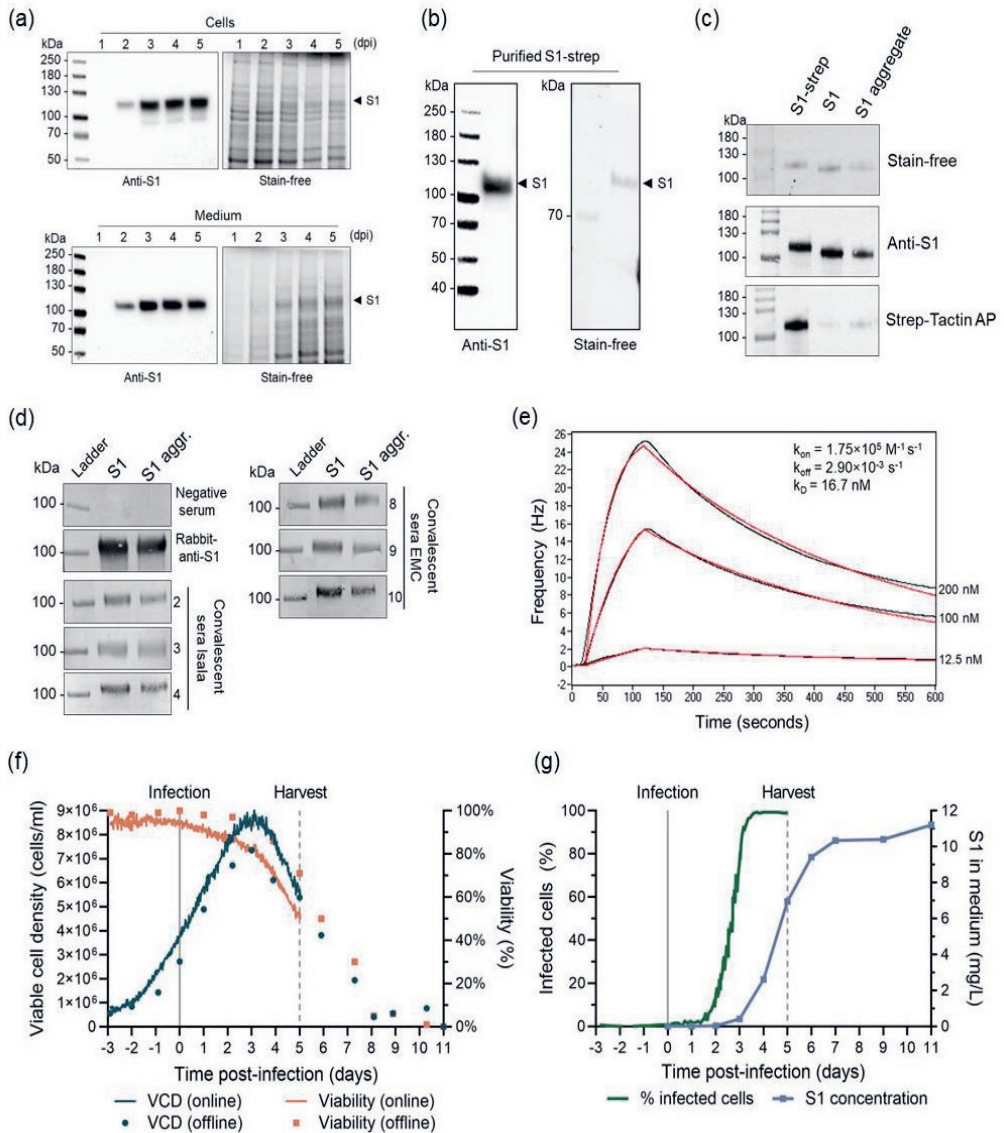


**Figure 3.** Production and analyses of recombinant S1 protein in shake flasks and bioreactor. (a) S1 was produced with the ExpiSf9 expression system in chemically defined medium and was detected in cells and culture fluid on SDS-PAGE (stain-free) and Western blot (anti-S1). (b and c) S1 was purified from the culture fluid (b) and fractions before strep-tag removal (S1-strep) and after (S1 and S1 aggregate) were analyzed (c). (d) S1 and S1 aggregate (S1 aggr.) bind to COVID-19 convalescent-phase sera from Isala Zwolle (serum numbers 2, 3, 4) or from EMC Rotterdam (serum numbers 8, 9, 10) on Western blot. COVID-19 naive serum served as a negative control (Isala 7) and rabbit-anti-S1 (Sino Biological) as a positive control. (e) S1 also binds to immobilized ACE2, where real-time binding (black curves) was fitted in a 1:1 simple binding model (red curve). (f and g) Production of S1 was scaled up from shake-flask cultures to a 3-liter bioreactor. At time  $-3$  days, ExpiSf cells were seeded, at  $t=0$  (straight line), and the cells were infected at an MOI of 0.01. The reactor was harvested at 5 dpi (dotted line), where 60 ml of the culture was transferred to a shake flask and

continued (offline) sampling. (f) Viable cell density (VCD) and viability were monitored continuously (line), and samples were taken daily for extra offline measurements (dots). (g) Fraction of infected cells from total cells in the bioreactor and SARS-CoV-2 spike protein secreted in the culture supernatant measured by ELISA in milligrams per liter of culture.

### Analyses of S1 structure, folding, and glycosylation

The structure, folding, and glycosylation of insect cell-derived S1 were analyzed by several methods. The secondary structure content was calculated from the far-UV circular dichroism (CD) spectrum of S1 (Figure a). With 6.8%  $\alpha$ -helices and 38.4%  $\beta$ -sheets, the secondary structure content of S1 was highly similar to what was expected based on the wild-type (WT) SARS-CoV-2 spike structure (Figure b and c) (i.e., 2.3% helices, 41.2% sheets). Thus, CD confirms that at 20°C the purified spike S1 domain mostly retained its structural elements.

The oligomerization state, molar mass, and glycosylation of S1 were determined by duplicate size-exclusion chromatography coupled with multiangle light scattering (SEC-MALS) experiments. Three oligomerization states could be distinguished in the chromatograms, as monitored by absorbance of UV light at 280 nm (Abs<sub>280</sub>), refractive index (dRI), and light scattering (LS) (Figure d, Supplementary figure 3). Conjugate analysis revealed that peak 1 represented a glycosylated protein species with a molecular weight of  $90.9 \pm 0.2$  kDa. This glycosylated protein consisted of a protein component ( $82.4\% \pm 1.1\%$ ) with a molecular weight of  $74.9 \pm 1.0$  kDa and a glycan component ( $17.6\% \pm 1.1\%$ ) with a molecular weight of  $16.0 \pm 0.2$  kDa. The molecular weight of the protein component in peak 1 is in good agreement with the 77.1 kDa that is expected for the S1 protein monomer based on the amino acid sequence. The  $dn/dc$  value (i.e., the refractive index increment) for the conjugate (i.e., 0.1775 ml/g) was obtained and was used to calculate the molecular weights of the species in elution peaks 2 and 3. The protein species were found to be  $183.4 \pm 0.4$  kDa for peak 2 and  $279.8 \pm 1.6$  kDa for peak 3. Thus, the protein species eluting in peaks 1, 2, and 3 corresponded to an S1 monomer, dimer, and trimer, respectively. Under these conditions, the monomer is clearly the predominant S1 form.

Glycosylation of S1 was further confirmed by PNGase-F treatment and Periodic acid-Schiff (PAS) staining of the protein. The PNGase-F treatment, which removes N-linked glycans, caused a shift in protein migration on SDS-PAGE gel and a loss of PAS staining of the Western blot membrane (Figure e). Together, they substantiate the results obtained with SEC-MALS. Thus, S1 produced in Sf9 cells is heavily glycosylated, akin to SARS-CoV-2 proteins that were produced in HEK293 cells (D. Wang et al., 2020).

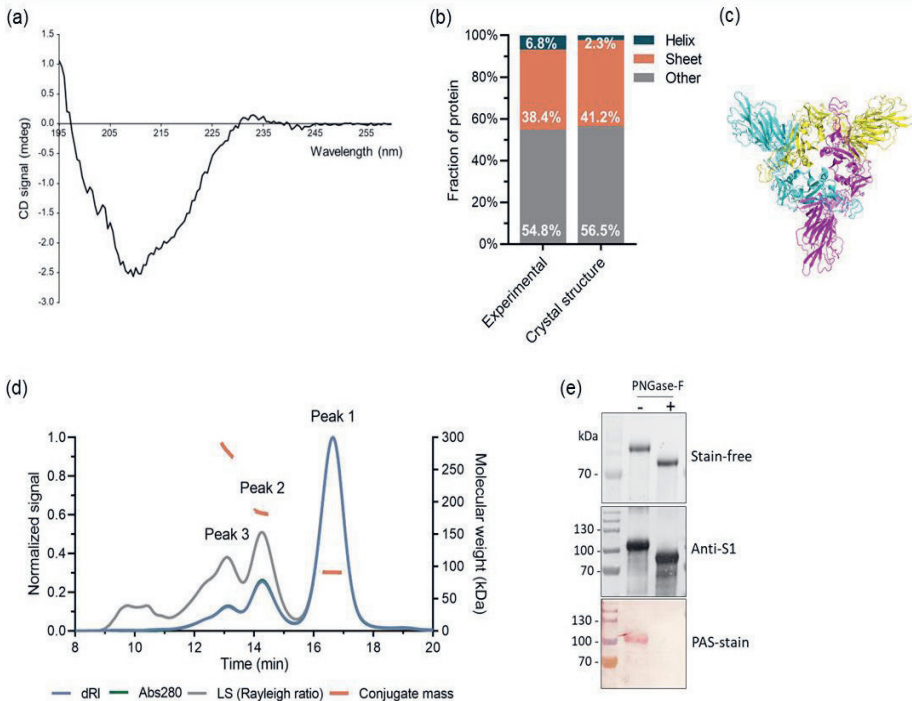


**Figure 4.** Analysis of glycosylation and oligomerization of Sf9-cell-produced S1 protein. (a) Far-UV CD spectrum of S1 at 20°C and the resulting percentage of helices, sheets, and other structures within S1. (b) Data derived from CD measurements (experimental) were compared to those from wild-type S1 (crystal structure). (c) The proposed structure of S1 in trimeric conformation, based on the truncation of the full-length SARS-CoV-2 structure (Wrobel et al., 2020). (d) A representative chromatogram of S1 on a Superdex 200 increase 10/30 column, as detected by differential refractive index (dRI), absorption at 280 nm (A280), and light scattering (LS). The molecular weight of the species eluting in each indicated peak is shown in orange (conjugate mass). (e) S1 N-linked glycosylation was further confirmed by PNGase-F treatment and PAS staining. TEV-cleaved S1 was treated with PNGase-F. Treated (+) and nontreated (-) samples were analyzed on SDS-PAGE (stain-free) and Western blot (anti-S1). Glycosylation was confirmed by PAS stain.

### Display of S1 on AP205 VLPs

To improve the immunogenicity of the prototype vaccine, the S1 and S1 aggregate fractions were individually mixed in equimolar ratios with catcher-VLPs in an overnight coupling reaction (Figure a). We included the S1 protein that still contained the C-terminal strep-tag (S1-strep) as a control. The coupling efficiency was assessed on a reducing SDS-PAGE as shown in Figure b. An additional band of higher molecular mass appeared on the SDS-PAGE gel, corresponding to one S1 molecule covalently bound to one AP205 capsid. Removal of the C-terminal strep-tag by TEV protease cleavage improved the coupling efficiency. In that case, the coupling efficiency was estimated as at least 10%. This suggests that, on average, each VLP displayed at least 18 S1 proteins on its surface. A centrifugation step after coupling (stability spin test) revealed that the coupling was stable and the

S1-VLP was not prone to aggregation. These results are similar to what was seen for a previously developed RBD-VLP vaccine (Fougeroux et al., 2021). After purification of the VLPs from the remaining soluble S1, the VLPs are intact and of good quality, and the S1 domains are uniformly distributed among the VLP particles, as seen by transmission electron microscopy (TEM) (Figure c).

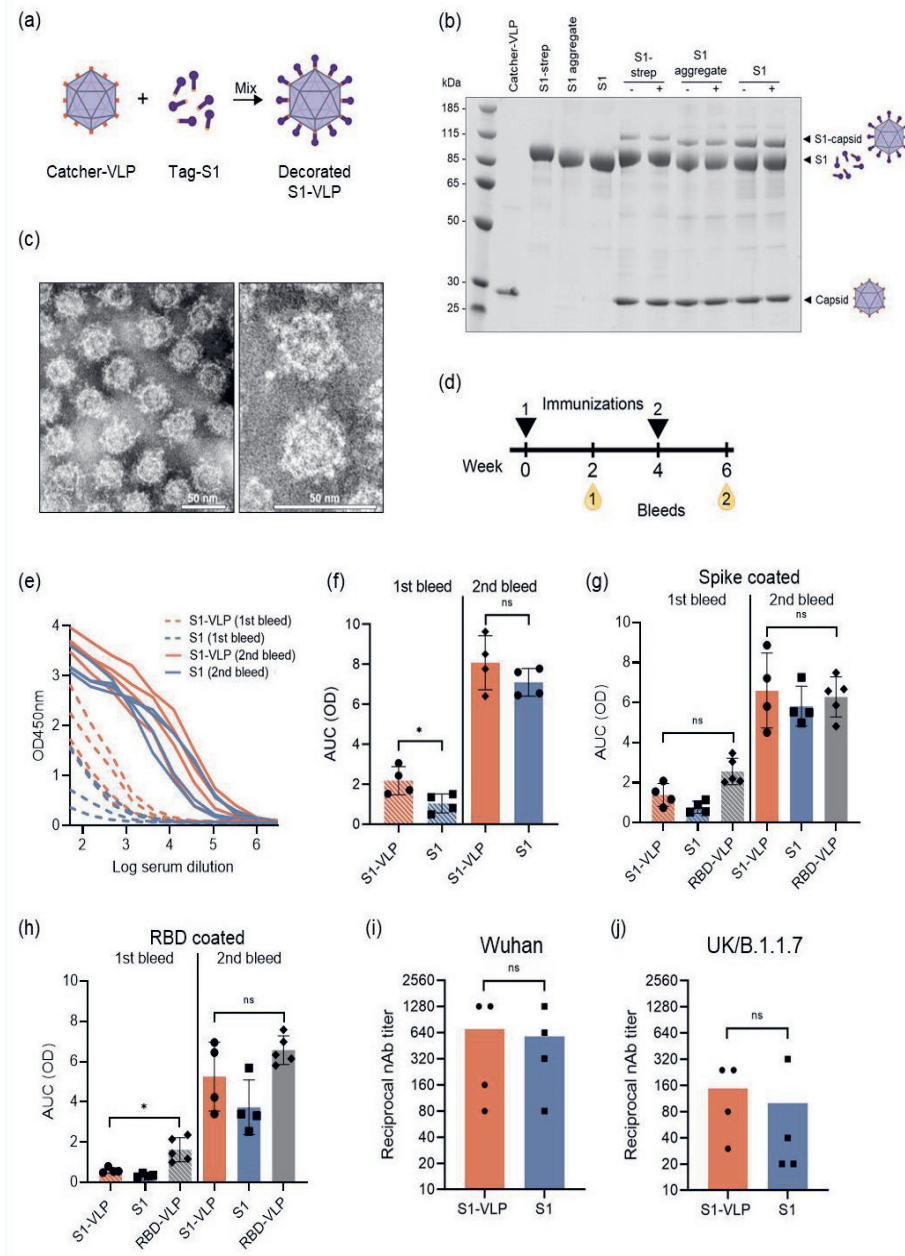


**Figure 5.** Low-dose vaccination of BALB/c mice with soluble S1 and S1-VLP induces potent neutralizing antibody responses. (a) S1 was coupled to VLPs by a coupling reaction as schematically represented. The catcher-VLPs are mixed with tag-S1, which results in a covalent display (decorated S1-VLP) that is visible on a reduced, denaturing SDS-PAGE gel. The individual components (catcher-VLP and S1) are shown. (b) Antigens were mixed with VLP and were analyzed again before (–) and after (+) a centrifugation step. An extra band appears representing the covalently fused S1 to a single AP205 capsid (S1-capsid). (c) The VLPs were purified from the uncoupled S1 subunits and visualized by negative-stain transmission electron microscopy (TEM). The scale bar represents 50 nm. (d) BALB/c mice ( $n = 4$  per group) were vaccinated with 0.5  $\mu\text{g}$  soluble S1 or 0.5  $\mu\text{g}$  S1-VLP with Addavax adjuvant. Blood was collected 2 weeks postprime (1st bleed) and 2 weeks postboost (2nd bleed). (e) IgG antibodies against SARS-CoV-2 spike were analyzed in a dilution series in an ELISA. (f to h) The IgG titers were expressed as area under the curve (AUC) values. (f) The IgG titers in plates coated with SARS-CoV-2 spike were compared for mice vaccinated with S1 or S1-VLP. (h and g) Sera were measured on ELISA plates coated with RBD (g) or coated with full spike (h) and were compared to sera of mice vaccinated twice with 5  $\mu\text{g}$  RBD-VLP. (i and j) The reciprocal neutralizing antibody titers after the second vaccination are shown for neutralizing SARS-CoV-2 Wuhan (L008) (i) or UK/B.1.1.7 (j) strain. A two-sided nonparametric Mann-Whitney  $t$  test was used for statistical comparison. ns, nonsignificant; \*,  $P < 0.05$ . Significance is marked with an asterisk in panels e ( $P = 0.0286$ ) and g ( $P = 0.0159$ ).

### Immunogenicity of the S1-VLP nanoparticle vaccine.

The immunogenicity of the S1-VLP was assessed in a mouse immunization study and was compared to mice vaccinated with soluble S1 protein. Before vaccine formulation of S1-VLP, the unbound S1 was removed from the coupling reaction mix by using ultracentrifugation. BALB/c mice ( $n = 4$ ) received two intramuscular immunizations containing only 0.5  $\mu\text{g}$  S1-VLP or 0.5  $\mu\text{g}$  S1 per dose, formulated with Addavax, and blood was collected 2 weeks after each vaccination (Figure d). All mice showed potent immune responses, especially after the second immunization, as measured in an IgG protein enzyme-linked immunosorbent assay (ELISA) (Figure e). The areas under the curve (AUC) were derived from the ELISA data and showed a slight difference in IgG levels after the first immunization between the two groups, with the S1-VLP vaccine performing better (Figure f). After the second immunization, however, the effect of the VLP coupling was less clear, possibly because in both groups an adjuvant was used.

These sera were compared to sera of mice vaccinated with 5  $\mu\text{g}$  of the previously developed RBD-VLP vaccine (Fougeroux et al., 2021). Even though the antigen concentration in the S1-VLP vaccine trial was 10-fold lower, all groups had comparably high antibody responses to the spike protein, as determined by ELISA (Figure g). The IgG titers specific for the SARS-CoV-2 RBD domain were higher in the RBD-VLP vaccinated mice than our S1- and S1-VLP-vaccinated mice after the first bleed but not after the second bleed (Figure h).

Finally, after the second vaccination, all sera contained substantial virus-neutralizing antibody titers against the Wuhan (L008) SARS-CoV-2 strain, on which the vaccine was based (Figure i). Importantly, sera were also able to neutralize the UK (B.1.1.7) strain of SARS-CoV-2 (Figure j).

### Discussion

The development and/or improvement of effective SARS-CoV-2 vaccines are still a priority worldwide. Protein-based vaccines are needed to vaccinate the world population and to boost immunity against emerging variants. These vaccines are known for their inherent long-term safety and efficacy after administration and lack of preexisting antivector immunity (Moore & Klasse, 2020). Moreover, the production safety, production costs, and vaccine storage temperatures are advantageous compared to mRNA and adenovirus vector vaccines, especially for scale-up manufacturing and global distribution (Nagy & Alhatlani, 2021). In this study, we have used the versatile and scalable baculovirus expression vector system to generate a two-component nanoparticle vaccine that induced a potent neutralizing antibody response against SARS-CoV-2 variants.

Both secreted S and S1 were produced with the ExpiSf9 expression system in chemically-defined medium, which is both serum-free and protein-free. A yield after purification of 0.18 mg/L for S was obtained. This is relatively low, although production yields of prefusion-stabilized S vary greatly between expression systems. Yields of 0.5 mg/L S have been reported for FreeStyle 293 cells, 5 mg/L for HEK293 cells (Esposito et al., 2020), and up to 200 mg/L for stably transfected CHO cells (Wu et al., 2021). Whereas trimeric S is often unstable (Juraszek et al., 2021; Stuible et al., 2021), smaller spike protein domains, for example the S1 or RBD, are generally more stable and result in higher yields. RBD is produced up to 50-60 mg/L in Schneider-2 insect cell lines and Expi239F cells, respectively (Fougeroux et al., 2021; Walls, Fiala, et al., 2020), but production yields of the S1 subunit have not been reported to our knowledge. During our scale-up of S1 production in a stirred-tank bioreactor, we measured a maximum yield of 11 mg/L culture, which might be further increased by subsequent parameter optimization that could be facilitated by online monitoring of the baculovirus infection process. The clear advantages of baculovirus expression over other expression platforms are its excellent safety profile, the rapid scalability to bioreactors up to several thousand liters, and its demonstrated use in the production of protein and VLP-based human vaccines (Buckland et al., 2014; Felberbaum, 2015; Van Oers et al., 2015). Based on the dosage of SARS-CoV-2 subunit vaccines in current phase 3 clinical trials (5 µg/dose, Novavax, NCT04583995; 10 µg/dose, Sanofi Pasteur, NCT04904549), and a licensed subunit vaccine made with the BEVS (135-180 µg/dose,

FluBlok (Treanor et al., 2007), a million-dose vaccine batch of S1-VLP can theoretically be produced in a single insect-cell bioreactor. Moreover, as demonstrated for the Flublok® influenza vaccine, the production process can easily be adapted to new protein variants in only six weeks (Buckland et al., 2014; Cox & Hashimoto, 2011).

Using multiple analyses, we have demonstrated correct folding, ACE2 affinity, and extensive glycosylation of the insect cell-derived S1. While glycosylation patterns in insect cells are less complex and more homogeneous than in mammalian expression systems (Harrison & Jarvis, 2006; D. Wang et al., 2020), there are no indications that insect glycosylation patterns positively or negatively affect the immunogenicity of SARS-CoV-2 or other glycoprotein based vaccines (Cox et al., 2015; Keech et al., 2020; Sadoff et al., 2021).

In a first attempt to investigate the immunogenicity of insect-cell-derived SARS-CoV-2 antigen, adjuvanted S was tested in a vaccination-challenge experiment in K18-hACE2 transgenic mice, but only partial protection against sublethal SARS-CoV-2 challenge was obtained. The impurities in the his-tag purified S subunit, including glycosylated insect cell proteins, lower the effective dose to induce a specific antibody response against S. This is in line with clinical studies in which low immune responses of baculovirus-expressed, adjuvanted S protein subunit in certain age groups were reported, and this can possibly lead to a higher reactogenicity of the vaccine (Goepfert et al., 2021). Thus, a better SARS-CoV-2 antigen presentation was needed and this was accomplished by coupling S1 subunits to AP205 VLPs (Fougeroux et al., 2021).

The tag/catcher coupling of S1 to the VLPs was increased after removal of the strep-tag and was estimated to be at least 10%. Display of the SARS-CoV-2 RBD domain onto AP205 VLPs showed 33-45% coupling efficiency (Fougeroux et al., 2021) and display of other proteins ranged from 22-88%, which negatively correlated to the size of the antigen (Thrane et al., 2016). The coupling efficiency might be further improved by increasing the coupling pressure where the antigen is present in excess in the mixture. Also, the coupling is potentially facing partial steric hindrance between the relatively large, glycosylated S1 antigens and it may be useful in future studies to experiment with flexible linkers at the S1 C-terminus to provide additional space to further improve antigen coupling. Moreover, S1 is highly glycosylated and these glycans might further impair efficient coupling by steric hindrance between S1 domains. We have displayed an average of 18 relatively large S1 proteins on

each 30 nm VLP, which is comparably spaced as the spikes on the wildtype SARS-CoV-2 virion (Bachmann et al., 2021; Ke et al., 2020; Liu et al., 2020).

The S1-VLPs (and S1 subunit for comparison) were used to immunize BALB/c mice twice with a low dose of 0.5 mg per mouse. The vaccines were adjuvanted with AddaVax, an MF59-like oil-in-water emulsion. Comparison between adjuvants in SARS-CoV-2 subunit vaccines has shown that these squalene-based oil-in-water emulsions are among the most potent adjuvants (Arunachalam et al., 2021; Haun et al., 2020; Liang et al., 2021). An adjuvating effect of the VLP was observed only after the first immunization, where a significant difference between S1 subunit and S1-VLP was observed in the amount of IgG produced. After the second immunization, the S1 subunit and S1-VLP performed similarly in inducing potent immune responses. The boosting effect of the second immunization and the addition of Addavax adjuvant in both vaccine groups might be obscuring the intrinsic adjuvating effect of the AP205 VLP (Zhang et al., 2020).

An RBD-VLP prototype vaccine is currently under evaluation in the COUGH-1 clinical phase I/II trial (National Library of Medicine, NCT04839146) and makes use of the same AP205 VLPs, but with an RBD antigen expressed in S2 Drosophila cells (Fougeroux et al., 2021). We show that our S1-VLP vaccine reaches comparable IgG titers compared to the RBD-VLP but with a 10-times lower antigen dose (0.5 mg for S1-VLP vs. 5 mg for RBD-VLP). In line with this result, a comparison of HEK293-cell-derived S1 and RBD subunits showed that S1 gave superior immune responses when formulated as subunit vaccine (Y. Wang et al., 2020). It remains to be seen if enhanced immunogenicity of S1 compared to RBD can compensate for the less efficient S1-VLP coupling. In our study, both vaccines appear equally potent in generating SARS-CoV-2 specific antibodies.

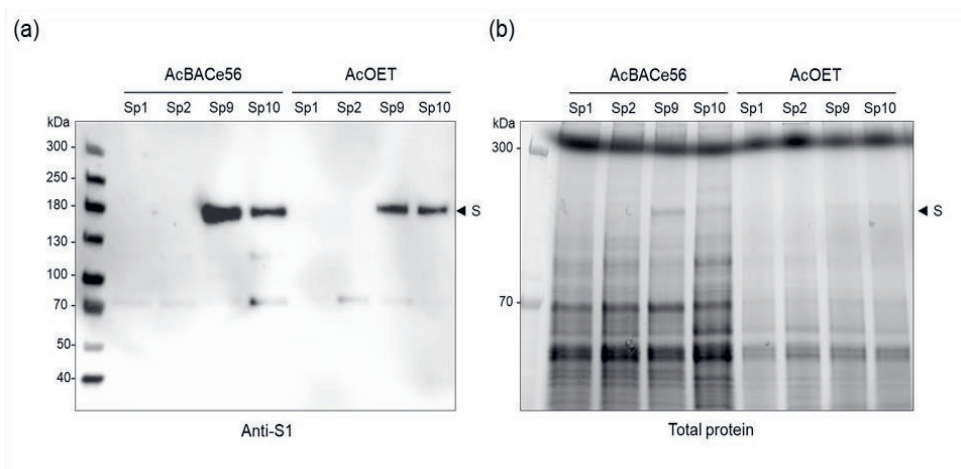
Neutralizing antibodies are an important immune correlate of protection (Addetia et al., 2020; Carrillo et al., 2021; Sui et al., 2021) and therefore it was an important finding that all mice generated high neutralizing antibody titers for both the Wuhan L008 as well as the B.1.1.7. UK variant of SARS-CoV-2. The neutralizing antibody titers determinations have been performed in separate assays and thus cannot be directly compared, but it is feasible that protection against the B.1.1.7 is somewhat reduced due to the presence of several mutations in the S1 domain (HV69-70del, Y144del, N501Y, A570D, D614G). With RBD-based vaccines, this difference would only be a single amino acid (N501Y) (Socher et al., 2021). Immunogenicity against current and emerging variants might be further improved by the development of a multivalent vaccine, i.e. a VLP displaying a mixture of S1

variants. This can result in a more focused immune response toward conserved protein domains and broader protection against variants as was shown for HIV (Brouwer et al., 2019). Neutralizing antibody responses against other SARS-CoV-2 variants of concern as B.1.1.7. are important for future vaccine designs and for the progression of vaccine candidates through clinical trials towards licensing (Z. Wang et al., 2021). With novel SARS-CoV-2 variants emerging in the years to come, these two-component nanoparticle vaccines can be quickly adapted as booster vaccines by simply updating the antigen component.

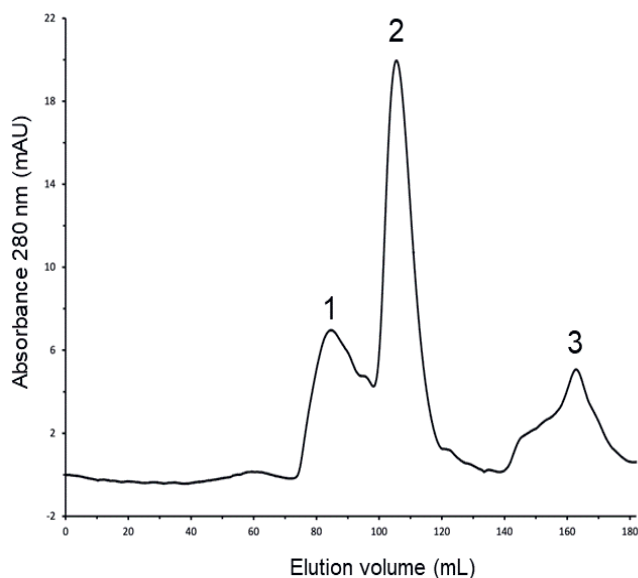
## Acknowledgments

We thank Els Roode, Gwen Nowee, Marleen Abma-Henkens, and Jelmer Vroom (Laboratory of Virology, Wageningen University) for their technical assistance. We acknowledge Corine Geurts van Kessel and Marion Koopmans (Erasmus MC, Rotterdam, The Netherlands) and Jacky Flipse (Isala, Zwolle, the Netherlands) for sharing sera of COVID-19 convalescent patients. We also acknowledge Arthur Oudshoorn (Applikon Biotechnology) for his assistance in the bioreactor production runs. This research was funded through European Union's Horizon 2020 research and innovation program (grant agreement no. 101003608) and conducted in the H2020 Prevent-nCoV consortium.

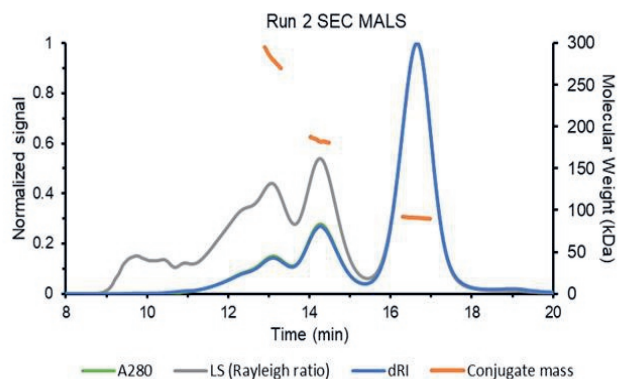
## Supplementary information



**Supplementary figure 1.** Spike protein secretion. Both full spike with transmembrane domain (Sp1-2) and spike without transmembrane domain (Sp9-10) were expressed with HBM or Gp64 as a signal sequence. Recombinant baculovirus was constructed with the AcBACE56 and the AcOET virus backbones. Sf9 cells were infected with recombinant baculovirus, and protein secretion in the medium was analyzed by SDS-PAGE (stain-free) (b) followed by Western blotting with polyclonal anti-S1 serum (a).



**Supplementary figure 2.** Removal of C-terminal triple strep-tag from S1 by TEV protease cleavage. The purified S1 was incubated overnight with 10:1 (wt/wt) TEV protease to S1. The cleaved product was run over a preparative Superdex S200 column, resulting in the pooled separation of S1 aggregate (peak 1, 75 to 98 ml), S1 (peak 2, 99 to 117 ml), and other proteins, including TEV protease (peak 3, 135 to 175 ml).



**Supplementary figure 3.** Duplicate run SEC-MALS of S1. Chromatogram of S1 on a Superdex 200 increase 10/30 column, as detected by differential refractive index (dRI), absorption at 280 nm (A280), and light scattering (LS). The molecular weight of the species eluting in each indicated peak is shown in orange.



3

# Chapter 3

---

## Real-time online monitoring of insect cell proliferation and baculovirus infection using digital differential holographic microscopy and machine learning

---

Jort J. Altenburg<sup>1</sup>, Maarten Klaverdijk<sup>1</sup>, Damien Cabosart<sup>2</sup>, Laurent Desmecht<sup>2</sup>, Sonja S. Brunekreeft-Terlouw<sup>1</sup>, Joshua Both<sup>1</sup>, Vivian I.P. Tegelbeckers<sup>1</sup>, Marieke L.P.M. Willekens<sup>1</sup>, Linda van Oosten<sup>3</sup>, Tessy A.H. Hickl<sup>3</sup>, Tom M.H. van der Aalst<sup>1</sup>, Gorben P. Pijlman<sup>3</sup>, Monique M. van Oers<sup>3</sup>, René H. Wijffels<sup>1</sup>, Dirk E. Martens<sup>1</sup>

<sup>1</sup> Bioprocess Engineering, Wageningen University & Research, Droevendaalsesteeg 1, 6708 PB Wageningen, The Netherlands

<sup>2</sup> Ovizio Imaging Systems, Av. Kersbeek 306, 1180 Ukkel, Belgium

<sup>3</sup> Laboratory of Virology, Wageningen University & Research, Droevendaalsesteeg 1, 6708 PB Wageningen, The Netherlands

### Abstract

Real-time, detailed online information on cell cultures is essential for understanding modern biopharmaceutical production processes. The determination of key parameters, such as cell density and viability, is usually based on the offline sampling of bioreactors. Gathering offline samples is invasive, has a low time resolution, and risks altering or contaminating the production process. In contrast, measuring process parameters online provides more safety for the process, has a high time resolution, and thus can aid in timely process control actions. We used online double differential digital holographic microscopy (D<sup>2</sup>HM) and machine learning to perform non-invasive online cell concentration and viability monitoring of insect cell cultures in bioreactors. The performance of D<sup>2</sup>HM and the machine learning model was tested for a selected variety of baculovirus constructs, products, and MOIs. The results show that with online holographic microscopy insect cell proliferation and baculovirus infection can be monitored effectively in real time with high resolution for a broad range of process parameters and baculovirus constructs. The high-resolution data generated by D<sup>2</sup>HM showed the exact moment of peak cell densities and temporary events caused by feeding. Furthermore, D<sup>2</sup>HM allowed us to obtain information on the state of the cell culture at the individual cell level. Combining this detailed, real-time information about cell cultures with methodical machine learning models can increase process understanding, aid in decision-making, and allow for timely process control actions during bioreactor production of recombinant proteins.

## Introduction

The baculovirus-insect cell expression vector system (BEVS) is used for the production of recombinant proteins and is one of the most used eukaryotic expression platforms to produce virus-like particles (VLPs) (T. Kost, 1999; Luckow & Summers, 1988; Pijlman, 2015; Robert D Possee, 1988). With this expression platform, VLP quantities comparable to those achieved in yeast can be produced. In addition, with BEVS it is possible to perform post-translational modifications (PTMs), such as glycosylation, comparable (but not identical) to that of mammalian cells (T. A. Kost et al., 2005; Roldão et al., 2010; van Oers, 2011). The baculovirus vector constructs required for the expression of the desired proteins (e.g., VLPs, viral glycoproteins, gene therapy vectors, enzymes, biologicals) can be generated in a matter of weeks. The ability to quickly express the desired protein and scale up the production makes the BEVS an excellent platform to respond to emerging virus threats, as witnessed recently during the global COVID-19 pandemic and earlier during outbreaks of the Zika virus (M. Cox, 2017; Shinde et al., 2021; van Oosten et al., 2021).

When scaling up the BEVS in bioreactors, it is important to determine three key parameters that interact with each other; the cell density at infection (CCI), multiplicity of infection (MOI), and the optimal time of harvest (TOH). First, cells are grown to the CCI at which point the baculovirus particles are added at a certain MOI, i.e., number of infectious virus particles per viable cell. Approximately 20-24 hours after the insect cells are infected by the baculoviruses they start producing the protein of interest. Next, at approximately 48-72 hours after infection, the cells start to lyse and release their contents in the medium among which proteases. This may affect product quality and complicate downstream processing, essentially lowering the product yield. On the other hand, performing the harvest too early leads to reduced yields as well. Harvesting at the right TOH is therefore critical for obtaining optimal yields of a high-quality product. Being able to precisely determine the values for CCI, MOI, and TOH during process development is essential for obtaining optimal volumetric productivity and product quality in the final production process.

Key process parameters describing the state of the culture, like viable cell density, viability, and infection state of the culture, are usually measured only once or twice per day. As a result, the time resolution (once every 12-24h) is low and important information to determine for example cell growth or infection stage may be obtained too late or even completely missed. This leads to suboptimal control and potential failure of production runs. (Anurag S Rathore & Helen Winkle, 2009) In addition, insufficient information is obtained for a proper mechanistic understanding of the

system. For example, when developing mathematical models based on scattered, offline sample data, the low time resolution of the data will impact the quality of these models. Finally, such manual sampling also introduces the risk of contaminating the culture and is prone to operator variance leading to less reliable datasets. Thus, online, and real-time measurement of key parameters like viable cell density, viability, and infection state of the culture appears to be important for a proper understanding of the BEVS and timely control of the production process.

Currently, several physical probes are available to allow online measurements of biomass, such as dielectric spectroscopy and light scattering. Dielectric spectroscopy measures viable biomass based on biomass capacitance, whereas light scattering methods measure total biomass. (Carvell & Dowd, 2006; Kiviharju et al., 2007; Ude et al., 2014) These methods are well suited for measuring cell biomass, however, they cannot directly measure the viability or infection stage of a single cell. Image-based cell culture monitoring is a more direct approach, where cells can be visualized individually to extract both the cell density and information on the state of the cells. An example of such an online imaging tool is online double digital differential holographic microscopy (D3HM) (Janicke et al., 2017; Rappaz et al., 2014). With this technique, the cell density is measured as well as a large number of optical parameters among which cell diameter and circularity, as well as quantitative parameters associated with the light phase and light intensity of each cell. These parameters can be related to the physiological states of the cells using machine learning models and specific training data sets. There is currently only one study that demonstrated the ability of online double digital differential holographic microscopy to monitor the BEVS in bioreactors (Pais et al., 2020). In that study by Pais et al. (2020), two bioreactor batch runs of Sf9 cells in SF900 II medium were performed where the insect cell concentration was measured online and the viability and AAV production titer was predicted. One growth batch without baculovirus infection and a single AAV production run using a two-baculovirus infection strategy at an MOI of 0.05 TCID<sub>50</sub>/cell were monitored.

The current work aims to obtain more insight into the performance of online digital differential holographic microscopy to monitor baculovirus-infected cell cultures in bioreactors. Several baculovirus constructs were included, producing various recombinant proteins, and under varying process conditions, using the ExpiSf9 cell line as a model (Yovcheva et al., 2018). First, training data sets were generated to develop machine learning models. Then the performance of the D3HM tool and machine learning model was evaluated during online monitoring of bioreactor runs. Results showed that after training the machine algorithm with a training data set, the cell density, cell viability,

cell diameter, and the fraction of infected cells could be accurately determined for a variety of bioreactor processes. Furthermore, the continuous online measurements allowed for the construction of high-resolution time-series profiles of these parameters. These high-resolution time-series profiles gave more insight into the state of the cell culture inside the bioreactor. Infected cells could be detected earlier compared to offline methods and the effect of process interventions such as feeding became distinguishable. Improved training data sets can further increase the accuracy of the online prediction, allowing for more advanced process control strategies and increased process understanding of recombinant protein production processes.

### Materials & Methods

#### Cell Lines, Media, and Virus Stocks

ExpiSf9 cells (Thermo Fisher) adapted to ExpiSf chemically defined medium (Thermo Fisher) were used in all batch and shake flask cultures. Recombinant baculoviruses of *Autographa californica* multicapsid nucleopolyhedrovirus (AcMNPV) were generated in two ways. Baculovirus expressing His-tagged GFP (hisGFP) or mCherry from the polyhedrin promoter, and a dual fluorescence baculovirus (AcBac-2FL) with GFP driven by the OpMNPV IE2 promoter and mCherry from the polyhedrin promoter were constructed by bac-to-bac transposition in *E.coli* (Thermo Fisher), followed by transfection of the bacmid into Sf9 insect cells with Express2TR transfection reagent (Express2ion Biotechnologies). Baculovirus expressing the strep-tagged SARS-COV-2 S1 spike subunit from the polyhedrin promoter was constructed by using pOET1-derived plasmids to transfect insect cells with the flashBAC Ultra kit (Oxford Expression Technologies, van Oosten et al., 2021). All baculovirus stocks were amplified in ExpiSf9 cells, and viral titers were determined by endpoint dilution assay on Sf9-easy titer cells using the Reed-Muench method (Hopkins & Esposito, 2009). Viral titers are defined as 50% tissue culture infectious dose (TCID<sub>50</sub>) units per ml.

#### Bioreactor Cultures

Cells were grown in 0.5L miniBio or 3L glass reactor vessels (Gethinge) controlled by myControl bioreactor controllers (Gethinge). The working volume of each reactor vessel was 0.3-2L. Reactors were inoculated at target starting densities of  $0.5-1.0 \cdot 10^6$  viable cells/mL. The liquid temperature was controlled at 27 °C. The pH was not controlled but maintained by the buffering capacity of the medium. Measured values remained between pH 5.7-6.1. Dissolved oxygen was controlled at 30% of air saturation using Lumisens optical dissolved oxygen sensors (Gethinge) and sparging of pure oxygen through open pipe spargers. In addition, a constant headspace aeration rate of 0.01 vvm air was applied. Agitation with marine impellers was set to 266-600 rpm by keeping the tip speed constant among the different reactor sizes.

#### Analytical Methods

Cells were counted by trypan blue exclusion using a TC20 Automated Cell Counter (Bio-Rad) or by manual counting using DHC-F01 cell counting chambers (INCYTO). Online measurements of viable and total cell density, viability, and infected cells were performed by differential digital

holographic microscopy (D3HM) using iLine F holographic microscopes (OVIZIO). Data acquisition and quantitative data analysis were performed using OsOne software (OVIZIO). Infected cells were visualized by expression of GFP or mCherry detected by a C6 Plus Flow Cytometer (BD Accuri). SARS-CoV-2 S1 subunits were quantified using a SARS-COV-2 Spike S1 Protein ELISA kit (AssayGenie).

### Results & Discussion

#### Training of the machine learning model

We assessed the ability of the iLine F online microscope to monitor cell growth, viability, and virus infection in bioreactors. Cell culture fluid was continuously pumped from the reactor through the iLine F flow cell and back into the reactor again. In this flow cell, holograms of the cells were captured. These holographic pictures allowed for direct calculation of the cell concentration and analysis of a large set of optical cell parameters that can be linked to the state of the cell. For example, upon baculovirus infection, distinct changes in cell morphology occur such as cell enlargement and changes in the granularity of the cell. (Kamen et al., 1996; Palomares et al., 2001b; Schopf et al., 1990; Taticek & Shuler, 1997) Specific optical changes also occur if the cell loses viability. Changes in measured optical parameters were then linked to the infection state and viability of each separate cell by a machine-learning model (Figure 1). The model was trained by monitoring bioreactor cultures of baculovirus-infected ExpiSf9 suspension cells in ExpiSf chemically defined medium. The training was done for the parameters of viability and infection percentage. Data from 6 runs with around 7 captures per run were used to train the initial machine learning model. To calculate the cell concentration, a segmentation model was used to detect the objects on the images. The objects were then filtered to remove non-cell objects like cell debris by specifying criteria such as particle size. Since the segmentation algorithm was not a machine learning model, no training step was required but only model parameter tuning. Part of the training was a bioreactor run with ExpiSf9 cells that were infected with a baculovirus expressing two fluorescent protein genes at high MOI (3 TCID<sub>50</sub>/cell) (Figure 2). The training data set for the live and dead cell detection algorithm was calibrated using offline samples and standard manual haemocytometer cell counting techniques using trypan blue exclusion. Viable cell percentages were very similar for the online measurement and offline samples except for 96 hours post-inoculation (hpi) when offline measured viability was notably higher (Figure 2A). The machine learning model might have detected dead or dying cells before this was discernable by trypan blue exclusion.

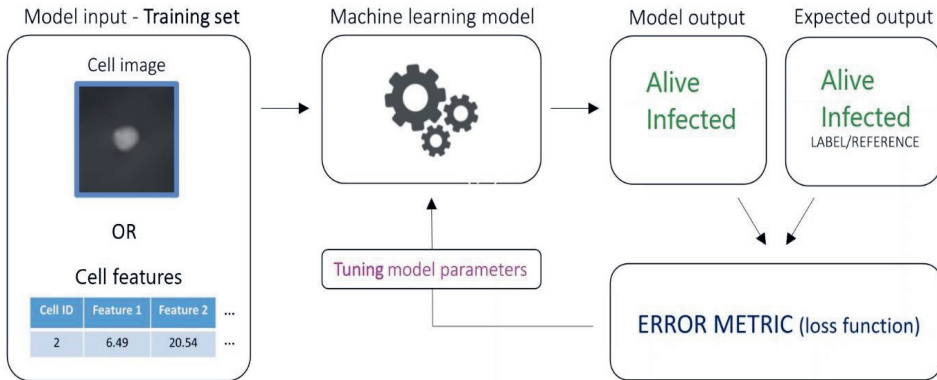


**Figure 1.** Workflow for training the machine learning model to detect alive and dead cells.

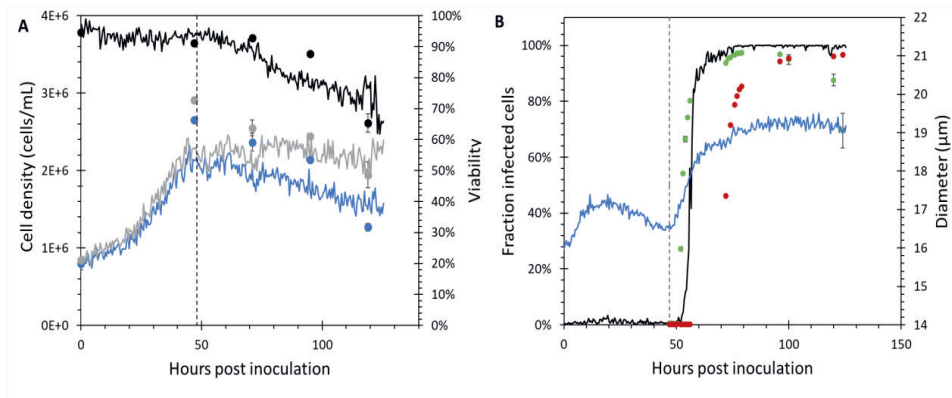


**Figure 2.** Time-course profiles for a training bioreactor run where ExpiSf9 cells were infected with a baculovirus expressing GFP and mCherry at an MOI of 3. The used baculovirus construct, AcBac-2FL, contained a gene for GFP located behind the immediate early OpIE2 promoter and a mCherry gene located behind the very late polyhedrin promoter. The dashed lines indicate the moment of baculovirus infection. (A) Viable online (-) and offline (●) and total online (-) and offline (●) cell densities. Online (-) and offline (●) viable cell percentages. (B) Online predicted infected cell fraction (-), offline measurements of fraction of GFP (●) and mCherry (●) expressing cells and average online cell diameter (-). Error bars represent duplicate measurement values.

The infected cell detection algorithm was calibrated to offline data from the same baculovirus-infected bioreactor cultures of ExpiSf9 cells in ExpiSf chemically defined medium. To calibrate the algorithm, a purpose-built dual fluorescence baculovirus construct was engineered. This dual fluorescence baculovirus, AcBac-2FL, was constructed to express the GFP gene behind the immediate early OpIE2 promoter, and the mCherry gene behind the very late polyhedrin promoter. The expression of GFP behind the OpIE2 promoter allowed us to spot early infection as the OpIE2 promoter becomes active immediately after baculovirus infection (Ramachandran et al., 2001; Shippam-Brett et al., 2001). The expression of mCherry was regulated by the very late polyhedrin promoter commonly used in the BEVS. This polyhedrin promoter becomes active around 20-24 hours after baculovirus infection (Massotte, 2003). To generate the training data set, the bioreactor culture was infected with AcBac-2FL at an MOI of 3 TCID<sub>50</sub>/cell. The early and very late phases of baculovirus infection could clearly be distinguished since cells showing green fluorescence were detected one day before the appearance of red fluorescent cells (Figure 2B). Using the early expression of GFP in insect cells, the machine learning model for the detection of infected insect cells was then calibrated to offline samples measuring the percentage of green fluorescent cells with a flow cytometer. The iLine F detected the percentage of infected cells before mCherry was detected by the flow cytometer (about 16 hours). However, detection of infection by the iLine F was still slightly delayed (about 4 hours) compared to the percentage of infection as determined by immediate early expression of eGFP manually. The eGFP was detected by flowcytometry about 5 hours after infection of the culture. This indicated that the expression of early genes preceded detection of optical changes to the cells by the microscope and the machine learning algorithm.

### Verification run of baculovirus infection at low MOI

After the machine learning model was trained using this training data set, the model was tested using new verification data sets. ExpiSf9 cells were infected with AcBac-2FL at an MOI of 0.01 at a CCI of  $1.1 \cdot 10^6$  cells/mL. The bioreactor culture was monitored by the iLine F holographic microscope (Figure 3). Using a low MOI of 0.01 would lead to multiple infection cycles before the complete culture would be infected with baculovirus.

Although online measurements showed a similar trend in measured viable cell density and total cell density compared to offline measurements, both viable and total cell densities were higher for the

online measurements (Figure 3A). Since the cell counts are based on image analysis of the flow cell with a known volume and are extensively verified by the supplier, it might be that the difference is caused by the loss of cells during the offline sample handling. When taking samples offline and measuring them manually with the iLine F, cell counts were more similar between haemocytometer and holographic cell count methods (data not included). This indicates that cells might be lost due to cell attachment, disintegration, or other reasons during sampling, diluting, and mixing of cell suspension samples from the bioreactor. The online measurement showed a clear peak in the viable cell density, whereas the manual counts showed a plateau in the viable cells followed by a decrease in viable cells. This demonstrated that due to the high resolution of online measurements, the exact moment where the cells stop growing could be determined. The viability estimated by the online microscope showed a similar trend as the manual value, although the offline measured values were higher towards the end of the cell culture when the viability dropped (Figure 3A). This could be due to the difference in measurement principle. The manual method is based on membrane permeability. The microscope method is based on alterations in the optical properties of the cell, which may occur before the membrane becomes permeable, thus resulting in lower viable cell percentages. Furthermore, as cells start to die, the morphology of the cell population becomes more heterogeneous. The increase in heterogeneity complicates cell measurements and can cause inaccuracies in both offline and online methods mainly due to cell clumping and decreasing cell circularity.

Based on offline flow cytometer measurements of low MOI infected cells, expression of green fluorescence was detected only slightly earlier than red fluorescence and this was well predicted by the iLine F. The start of mCherry expression was almost at the same moment as the start of eGFP expression, where it is expected to start 16-20 hours later as observed previously for high MOI infections. Possibly this is due to the low resolution of offline measurements with only one measurement taken when baculovirus infection started to spread throughout the cell culture. In contrast, the iLine F was able to continuously follow the progression of baculovirus infection and predict the percentage of infected insect cells in real-time, in this case also for infections that were started at a low MOI and thus requiring multiple infection cycles to infect all the cells at 93 hpi (Figure 3B). This moment coincided with the stabilization of the total cell density as measured in real-time by the iLine F. Viable cell density peaked and the cell viability started to decrease around the same moment. Slower cell growth was observed before the first infected cells were detected between 70-

80 hpi. This could be due to the delay between actual infection and the appearance of optical changes in the cell as discussed with the calibration experiments. In addition, it could also partly be due to the multiple infection cycles needed to infect all the cells. However, it was not possible to make a clear distinction between sequential infection cycles from the online measurements of infected cells. When infecting with an MOI of 0.01, <1% of the cells are expected to be initially infected. This is close to the detection limit of the system. Some measurement noise existed in the online signal of the fraction of infected cells, especially during the first 24 and final 10 hours. During cell culture, there are typically moments where cells experience high stress due to respective inoculation, apoptotic signals, budded virus production, and cell death. (Byun et al., 2015; Huang et al., 2011; Kiehl et al., 2011; Weidner et al., 2017) These events may influence cell morphology, such as average cell diameter, which in turn affects the infected cell prediction. Additional training with new datasets could improve the accuracy and sensitivity of the infected cell detection algorithm to reduce this measurement noise and possibly detect the different infection cycles during low MOI baculovirus infection processes.

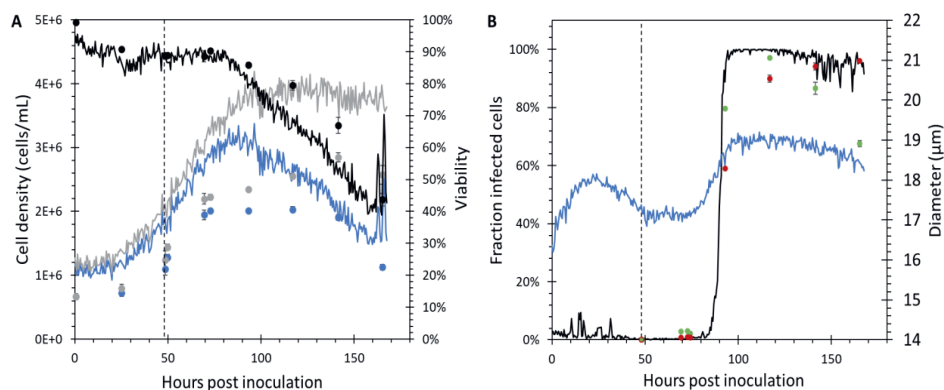


**Figure 3.** Time-course profiles for a verification bioreactor run where ExpiSf9 cells were infected with a baculovirus expressing GFP and mCherry at an MOI of 0.01. The used baculovirus construct, AcBac-2FL, contained a gene for GFP located behind the immediate early OpIE2 promoter and a mCherry gene located behind the very late polyhedrin promoter. The dashed lines indicate the moment of baculovirus infection. (A) Viable online (-) and offline (●) and total online (-) and offline (●) cell densities. Online (-) and offline (●) viable cell percentages. (B) Online predicted infected cell fraction (-), offline measurements of fraction of GFP (●) and mCherry (●) expressing cells, and average online cell diameter (-). Error bars represent duplicate measurement values.

### Online monitoring of baculovirus infection at different MOIs

Using the machine learning model calibrated on immediate early expression, ExpiSf9 cell infection was monitored for bioreactor processes where fluorescent proteins were expressed behind the very late polyhedrin promoter, which is the strongest baculovirus promoter and most commonly exploited for the expression of recombinant proteins with the BEVS (Smith et al., 1983; Van Oers et al., 2015). All bioreactor runs were monitored with the iLine F microscope to follow baculovirus infection inside the cells. MOIs between 0.01 and 10 were used to investigate differences between immediate cell infection and slower infection processes involving multiple infection cycles inside the production bioreactor.

With the iLine F, it was possible to monitor the fraction of infected cells in real time for different MOIs. For the high MOI processes, infection development was faster and 100% cell infection was reached within 9 hours after infection for MOI 10 and within 17 hours for MOI 1 (Figures 4-5 B). With the iLine F, infected cells could be detected before offline detection of fluorescent cells by flow cytometry. For the lower MOI process, infection development was slower and 100% of infected cells were detected only 45 hours after infection (Figure 3B). Real-time measurements of average cell diameters showed a similar pattern. Average cell diameters increased more rapidly for the process infected with a high MOI (Figures 4-5 B).

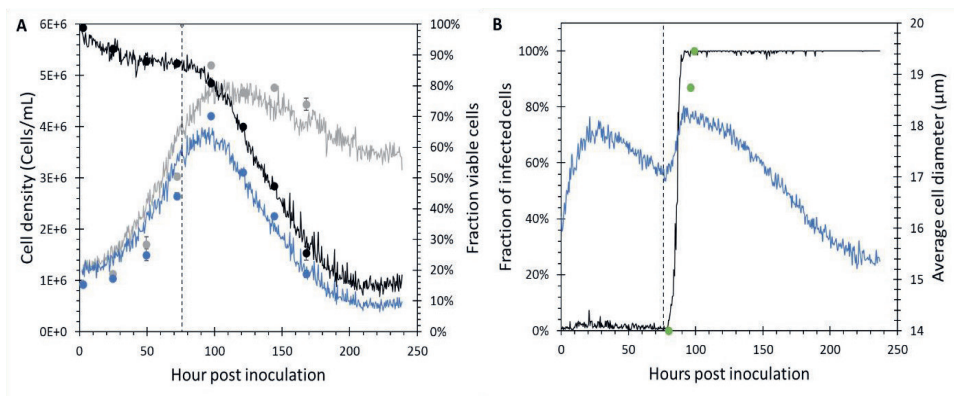


**Figure 4.** Time-course profiles of a bioreactor infected with MOI 10. ExpiSf9 cells were infected with a baculovirus expressing GFP from the very late polyhedrin promoter at an MOI of 10. The dashed lines indicate the moment of baculovirus infection. (A) Viable online (-) and offline (●) and total online (-) and offline (●) cell densities. (B) Online predicted infected cell fraction (-), offline measurements of fraction of GFP expressing cells (●), and average online cell diameter (-). Error bars represent duplicate measurement values.

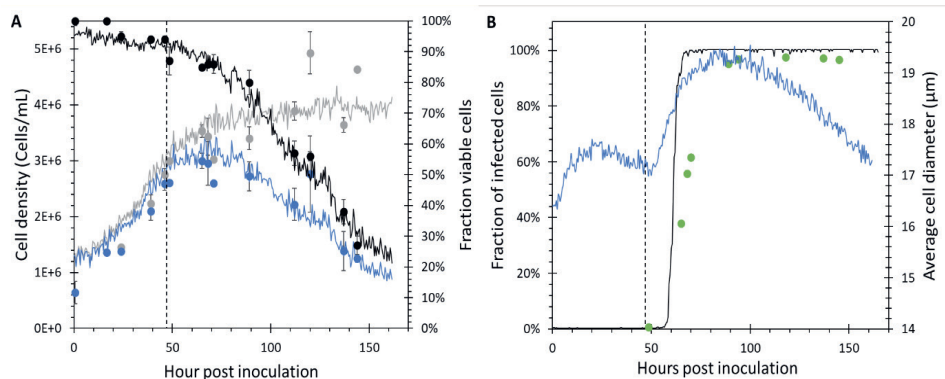


**Figure 5.** Time-course profiles of a bioreactor infected with MOI 1. ExpiSf9 cells were infected with a baculovirus expressing GFP at an MOI of 1. This baculovirus construct contained a gene for GFP located behind the very late polyhedrin promoter. The dashed lines indicate the moment of baculovirus infection. (A) Viable online (-) and offline (●) and total online (-) and offline (●) cell densities. Online (-) and offline (●) viable cell percentages. (B) Online predicted infected cell fraction (-), offline measurements of fraction of GFP expressing cells (●), and average online cell diameter (-). Error bars represent duplicate measurement values.

### Verification of baculovirus-infected insect cell culture with butyrate addition

The high resolution of the online measurements ideally would allow for spotting small process deviations that might be invisible with daily manual sampling. The sensitivity of the online microscope to spot temporary effects of butyrate addition was, therefore, investigated. Butyrate was added to improve baculovirus gene expression (Guo et al., 2010; Yovcheva et al., 2018). ExpiSf9 cells were grown until they reached a density of  $4 \cdot 10^6$  cells/mL at 72 hpi, at which point butyrate was added at a final concentration of 2mM. Immediately afterward, cells were infected with an MOI of 0.01 with a baculovirus construct containing GFP behind the polyhedrin promoter. Online measurements of viable cell density and total cell density, and online predictions of cell viability and infection state were compared to offline measurements. Offline measurements of cell densities and cell viability showed a similar trend to online measurements although offline-measured cell densities were lower (Figure 6A). The online measurements showed a clear peak in the viable cell density and a sharp switch from growth to death phase, whereas the manual counts showed a plateau in the viable cells followed by a decrease in viable cells. This demonstrates once more that due to the high resolution of online measurements, the exact moment when the cells stop growing can be determined. Together with the virus, butyrate was added to the cell culture at 72 hpi. to enhance GFP production. A temporary slowdown of cell growth was visible between 72-85 hours in the high-resolution data of

the online viable cell and total cell density measurement (Figure 6A). This is in agreement with the fact that butyrate can cause a cell-cycle arrest (Peng et al., 2007). Note that this arrest is not visible in the low-resolution offline data, showing the importance of having a high-resolution online measurement. Online monitoring of the infected percentage of cells showed a small peak around 80 hpi after which the fraction of infected cells stays slightly elevated at about 5%, followed by a sharp increase around 120 hpi (Figure 6B). Such a small peak was not expected when infecting with an MOI of 0.01. It could be caused by the diameter increase of the cells directly after butyrate addition since the prediction algorithm mainly makes predictions based on the size of the cell. This indicates the potential limitation of the current model of having a strong dependency on certain parameters when using a machine learning modelling approach. Generating additional training sets specifically aimed at breaking this correlation, for instance by changing culture osmolality, could potentially improve the accuracy of the infection prediction algorithm. The small peak around 80 hpi was not clearly visible with the offline measurements GFP fluorescence at this point is unexpected as the polyhedrin promoter becomes active at 20 hpi. (Massotte, 2003)

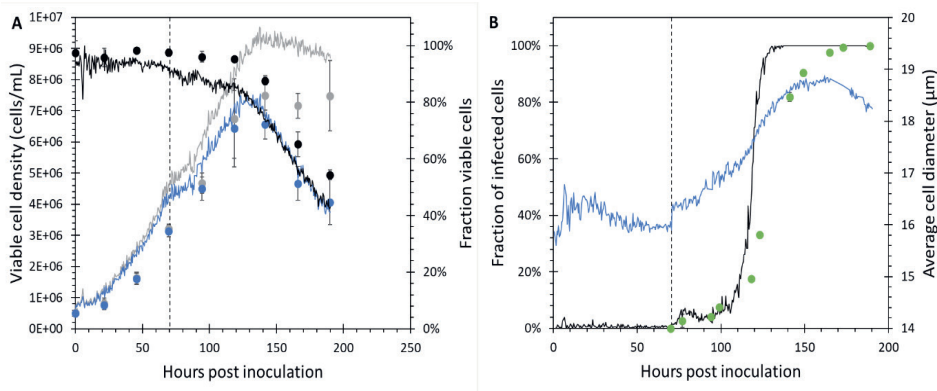


**Figure 6.** Time-course profiles of the GFP production run with butyrate addition. ExpiSf9 cells were infected with a baculovirus expressing GFP at an MOI of 0.01. This baculovirus construct contained a gene for GFP located behind the very late polyhedrin promoter. The dashed lines indicate the moment of baculovirus infection and butyrate addition. (A) Viable online (-) and offline (●) and total online (-) and offline (●) cell densities. Online (-) and offline (●) viable cell percentages. (B) Online predicted infected cell fraction (-), offline measurements of fraction of GFP expressing cells (●), and average online cell diameter (-). Error bars represent duplicate measurement values.

### Online monitoring of SARS-CoV-2 spike protein production using a low MOI

To follow the infection process for non-reporter-secreted proteins, the holographic microscope was used to monitor a SARS-CoV-2 spike protein production process (Figure 7). In contrast to reporter

proteins such as GFP and mCherry, which accumulate inside the cells (Oker-Blom et al., 1996), the S1 subunit of the SARS-CoV-2 spike protein is excreted into the medium (van Oosten et al., 2021). To produce SARS-CoV-2 S1, insect cells were infected with an MOI of 0.01 at 70 hpi. S1 was detected for the first time in the culture fluid at 140 hpi and S1 concentration continued to increase until harvest at 190 hpi. Using the holographic microscope and the previously calibrated infected cell detection algorithm, the moment of 100% infected cells was detected at 155 hpi (Figure 7B). Peak viable cell density was reached a little bit earlier, at 150 hpi (Figure 7A). The reactor content was harvested when cell viability dropped below 70%. Again, the cell densities measured by the iLine F were slightly higher and the viability slightly lower than the offline samples. For the percentage of infected cells, a small increase could be observed at about 10 hours after infection (80 hpi), which might represent the start of the second infection cycle. Next, the infection increased to 100% between 100 and 150 hpi (30-80 hours after infection) for a low MOI process. About 30 hours after the infection percentage started to rise, at 118 hpi, the secretion of the spike protein started, which is within the range expected for very late gene expression (Ramachandran et al., 2001).

The ideal TOH depends on product concentration and product quality. Since both parameters are relatively difficult to measure in real-time, the online measured viability, diameter, and percentage of infected cells can be used as indicators for determining the best moment of harvest. Low viability can affect protein quality, as proteases are released from dead cells (Pyle et al., 1995) (Heitz et al., 1997). Harvesting too early, however, can negatively affect product yield. Sander et al. (2007) already demonstrated that peak protein production was reached one or two days after the point of maximum average cell diameter, showing diameter to be a good indicator for determining optimal harvest time in terms of peak protein yield (Sander & Harrysson, 2007). The combination of a real-time percentage of infected cells, average cell diameter, and cell viability can present a clearer picture of the state of the cell culture to determine the optimal moment of harvest. As all these parameters are measured in real-time, trends can be spotted faster, and bioreactor harvest can commence instantaneously once the desired parameter criteria are met. This removes the need for offline sampling, reducing delays and inaccuracies associated with offline sample handling. Furthermore, monitoring the progress of infection is crucial to spot process deviations early on and determine the exact moment when all cells have been infected. In case of a delay, process deviations are spotted later by offline measurements, and the timings of process decisions are sub-optimal. For low MOI processes, this delay affects robustness and reproducibility to a greater extent. Since several infection

cycles are necessary to reach 100% infected cells, the time to reach 100% infection can be significantly influenced by relatively small deviations at the moment of infection, for example in the titer of the baculovirus stock and amount of virus stock added. This makes low MOI processes generally less predictable. Being able to consistently execute low MOI processes with high reproducibility is highly advantageous from a process development point of view. Small virus stocks can be used, avoiding the need for a separate large-scale virus production run and subsequent virus titer determination. This leads to considerable time savings at the industrial production scale (Maranga et al., 2003a). Such time savings are of utmost importance to speed up process development, especially when a rapid response to pandemic outbreaks, such as the recent SARS-CoV-2 outbreak, is needed. This study shows that with a limited training set (limited number of process conditions and virus constructs) the microscope and machine learning algorithm can predict cell numbers, viability, and infection percentage for different viral constructs, MOIs, and butyrate addition. However, the model heavily relies on the increase in cell size for predicting the infected cell percentage. This could be a limitation in case process conditions are introduced that cause changes in cell size. Further training of the model using such conditions could further improve the accuracy and applicability of the model. The high resolution of the online measurements enables the detection of small events or process deviations that would have otherwise been missed by manual sampling. Detecting these deviations gives more insight into the state of the culture and could aid in process understanding and process control.

3

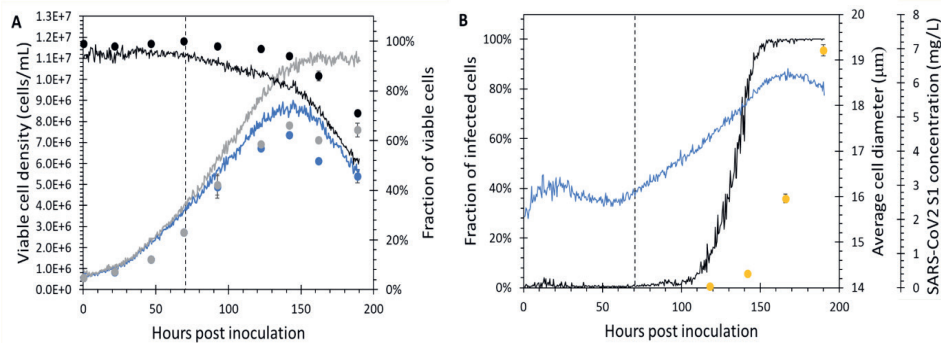


**Figure 7.** Time-course profiles of a SARS-CoV-2 S1 production run. ExpiSf9 cells were infected with a baculovirus expressing SARS-CoV-2 S1 subunits at an MOI of 0.01. The gene for expression of SARS-CoV-2 S1 was located behind the very late polyhedrin promoter. The dashed lines indicate the moment of baculovirus infection and butyrate addition. (A) Viable online (-) and offline (●) and total online (-) and offline (●) cell densities. Online (-) and offline (●) viable cell percentages. (B) Online predicted infected cell fraction (-), average online cell diameter (-), and offline measured SARS-CoV-2 S1 concentrations (●). Error bars represent duplicate measurement values.

### Conclusion

Online double differential digital holographic microscopy (D3HM) and machine learning modeling was used for real-time monitoring of insect cell proliferation and baculovirus infection in bioreactors. Training and verification data sets were generated using a purpose-built baculovirus construct. Calibration of the machine learning model was based on infection with a baculovirus that had eGFP behind an early promoter. With the online microscope, it was possible to accurately monitor viable and total cell densities, viable cell percentages, and insect cell infection states for a variety of baculovirus constructs, MOIs, and produced proteins based on this calibration data set. Moreover, the high resolution of the online measurements made it possible to accurately determine changes in the culture like the exact moment of peak cell densities and detection of growth arrest due to butyrate addition. Accurate online monitoring of bioreactor cell cultures with high resolution is important to enhance process understanding and may aid in the timing of important process steps such as the time of infection or the time of harvest. Each newly generated data set can be used to improve the machine learning algorithms and can be used retroactively by re-calculating old data sets. The variety of cell parameters computed by the microscope potentially hides a wealth of information on the biological state of the cells. Interpreting this information to obtain further insight into the state of the cell culture, and in real-time, is a future challenge.

## Acknowledgments

We thank Els Roode, Gwen Nowee, Fred van den End, and Wendy Evers (Wageningen University & Research) for their technical assistance. We also acknowledge Jérémie Baurbau, Jan van Hauwermeieren, Nicolas Janssen, Laurent Desmecht, Willem Hoérée, and Thomas Guyon (Ovizio) for their assistance and advice in using the iLine F. We thank Tom van Arragon and Timo Keijzer (Getinge) for their bioreactor support. This publication is part of the BACFREE project with project number 16762 of the Open Technology Programme which is (partly) financed by the Dutch Research Council (NWO). Damien Cabosart and Laurent Desmecht are employees of Ovizio.

4

# Chapter 4

---

## Novel temperature-sensitive baculovirus expression vector system with upstream reduction of baculovirus contaminants (BacFree)

---

Jort J. Altenburg<sup>1\*</sup>, Linda van Oosten<sup>2\*</sup>, Gwen Nowee<sup>2</sup>, Tessa Neef<sup>1</sup>, Thomas Rouw<sup>1</sup>, Vivian I.P. Tegelbeckers<sup>1</sup>, Jans van der Heijden<sup>2</sup>, René H. Wijffels<sup>1</sup>, Monique M. van Oers<sup>2</sup>, Dirk E. Martens<sup>1</sup>, Gorben P. Pijlman<sup>2</sup>

<sup>1</sup>Bioprocess Engineering, Wageningen University & Research, The Netherlands

<sup>2</sup>Laboratory of Virology, Wageningen University & Research, The Netherlands

\*equal contribution

*The European patent application 'BacFree' has been filed (Applicant nr. 23170183.0)*

### Abstract

The baculovirus expression vector system (BEVS) is a widely used platform for the production of virus-like particles (VLPs). It relies on the infection of insect cells with budded baculoviruses (BV) expressing the gene(s) of interest. However, separating the VLPs from the contaminating budded baculovirus particles during downstream processing is complex, as both VLP and BV have similar physical properties. To address this key issue, we have developed a baculovirus contaminant-free (BacFree) BEVS that utilizes a temperature-sensitive (TS) baculovirus strain with a mutation in *gp41* mutation to avoid BV contaminant production at the elevated, non-permissive temperature. The TS virus was constructed by expressing *gp41<sup>ts</sup>* from the very late p10 promoter, whereas the original *gp41* gene was deleted from the baculovirus genome. At standard culturing conditions (27°C), the TS virus could be amplified to high viral titers. In contrast, at elevated temperatures ( $\geq 34^\circ\text{C}$ ), the BV contaminant production was strongly inhibited. The production of chikungunya VLPs was retained at elevated temperatures. This BacFree strategy was successfully scaled up to stirred-tank bioreactors, where at least a 100-fold reduction in contaminating BV titers was achieved for both high multiplicity of infection (MOI) and low MOI infection strategies. For the low MOI strategy, real-time online monitoring of the cell diameter using double-differential digital holographic microscopy was an effective tool for determining the optimal timing of the temperature shift from 27° to 34°C. These findings are the first demonstration that a TS baculovirus can effectively reduce BV contamination while maintaining VLP productivity. The BacFree system is compatible with most commercial baculovirus expression plasmids and insect cell lines. Moreover, BacFree is scalable to stirred-tank bioreactors and suitable for high MOI and low MOI processes. The development of BacFree marks a significant advancement in the field of VLP production for large-scale manufacturing of VLP-based vaccines and therapeutics.

## Introduction

The baculovirus expression vector system (BEVS) has been a prominent platform for recombinant protein production for many years (Possee et al., 2020; Targovnik et al., 2021; Van Oers et al., 2015). It provides a safe, scalable production platform for recombinant proteins, protein complexes, virus-like particle (VLP) vaccines, and adeno-associated virus (AAV) gene therapy vectors. The baculovirus *Autographa californica* multiple nucleopolyhedrovirus (AcMNPV) is commonly used as a viral expression vector in combination with *Spodoptera frugiperda* (e.g., Sf9) or *Trichoplusia ni* insect cells (Hi5). An important aspect of this system is that recombinant baculoviruses, carrying the gene(s) of interest behind the strong baculoviral polyhedrin (polh) or p10 promoter can be rapidly constructed, making the system well-suited for vaccine development. Recombinant proteins are expressed at high levels upon infection of insect cells. Especially VLPs are promising protein-based vaccine candidates since their immunogenicity is typically higher than peptide- or subunit-based vaccines (Metz, Martina, et al., 2013; Mohsen & Bachmann, 2022).

Besides expression of the gene of interest in the very late phase of infection, the baculovirus-infected cells produce large amounts of new budded viruses (BVs). The BVs are enveloped nucleocapsid particles containing a single copy of the baculoviral double-stranded DNA genome. Each cell will produce many new infectious BVs, resulting in up to  $10^9$  infectious BV per milliliter of culture fluid. BVs are regarded as unwanted contaminants in the final product, especially when it concerns pharmaceutical products or vaccines for human use, therefore these BVs have to be removed. However, the physical properties such as size, density, and charge of BVs are often similar to those of secreted (enveloped) VLPs, which makes downstream purification challenging (Cervera et al., 2019; Cox, 2021; González-Domínguez et al., 2020; Vicente et al., 2011) and often results in decreased product yields.

A solution to this BV contamination problem could be to prevent the formation of BVs during the production phase. A baculovirus-free expression system has been constructed before by deletion of the essential baculovirus genes *gp64* (Chaves et al., 2018), *vp80* (Marek et al., 2011), or *lef-5* (Hu et al., 2023). In these systems, a deletion of a specific baculovirus gene from the AcMNPV genome results in the inability of BV production in conventional insect cell lines, while very late gene expression from polh and p10 promoters is largely unaffected. Amplification of BV seeds needed for infection in the production reactor is therefore achieved by complementing the deleted protein *in trans*. The downside of such a system is that two different cell lines are needed for BV production;

the transgenic cell (for trans-complementation of the deleted gene) and the production cell line for the expression of the gene of interest. A potential problem is the instability of transgene expression and the ability of the baculovirus to regain the deleted gene from the transgenic cell by recombination (Hu et al., 2023). Recently, a CRISPR-Cas-based approach was developed to mediate this gene disruption and this approach relies on a CRISPR-Cas-expressing cell line (Bruder & Aucoin, 2023). This approach also requires two cell lines and the production cell line needs to be infected with a high multiplicity of infection (MOI) for efficient VLP production, which means that relatively large volumes of BV seeds are required.

Here we propose to use a temperature-sensitive (TS) baculovirus expression vector for the production of VLPs, in which the production of BV contaminants can be switched off by an elevation in production temperature. A single TS baculovirus would provide for both BV amplification and VLP production in the same cell line (e.g., standard Sf9). This approach eliminates the need for stable cell line development and provides flexibility in the choice of cell lines and MOI.

Several baculovirus TS mutants have previously been isolated and characterized after mutagenesis with N-methyl-N-nitro-N-nitrosoguanidine or 5-Bromodeoxyuridine (Brown et al., 1979; Lee & Miller, 1979; Partington et al., 1990). These TS mutants were useful for fundamental research on baculovirus replication and creation of the genetic map of AcMNPV. Most baculovirus TS mutants appeared to be defective in early gene expression (Miller et al., 1983; Ribeiro et al., 1994), DNA replication (Gordon & Carstens, 1984), or very-late gene expression (Carstens et al., 1994; McLachlin & Miller, 1994; Partington et al., 1990). These TS baculoviruses would not result in significant protein expression from very late baculovirus promoters, making them unsuited for implementation into the BEVS.

Interestingly, however, a particular AcMNPV mutant, tsB1074, was described to only affect BV secretion, while polyhedrin was still produced in the very late phase of infection (Lee & Miller, 1979). Complementation analyses of tsB1074 revealed a point mutation in *ac80*, the baculovirus core gene encoding GP41 (Olszewski & Miller, 1997). GP41 is a 45 kDa protein of *Baculoviridae* that is O-glycosylated and oligomeric. It is known as the tegument protein of occlusion-derived viruses (ODV) but is also involved in the nuclear export of nucleocapsids on their way to the plasma membrane, where BVs leave the cell by budding. GP41 is essential for BV secretion but is dispensable for viral DNA replication or very-late gene expression (Li et al., 2018; Olszewski & Miller, 1997). The

tsB1074 mutant is characterized by an isoleucine-to-threonine mutation in residue 317 (I317T) of GP41. BV production appeared normal at 23°C (permissive temperature) but a single-cell infection phenotype was observed at 33°C (non-permissive temperature) (Lee & Miller, 1979; Olszewski & Miller, 1997).

In this research, we investigated if the TS mutation I317T in GP41 could form the basis for a BEVS with a temperature-inducible shutdown of BV production to aid the production of chikungunya enveloped virus-like particles (CHIKV VLPs) (Metz, Gardner, et al., 2013). Screening for the optimal switch temperature was done in a mini-bioreactor system. Next, the process was scaled-up to stirred tank bioreactors. Finally, the process was translated to a low MOI infection process, and the optimal time for the temperature switch was determined by real-time online monitoring of insect cell diameter using double-differential digital holographic microscopy.

## Materials & Methods

### Cell lines

*Spodoptera frugiperda* (Sf) insect cells were maintained in 250 mL shake flasks shaking at 110 rpm at 27°C. Sf9 cells were cultured in Sf900II serum-free medium (Gibco) supplemented with 50 µg/mL gentamycin. ExpiSf9 cells (ThermoFisher Scientific) were grown in ExpiSf chemically defined medium (Gibco) supplemented with 50 µg/mL gentamycin.

### GP41 plasmid design and construction

The *gp41* coding sequence containing the I317T mutation (ATA to ACA) and flanking XhoI and NheI restriction sites was ordered as a synthetic gene (Integrated DNA technologies). The DNA fragment was cloned into pJET1.2/blunt vector using the CloneJET cloning kit (ThermoFisher Scientific) and was confirmed by Sanger sequencing. pFastBacDual (pFBD, Gibco™) plasmids were constructed containing the *gp41* or *gp41<sup>I317T</sup>* sequence behind the p10 promoter as XhoI/NheI fragment. The chikungunya virus structural cassette (CHIKV str.) (Metz, Gardner, et al., 2013) was inserted downstream of the polyhedrin (ph) promoter as BamHI/XbaI fragment.

An N-terminal HA tag (MYPYDVPDYA) was added to *gp41* by digestion of pFBD-*gp41*-CHIKV str. with XmaI followed by plasmid dephosphorylation with CIAP. Two 5' phosphorylated oligos containing the HA-tag and part of the *gp41* N-terminus (Table 1) were mixed in equal molarity, melted at 95°C for 15 minutes, and slowly cooled to room temperature before ligation with the digested vector. Finally, all pFBD plasmids were confirmed by Sanger sequencing.

**Table 1.** Primers used in this research.

Primer	Sequence (5' - 3')
	Constructing GP41 HA virus
HA tag-F	CCGGGgccaccatgTACCCATACGACGTACCAGATTACGCTACAGATGAACGTGGCAATTTT ATTACAACACCCCTCCGCCGCTGAGGTATCCCTCTAATCCGGCAACGGCCATATTACC AGCGCGAAACTTACAACGCGC
HA tag-R	CCGGGCGCGTTGTAAGTTTGC GCGCTGGTGAATATGGCCGTTGCCGATTAGAGGGAT ACCTCAGCGCGGAGGGGTGTGTAATAAAAATTGCCACGTTTCATCTGTAGCGTAATC TGGTACGTCGTATGGGTACATGGTGCC

### Recombinant baculovirus construction

The AcMNPV bacmid with deletion of *gp41* (Ac $\Delta$ gp41) was received from Li. et al (2018). In this bacmid, a large part of the *gp41* open reading frame (including residue 317) had been replaced by a chloramphenicol acetyltransferase (*cat*) gene, and the gene coding for the enhanced green fluorescent protein (eGFP) downstream the heat-shock protein 70 (*hsp70*) promoter. The pFBD plasmids were inserted into the Tn7 site at the *polh* locus of the Ac $\Delta$ gp41 bacmid by bac-to-bac transposition (ThermoFisher Scientific). Recombinant bacmids were purified by alkaline lysis followed by isopropanol precipitation.

### Transfection and infection assays

The purified bacmids were transfected into Sf9 insect cells by ExpressS2TR transfection reagent (ExpressS2ion Technologies). Ten microliters purified bacmid and 5  $\mu$ l ExpressSTR transfection reagent were mixed with 90  $\mu$ l Sf900II medium, incubated for 15-20 minutes at room temperature, and added to the medium of ~60% confluent Sf9 cells. The medium containing the transfection reagent was replaced with new Sf900II medium with 50  $\mu$ g/mL gentamycin at 4 hours post-transfection. The clarified supernatant was harvested at 6-7 days post-transfection and used to infect healthy Sf9 cells. Virus stocks were further amplified on Sf9 cells at 27°C and were clarified and stored at 4°C after harvest. The transfection and infections were monitored by fluorescence microscopy.

### Baculovirus quantification

Two methods were applied for the quantification of infectious BV titers. Infectious BV titers were determined by end-point dilution assay (EPDA) at 27°C on Sf9-ET cells grown in Sf900II with 50  $\mu$ g/mL G418 and 5% FBS (Hopkins & Esposito, 2009), or on ExpiSf9 cells in CDM. The 50%

endpoint titer was calculated via the Reed and Muench method and is expressed as 50% Tissue Culture Infective Dose per mL (TCID<sub>50</sub>/mL). Alternatively, BV titers were determined using a flow cytometric titration assay based on the detection of the baculovirus envelope protein GP64 (ThermoFisher Scientific) and expressed as infectious viral particles per mL (ivp/mL). Values were read out with an Accuri BD C6 flow cytometer (BD Biosciences).

#### Viral infection experiments at elevated temperatures

Temperature-sensitivity of the viruses was assessed by infections with two different MOI at elevated temperatures. Sf9 cells were mixed with the virus at MOI=1 or at low MOI (0.01). The virus was mixed with the cells and aliquoted into a 60-wells microtiter plate. Triplicate plates were incubated at 27°C, 30°C, and 33°C. Viral infection was monitored by fluorescence microscopy at 96 hours post-infection (hpi).

#### Growth curves at elevated temperature

Growth curves were constructed of the wild type and TS virus at low and elevated temperatures in both monolayer cultures and suspension cultures. Sf9 cells were diluted in Sf900II supplemented with 5% FBS. The monolayers were seeded in 24-well plates containing  $0.25 \times 10^6$  cells per well, whereas suspension flasks contained 15 mL of  $1.0 \times 10^6$  cells/mL. Cells were infected with MOI=1 TCID<sub>50</sub>/cell and either kept at 27°C or shifted to 33°C at 4 hpi. Wells and flasks were sampled daily and BV titers in the clarified culture fluid were determined by end-point dilution assay.

#### Micro-bioreactor runs

The infection kinetics at a range of temperatures was screened in a high-throughput micro-bioreactor cultivation system (microMatrix) (Getinge Applikon Biotechnologies, Wiegmann et al., 2020). ExpiSf9 cells were diluted to  $1.0 \times 10^6$  cells/mL in ExpiSF CDM with 50 µg/mL gentamycin and infected with AcWT-VLP or AcTS-VLP virus at MOI=0.01 or MOI=0.3. Cells were incubated at 27°C for 30-45 minutes before aliquoting 5 mL per well of the 24-well micro-bioreactor cassette (Getinge Applikon Biotechnologies). The reactor was run for 96 hours shaking at 250 rpm, and the pH and DO were not controlled. The incubation temperature was set for each column of wells with a temperature difference between adjacent wells of 1°C and an accuracy of  $\pm 0.1^\circ\text{C}$ . Runs were performed with a temperature range of 22-27°C, 29-34°C, or 30-35°C.

The cell concentration at harvest was determined using the Countess II automated cell counter (ThermoFisher Scientific). The percentage of infected cells was measured by flow cytometry in the

BD Accuri C6 flow cytometer based on GFP expression (Green channel 553/30 nm). Data were analyzed in FlowJo, where single cells and (auto)fluorescence were gated with uninfected ExpiSF9 cells.

### Stirred-tank bioreactor cell cultures

ExpiSF9 cells were grown in 0.5 L miniBio or 3.0 L glass reactor vessels (Gefinge) controlled by myControl bioreactor controllers (Gefinge). The working volume of each reactor vessel was 0.3-2.0 L. Reactors were inoculated at target starting densities of  $0.5-1.0 \times 10^6$  viable cells/mL. The pH in the culture fluid was not controlled but was maintained by the buffering capacity of the medium and fluctuated between pH 5.7-6.1. The dissolved oxygen concentration was controlled at 30% of air saturation using Lumisens optical dissolved oxygen sensors (Gefinge) and sparging of pure oxygen through open pipe spargers. In addition, a constant headspace aeration rate of 0.01 vvm air was applied. Agitation with marine impellers was set to 266-600 rpm by keeping the tip speed constant among the different reactor sizes.

Cells were counted by trypan blue exclusion using a TC20 Automated Cell Counter (Bio-Rad) or by manual counting using DHC-F01 cell counting chambers (INCYTO). Online measurements of viable and total cell density, viability, and infected cells were performed by differential digital holographic microscopy (DDHM) using iLine F holographic microscopes (OVIZIO). Data acquisition and quantitative data analysis were performed using OsOne software (OVIZIO). Infected cells were visualized by expression of GFP detected by a C6 Plus Flow Cytometer (BD Accuri).

### eGFP quantification

The concentration of eGFP in a sample in the cell pellet and culture fluid was determined by fluorescence measurements relative to that of an eGFP standard. Samples were diluted 1 to 100 times with lysis buffer (containing 500 mM NaCl, 50 mM Tris(hydroxymethyl)methylamine (TRIS) and 0.1% Triton X-100, adjusted to pH 8 with HCl) according to their expected concentration, to ensure an appropriate fit within the calibration curve. The standard solution was prepared from *Aequorea victoria* His-eGFP (Chromotek) diluted to a final concentration of 10 ng/ $\mu$ L. A calibration curve was made from 0 to 4 ng/ $\mu$ L eGFP, with intervals of 0.8 ng/ $\mu$ L. Hundred microliter samples were measured in duplicate in a 96-well plate and fluorescence was determined using an FLx800 microplate reader (BioTek) with a 485/528 excitation/emission filter. For each sample, the total and extracellular eGFP concentrations were measured and quantified using the calibration curve. The internal eGFP concentration was determined by subtracting the external from the total eGFP.

### SDS-PAGE and western blot immunodetection

Cell suspension samples were pelleted by centrifugation for 5 minutes at 9000 rpm. The culture fluid was precipitated by the addition of 3 volumes of acetone and incubation at -20°C for 1 hour, followed by centrifugation for 10 minutes at 4000 rpm. The cell pellet and precipitated medium pellet were dissolved in 1xPBS with cOmplete™ protease inhibitor (Roche) and mixed with reducing SDS-PAGE loading buffer containing 10% β-mercaptoethanol or 50 mM DTT. Samples were heated for 10 minutes at 95°C before analyses on SDS-PAGE. As a positive control for CHIKV VLP production, an SDS-PAGE sample was prepared with CHIKV VLP from human HEK293 cells (The Native Antigen Company) diluted to 0.037 µg/µL in 1x PBS. Proteins in the SDS-PAGE gel were visualized by UV photography (stain-free gels, BioRad).

The proteins were subsequently transferred to a PVDF membrane, followed by immunodetection. Membranes were blocked with 1% skim milk powder in 1x PBS with 0.05% Tween-20 (PBS-T). The primary antibody was diluted in 1% milk powder in PBS-T. CHIKV VLPs were detected by staining for the E2 protein (E2dTm, Rabbit serum, 1:1000-1:5000). Baculovirus major capsid protein VP39 was stained with monoclonal Anti-VP39 (1:1500, from mouse). The Alkaline-phosphatase conjugated secondary antibodies Anti-rabbit IgG (Dako) or Anti-mouse IgG (Sigma-Aldrich) were diluted 1:2500 in PBS-T. Membranes were washed with PBS-T in between incubation steps and immunodetection was visualized with NBT/BCIP colorimetric stain (Roche).

## Results

### Construction of gp41 repair and TS mutant baculovirus expressing CHIKV VLPs

The I317T mutation in baculovirus GP41 has been identified to result in a temperature-sensitive virus for which BV production occurs at 23°C but is severely restricted at 33°C (Olszewski & Miller, 1997). We first verified this previous research by constructing a proof-of-concept TS baculovirus and determining its permissive and non-permissive temperatures. An AcMNPV bacmid was used in which the native *gp41* gene (including the codon for residue 317) was deleted (AcΔgp41). A GFP marker gene under control of the *hsp70* promoter is present at the original *gp41* locus (Li et al., 2018). The *gp41* gene expression was rescued from the very-late p10 promoter and the VLP cassette from CHIKV was expressed from the very-late polh promoter at the polh locus (AcWT-VLP, Figure a). The TS mutant was created in a similar way, but with a single point mutation in *gp41* that results in an I317T mutation (AcTS-VLP, Figure b). A transfection-infection experiment of the bacmids confirmed that AcΔgp41 bacmid could not spread after transfection, resulting in a single-cell infection

phenotype. Both wildtype and I317T mutant spread from cell-to-cell at 27°C (Figure c) and produced similar infectious BV titers of nearly  $10^8$  TCID<sub>50</sub>/ml (Figure d).

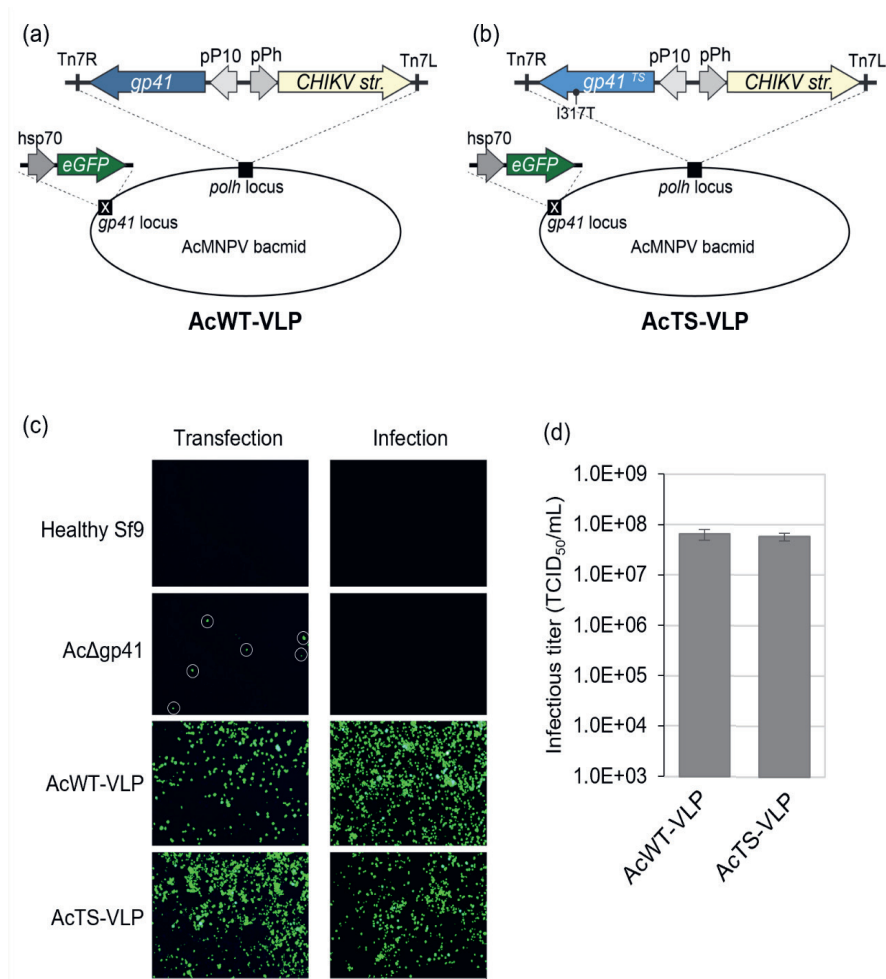


**Figure 1.** Construction of GP41 temperature-sensitive baculovirus vector expressing chikungunya virus-like particles. A bacmid containing a deletion in *gp41* (*AcΔgp41*) expressed GFP from the *hsp70* promoter served as the virus backbone. GP41 expression was rescued from the *p10* promoter (*pP10*) and was N-terminally HA-tagged. Both wildtype *gp41* (a) and GP41 containing the I317T TS mutation (b) were constructed. The CHIKV S27 structural cassette was expressed from the polyhedrin promoter (*pPh*). (c) Recombinant bacmids were transfected into Sf9 cells and the virus spread was monitored after transfection and secondary infection at 27°C. A single-cell infection phenotype is indicated with white circles. (d) Infectious budded virus production at 3 dpi after a high-MOI infection at 27°C.

### Temperature-sensitivity of GP41 mutant

Next, it was confirmed that the I317T mutant of *gp41*, expressed from a non-native locus and promoter, is indeed a temperature-sensitive baculovirus. Sf9 cells were infected with both viruses (AcWT-VLP and AcTS-VLP) at MOI 1 TCID<sub>50</sub>/cell and low MOI (0.01 TCID<sub>50</sub>/cell) at 27°C, 30°C, and 33°C. All cells show GFP fluorescence expressed from the *hsp70* promoter at elevated temperatures after a high MOI infection, indicating efficient baculovirus infection (Figure 22a). As expected, after a low MOI infection only AcWT-VLP could successfully spread at all tested temperatures. In contrast, the TS mutant could spread at 27°C, less efficiently at 30°C, and only single cells were infected at 33°C (Figure 22b).

Next, growth curve analyses were performed on adherent Sf9 cells at 27°C and the presumed non-permissive temperature of 33°C (Figure 22c). AcWT-VLP was not affected by increased incubation temperature and replicated to similar BV titers at 33°C as at 27°C (Figure 22c, grey lines). The virus production of AcTS-VLP was somewhat slower at 27°C but eventually reached similar titers as the WT control virus (Figure 2c, blue dotted line). In contrast, at 33°C a large reduction in BV titers was observed for the TS mutant. BV production was only measured from 2 dpi onwards and plateaued at 10<sup>5</sup> TCID<sub>50</sub>/mL, which corresponds to a BV titer reduction of approximately 2.5 log scales. A similar experiment was performed in 250 mL shake flasks with Sf9 suspension cells (Figure 22d). Although not as pronounced, possibly by variations in incubator temperatures or infection kinetics, the BV titers of AcTS-VLP also plateaued at 2 dpi with 10<sup>6</sup> TCID<sub>50</sub>/mL remaining. In short, infectious BV secretion in the culture fluid could be reduced with several log-scales at 33°C but was not completely inhibited.

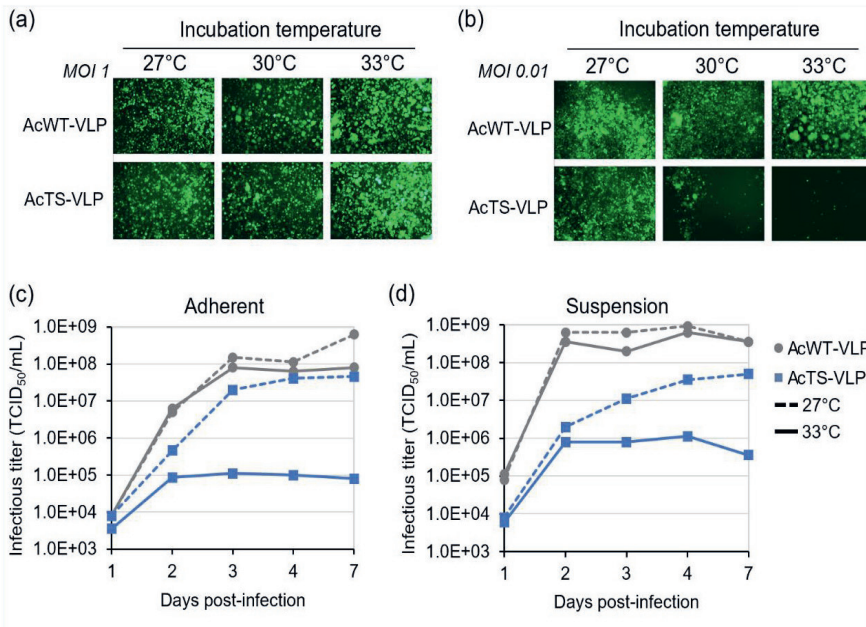


**Figure 22.** Temperature-sensitive phenotype of the baculovirus GP41 I317T mutant at 33°C. (a) All cells were infected after MOI 1 TCID<sub>50</sub>/cell infections with AcWT/TS-VLP incubated at 27°C, 30°C, or 33°C. (b) Low MOI (0.01 TCID<sub>50</sub>/cell) infections showed a reduced viral spread of AcTS-VLP at 33°C and a single-cell infection phenotype at 33°C. (c-d) Temperature sensitivity was confirmed by growth curve analysis on Sf9 cells incubated at 27°C or 33°C. Sf9 cells were either grown as adherent cells in a 6-well plate (c) or as suspension cells in 250 mL shake flasks (d) and were infected with AcWT-VLP or AcTS-VLP at MOI 1 TCID<sub>50</sub>/cell.

### Screening for permissive and non-permissive temperatures

The GP41<sup>TS</sup> mutant tsB1074 was selected based on viral spread at 23°C and single-cell infection phenotype at 33°C but the exact switching temperature was not studied (Lee & Miller, 1979; Olszewski & Miller, 1997). We performed a microMatrix micro bioreactor screening experiment to find the optimal permissive and non-permissive temperatures for the AcTS-VLP virus. ExpiSf9 cells ( $1.0 \times 10^6$  cells/mL) were infected at MOI 0.01 with AcWT-VLP or AcTS-VLP at 27°C for 30 minutes. Infected cells were aliquoted in duplicate into the wells of the microMatrix and, in two runs, incubated at low temperatures ( $22-27^\circ\text{C} \pm 0.1^\circ\text{C}$ ) or elevated temperatures ( $30-35^\circ\text{C} \pm 0.1^\circ\text{C}$ ) for 96 hours. AcWT-VLP retained efficient BV production within the entire temperature range of 22-34°C (Figure a, grey bars). However, past this endpoint of 35°C, BV titers declined rapidly most likely because this temperature is too high for efficient baculovirus replication in non-temperature adapted ExpiSf9 cells. The optimal BV production by the GP41 TS mutant ( $>10^8$  TCID<sub>50</sub>/mL) was found at

26°C, 27°C, and 30°C (28°C and 29°C not measured) (Figure 3a, blue bars). At 33°C, 34°C, and 35°C the BV concentration did not reach the detection limit of  $1.0 \times 10^3$  TCID<sub>50</sub>/mL. Interestingly, BV production was also slightly attenuated at reduced temperatures of 22-23°C. In conclusion, the temperature switch resulting in strongly reduced BV secretion was steep and within the small temperature range of 31-33°C.

The infection of AcTS-VLP was repeated at elevated temperatures using a slightly higher MOI (0.3 TCID<sub>50</sub>/cell) and with  $1.0 \times 10^6$  ExpiSf9 cells/mL. Replicate infections of AcTS-VLP were incubated in the microMatrix wells during multiple runs at either 29-34°C or 30-35°C. The GP41<sup>TS</sup> mutant was severely attenuated at 33°C, the temperature at which a measurable but reduced BV concentration of  $10^5$  TCID<sub>50</sub>/mL was found (Figure b). BV secretion was fully inhibited at 33-34°C ( $<10^3$  TCID<sub>50</sub>/mL). The attenuated or inhibited viral spread at  $\geq 33^\circ\text{C}$  was also reflected in increased total cell density (Figure c) and a reduced fraction of infected cells (Figure d). The physical reduction in BV contaminants at  $\geq 33^\circ\text{C}$  was confirmed by western blot analysis, which showed a lack of baculovirus capsid protein VP39 in the culture fluid (Figure e). This temperature effect was not observed for the control virus AcWT-VLP, which efficiently infected all cells and produced similar levels of BVs at all temperatures (Supplementary Figure S1).

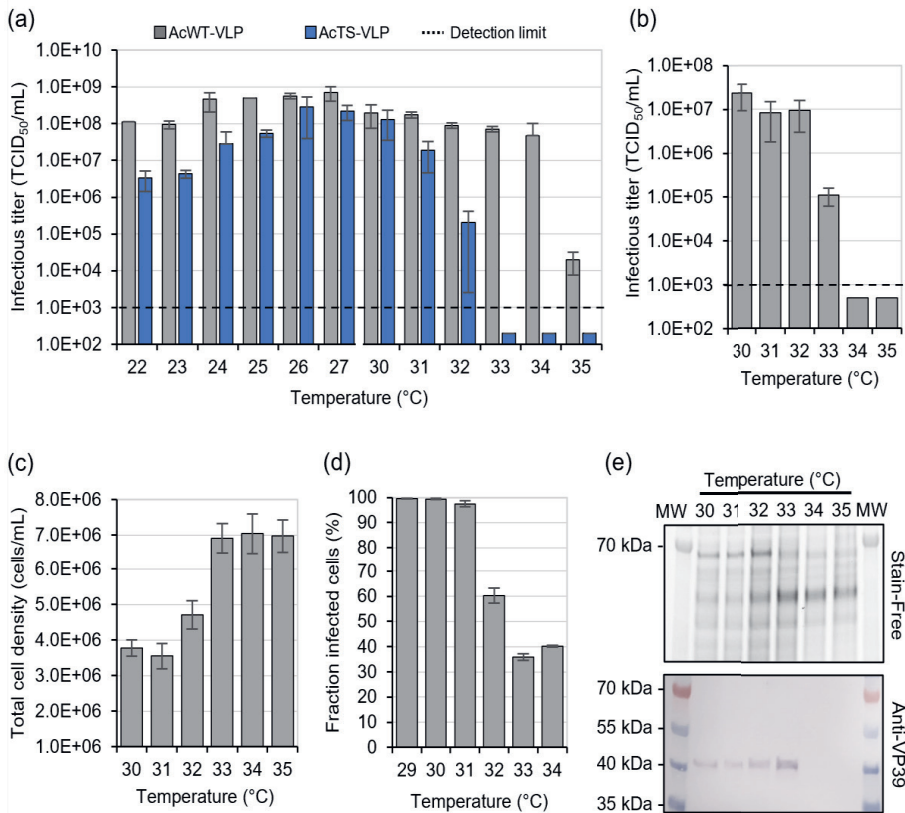


**Figure 3.** Microbioreactor characterization of GP41 TS mutant in suspension ExpiSf9 cells. (a) Infectious budded virus titers of WT and TS mutant after infection at MOI=0.01 were measured at 96 hpi (titrated at 27°C). The bar graph shows the average of two replicates. (b-d) ExpiSf9 cells were infected with the TS mutant at MOI=0.3. At 96 hpi, infectious BV titer (b), total cell density (c), and the percentage of infected cells (d) were determined. The average is shown as bar graphs +/- stdev. The cultures were sampled at 96 hpi and analyzed on a denaturing SDS-PAGE (e). The culture fluid was analyzed on a protein gel that was visualized by UV photography (stain-free) and western blot immunodetection against AcMNPV VP39 (anti-VP39). MW: Molecular Weight marker.

The AcTS-VLP virus expresses the structural cassette of CHIKV from the strong polh promoter. This cassette encodes the structural proteins capsid, E3, E2, 6K, and E1 that self-assemble into secreted, enveloped VLPs (Figure 4a) (Metz, Gardner, et al., 2013). The CHIKV VLP production of AcTS-VLP was measured by western blot immunodetection for E2 of the micro bioreactor samples (Figure 4 b-c). Immunodetection showed that E2 is produced in the cells (Figure 4b) and secreted in the culture fluid as VLPs (Figure 4c) at all temperatures. The elevated incubation

temperatures of  $\geq 33^{\circ}\text{C}$  resulted in a fainter band of E2 compared to lower temperatures, possibly caused by the low MOI of 0.3 and attenuated viral spread.

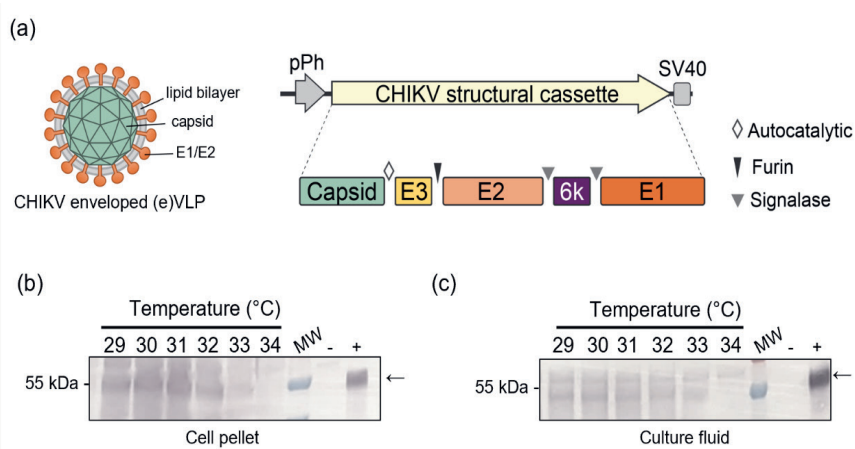


**Figure 4.** CHIKV VLP protein production by AcTS-VLP in the micro bioreactor screening experiment. AcTS-VLP expresses the structural cassette of CHIKV from the polyhedrin promoter (pPh). This cassette is post-translationally processed into the individual capsid and envelope (E) proteins by autocatalytic cleavage of capsid and processing by host furin and signalase. The CHIKV E2 protein (arrow) was detected in the cell pellet samples (b) or culture fluid samples (c) of ExpiSf9 cells infected with AcTS-VLP. Samples were collected at 96 hpi from the micro bioreactor run at 29-34°C after infection with MOI=0.3. MW: Molecular Weight marker. (-) mock-infected ExpiSf9 cells. The positive control (+) is purified CHIKV VLP derived from human HEK293 cells (The Native Antigen Company).

### Cell growth kinetics at elevated temperature

The microbioreactor screening experiments showed that the largest reduction in baculovirus titers could be achieved at 34°C. To further characterize the behavior of cell growth and infection at 34°C compared to the standard BEVS incubation temperature of 27°C, shake flask experiments were performed. ExpiSf9 cells were grown in shake flasks at 27°C and 34°C and the cell density and viability were monitored over time (Figure ). Similar growth kinetics were found in the first 72 hours for cells grown at 27 °C and 34 °C. After 72 hours post-inoculation, the viability and specific growth rate decreased at 34°C and were clearly lower than at 27°C.

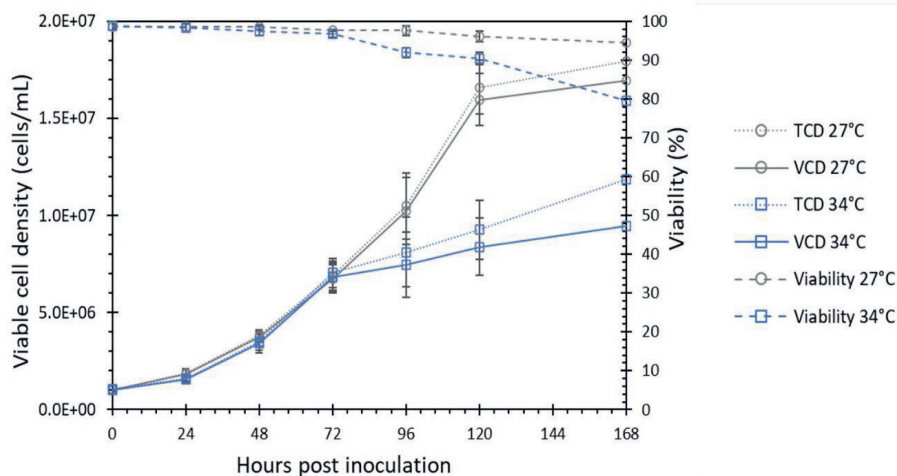


**Figure 5.** Cell growth and viability of suspension ExpiSf9 cells at elevated temperature. Viable cell density (VCD), total cell density (TCD), and viability of uninfected ExpiSf9 cells as a function of time at both 27°C and 34°C. Error bars indicate the variation between duplicate shake flasks.

#### Virus infection kinetics at elevated temperature

To characterize the infection of baculovirus AcTS-VLP in ExpiSf9 cells at elevated temperatures, virus uptake and infection at both 27°C and 34°C were measured for the first 11 hours of infection. Suspension cells were cultured in shake flasks and were infected at a cell concentration at infection (CCI) of  $0.9\text{--}1.3 \times 10^6$  viable cells/mL with AcTS-VLP at an MOI of 10 ivp/cell. The residual BV titer in the medium was measured in the first 11 hours post-infection. In the first hours post-infection, the virus titer in the culture fluid dropped exponentially at the same rate for both 27°C and 34°C (Figure a). The residual BV titer in the culture fluid remained around  $10^5$  ivp/mL at 11 hpi at 34°C.

Next to the BV titer, the increase in the percentage of infected cells was determined based on the percentage of cells showing eGFP fluorescence using flow cytometry (Figure b). From four hours post-infection, baculovirus-infected cells could be detected by eGFP fluorescence at 27°C, and close to 100% infection was reached at 11 hpi. At elevated incubation temperatures, the eGFP fluorescent cells were detected earlier, at three hours post-infection. The eGFP is expressed from the hsp70 promoter, and elevated incubation temperatures might activate this temperature-dependent promoter. To confirm this, the eGFP concentration was quantified at 11 hours post-infection. The total, external, and internal eGFP levels were indeed increased at 34°C compared to 27°C (Figure c). Thus, either the baculovirus infection proceeds more rapidly at 34°C, or the eGFP levels at 34°C are

elevated due to a more active hsp70 promotor and could therefore be detected earlier in the infection process. Nevertheless, the infection kinetics at 27°C and 34°C were similar in the first hours post-infection.

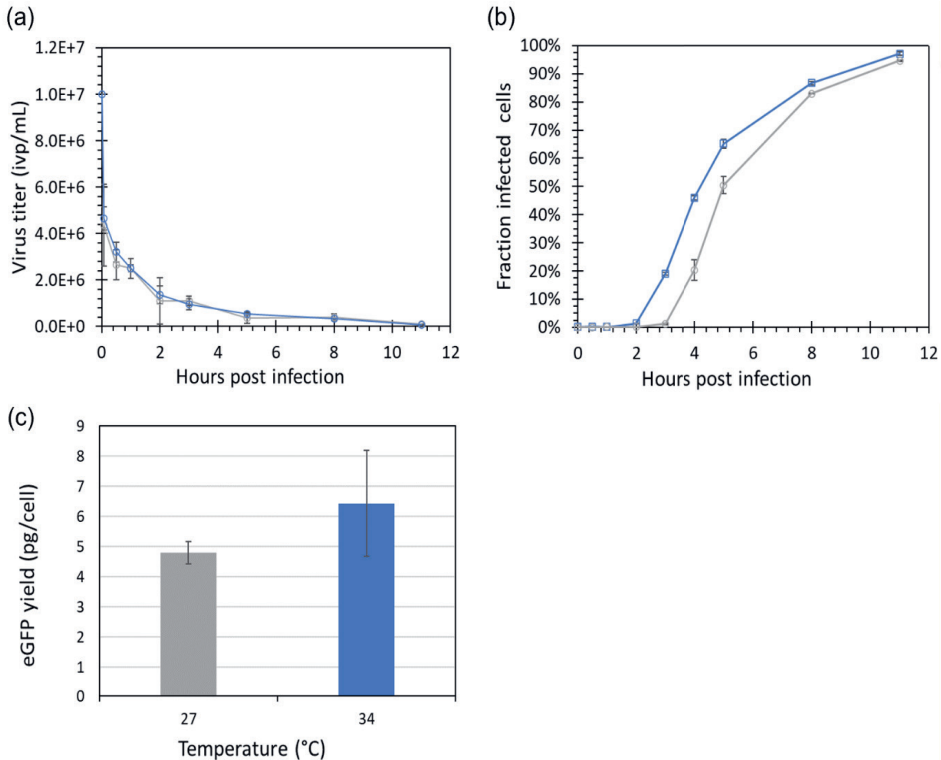


**Figure 6.** Virus entry and infection phenotype of AcTS-VLP at 27°C and 34°C. (a) Baculovirus titer was detected in the culture medium as a function of time after virus addition at MOI 10 and CCI 0.9-1.3x10<sup>6</sup> cells/mL at both 27°C and 34°C measured by the gp64 antibody assay. (b) Percentage of infected cells as a function of time after virus addition at MOI 10 and CCI 0.9-1.3x10<sup>6</sup> cells/mL measured by detecting eGFP fluorescent cells using flow cytometry. (c) eGFP concentration in picograms per cell in the total fraction at 11 hpi with the AcTS-VLP virus. Error bars indicate the variation between duplicate shake flasks.

### Scale-up to bioreactors with high MOI infection

To assess the scalability of the system, the temperature strategy was scaled up to stirred tank bioreactors. Cells were infected with the temperature-sensitive AcTS-VLP at a high MOI (8-10 TCID<sub>50</sub>/mL) and after 3 hours the temperature in the bioreactors was increased from 27°C to 34°C. In this 500 mL bioreactor with 400 mL working volume, the required time to shift the temperature from 27°C to 34°C was less than 10 minutes. Control shake flasks were either kept at 27°C, cultured

at 34°C, or shifted to 34°C at the same time as the bioreactor. The bioreactors and shake flasks were kept at setpoint until harvest at 96 hpi. In the control conditions cultured at 27 °C, BV titers significantly increased between 0 and 96 hpi. In contrast, in the bioreactor and shake flasks cultured at 34°C, new BVs were not produced (Figure 7). A similar reduction in BV titers was measured in bioreactors and shake flasks, demonstrating that the temperature strategy is suitable for scale-up. Moreover, the infected shake flasks that were directly incubated at 34°C, or shifted to 34°C at 3 hpi reached similar BV titers. This finding suggests that culturing at an elevated temperature of 34°C does not affect baculovirus entry into the insect cells compared to culturing at 27°C and supports the results shown in Figure 6a.

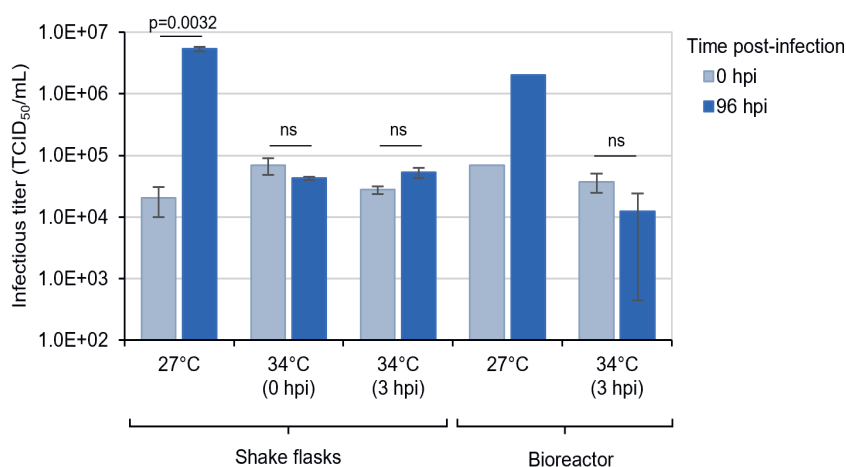


**Figure 7.** Characterization of infectious BV titers in bioreactors and shake flasks at different temperatures. Bioreactors and shake flasks were infected with AcTS-VLP at a high MOI (8-10 TCID<sub>50</sub>/mL). The temperature remained at 27°C, was increased to 34°C upon infection, or was shifted at 3 hpi. The infectious BV titer in the culture fluid was determined at 0 and 96 hpi. Error bars represent duplicate measurement values.

### Bioreactor infection at low MOI

Low MOI processes are highly advantageous from a process development point of view. Small virus seed stocks can be used, avoiding the need for a separate large-scale virus production run and subsequent virus titer determination. This leads to considerable time and resource savings at the industrial production scale (Maranga et al., 2003). Since the AcTS-VLP virus does not spread at 34°C, the temperature should be kept at 27°C for low MOI processes until all cells have become infected. Only then, the temperature is increased to 34°C to inhibit baculovirus contaminant release.

Choosing the optimal moment of temperature shift is therefore crucial for the implementation of a low MOI strategy. If the temperature shift is performed too early in the infection, it will result in incomplete infection and hence, lower product yields. On the other hand, performing the temperature shift too late will result in unnecessary high residual BV titers.

To assess the impact of timing on low MOI processes, several low MOI bioreactor infections with temperature shifts at different times post-infection were performed. In previous experiments with low MOI (0.01 TCID<sub>50</sub>/cell), complete baculovirus infection of all insect cells was observed around 40 hpi (Altenburg et al., 2022). Therefore, the temperature shift was conducted between 33-40 hpi. Reactors were inoculated at a target density of  $1 \times 10^6$  viable cells/mL at 27°C. At  $2.0 \times 10^6$  viable cells/mL, cells were infected with the temperature-sensitive baculovirus AcTS-VLP at an MOI of 0.01 TCID<sub>50</sub>/cell. The temperature was shifted to 34°C at 33 hpi, 35 hpi, or 40 hpi. One bioreactor acted as a control and was cultivated at 27°C with no temperature shift. For the temperature shifts performed at 33 and 35 hpi, an online microscope was used to measure the cell density, viability, cell diameter, and fraction of infected cells of the bioreactor cultures every 30 minutes.

Complete infection was achieved for all conditions (Figure 8a). The final contaminating BV titers were approximately 100-fold lower in the bioreactors that included a temperature shift, compared to the control run at 27°C (Figure 8b). The reduction in BV titers observed with this low MOI infection strategy was similar to the reduction observed with the high MOI infection strategy described in Figure 7 (about 100-fold). Nevertheless, residual BV titers were higher after low MOI infections ( $>10^6$  TCID<sub>50</sub>/mL), and BV titers still increased after the moment of the temperature shift. The online microscope detected an increase in cell diameter before infection could be detected by offline methods and therefore this is possibly a suitable parameter for determining the optimal timing of the temperature shift (Figure 8c).

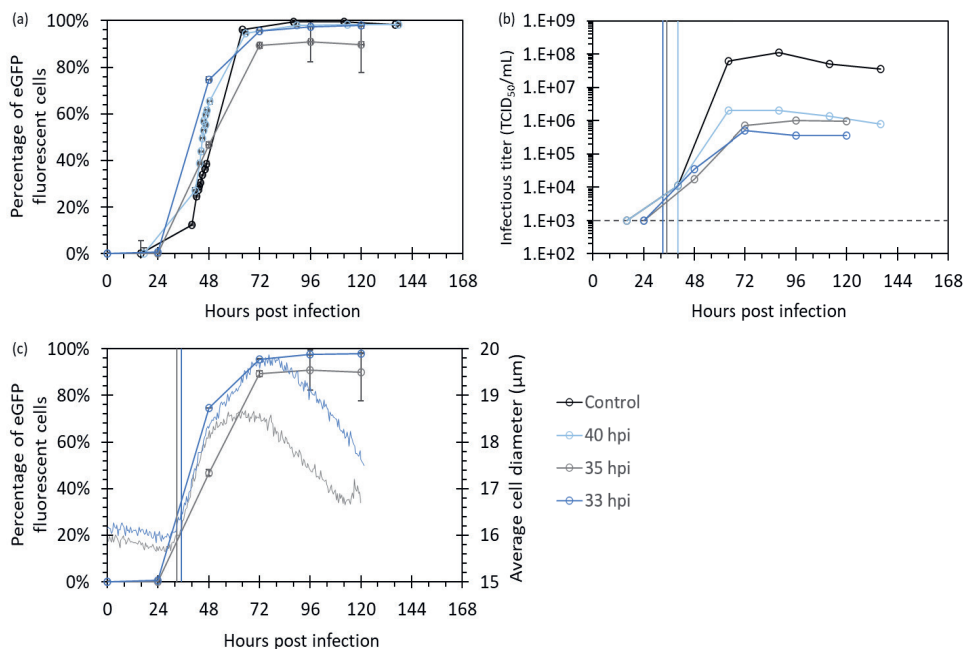


**Figure 8.** Temperature shift timing in low MOI infections with AcTS-VLP in bioreactors. Cells were infected with MOI 0.01 TCID<sub>50</sub>/cell AcTS-VLP at 27°C. The incubation temperature in the bioreactor was elevated to 34°C at 40 hpi (light blue), 35 hpi (light grey), or 33 hpi (dark blue). One control run remained at 27 °C (dark grey). (a) The percentage of infected cells after infection with AcTS-VLP at MOI 0.01. Error bars represent duplicate measurement values. (b) Infectious BV titers during bioreactor cultivations, measured by end-point dilution assay. The dashed grey line indicates the measurement threshold of the TCID<sub>50</sub> assay. The moment of the temperature shift (at 40, 35, or 33 hpi) is indicated in vertical lines. (c) Online average cell diameter was measured every 0.5h by a D3HM microscope for the bioreactor runs with temperature shift at 35 hpi (grey line) or 33 hpi (blue line). The moment of temperature shift is indicated by the vertical lines. Corresponding offline percentages of GFP fluorescent cells are also shown.

Western blot analysis was performed on the cell fraction and culture fluid to determine if CHIKV VLPs were still produced after the temperature switch of the bioreactor (Figure 9). The CHIKV E2 protein could be detected in the cell pellet (Figure 9a) and culture fluid (Figure 9b) at the standard culturing condition (27°C), but also after the temperature shift to 34°C.

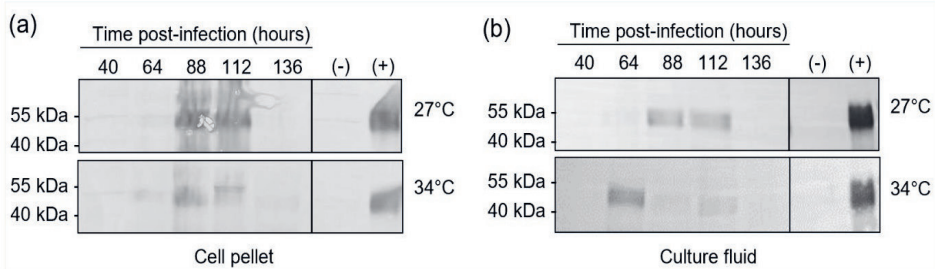


**Figure 9.** CHIKV VLP production with AcTS-VLP at different times post-infection in bioreactors. CHIKV proteins were analyzed on western blot stained with antibodies against the CHIKV E2 protein. (a) Cell fraction of cells infected with AcTS-VLP. (b) The supernatant (culture fluid) fraction of infections with AcTS-VLP. The cultures were sampled at 40, 64, 88, 112, and 136 hpi. The negative control (-) consists of ExpiSf9 cells at one hour before infection. The positive control (+) is purified CHIKV VLP derived from human HEK293 cells (The Native Antigen Company).

## Discussion

The aim of this study was to develop a novel baculovirus contaminant-free (BacFree) system based on a previously described temperature-sensitive baculovirus mutant. Baculovirus contaminant release during the production of (secreted) VLPs greatly hinders efficient downstream processing and was identified as one of the key issues of the BEVS for VLP production (F. Fernandes et al., 2013; Fuenmayor et al., 2017; Gupta et al., 2023; Mittal et al., 2022). By introducing the I317T mutation in GP41, we could significantly reduce the release of BV contaminants at elevated temperatures, while CHIKV VLPs production proceeded normally. TS mutants have been valuable tools for investigating the function of essential baculovirus genes (Lee & Miller, 1979; McLachlin & Miller, 1994; Olszewski & Miller, 1997; Ribeiro et al., 1994). In this research, however, a baculovirus ts mutant was utilized in a completely innovative way to improve the BEVS.

In our novel BacFree approach, BV secretion is regulated by changing the incubation temperature, and our strategy does not require the addition of (chemical) inducers, inhibitors, or the use of multiple cell lines. Although the TS baculovirus only contains one point mutation in *gp41*, we do not expect genetic instability as baculoviruses have low mutational rates (Boezen et al., 2022) and the virus is propagated at 27°C under non-selective conditions. Moreover, we show that BacFree can successfully be scaled up to stirred tank bioreactors and is suitable for both high MOI and low MOI

infection processes. This makes it favorable compared to alternative approaches based on trans-complementation (Chaves et al., 2018; Hu et al., 2023; Marek et al., 2011) or CRISPR-Cas9 knock-out (Bruder & Aucoin, 2023), which are only compatible with high MOI infections and require additional stable transgenic cell lines.

As a proof-of-concept for our BacFree BEVS, the GP41<sup>TS</sup> was expressed from the strong baculovirus p10 promoter, while the original *gp41* gene was deleted from the bacmid. Microbioreactor screening experiments showed that this virus was non-permissive at  $\geq 34^{\circ}\text{C}$ . The original tsB1074, harboring the I317T mutation at the *gp41* locus, was described to be non-permissive at  $33^{\circ}\text{C}$  (Olszewski & Miller, 1997). TS phenotypes can arise because, at the non-permissive temperature, the concentration of active protein is decreased below the required threshold for BV release, while it remains above this threshold at the permissive temperature. *Gp41* is a late baculovirus gene that is transcribed from 12 hpi onwards (Liu & Maruniak, 1995; Whitford & Faulkner, 1992b). We hypothesize that the overexpression of GP41<sup>TS</sup> from the very late p10 promoter affects the timing and concentration of GP41 in the cells, and thereby slightly affects the non-permissive temperature ( $34^{\circ}\text{C}$  instead of  $33^{\circ}\text{C}$ ).

The temperature sensitivity curve is steep, as only a few degrees difference in temperature results in a complete block of viral spread. The molecular basis of TS mutant phenotypes is often not well understood and could be related to protein stability, folding, or protein binding. GP41 is an oligomeric protein (Li et al., 2018) that is modified with O-linked N-acetylglucosamine (GlcNAc) (Stiles & Wood, 1983; Whitford & Faulkner, 1992a). GP41 localizes to the cytoplasm and nucleus (He et al., 2021) and interacts with other baculovirus and host proteins (Yue et al., 2017). Any of these steps could be affected by the I317T point mutation and further biochemical research is needed to fully understand the structural dynamics of GP41 as a function of temperature. It may also take some time before already formed GP41 becomes non-permissive, which would result in a delay of BV shut-off as seen in Figure 8b and affects the process optimization for low MOI processes. Furthermore, a temperature-dependent system might be sensitive to temperature fluctuations and requires close regulation of incubator temperatures. Further upscaling the BacFree BEVS to larger volume cultures can be challenging since increasing the culture temperature by multiple degrees (from  $27\text{-}30^{\circ}\text{C}$  to  $34^{\circ}\text{C}$ ) takes time and the temperature might not be homogenous throughout the entire reactor volume.

The BacFree system was successfully implemented in low MOI-infected bioreactors. There, it is critical to time the temperature shift correctly and we observed that residual BV titers were lower with earlier temperature shifts. Online monitoring of infection kinetics showed that an increased average cell diameter was an early indicator of infection progression. The phenomenon of increased cell diameter is commonly observed in baculovirus infections and is attributed to the elevation in viral DNA content and protein production (Braunagel et al., 1998; Chisti, 2000; Palomares et al., 2001; Rosinski et al., 2000). In addition, the cell diameter has proven to be a predictive indicator for both recombinant protein productivity and viral replication in culture (Janakiraman et al., 2006; Palomares et al., 2001). Therefore, online monitoring of cell diameter could be an effective tool for determining the optimal timing of the temperature shift. This underscores the substantial benefit of incorporating online monitoring tools for time or event-based process control of bioprocesses.

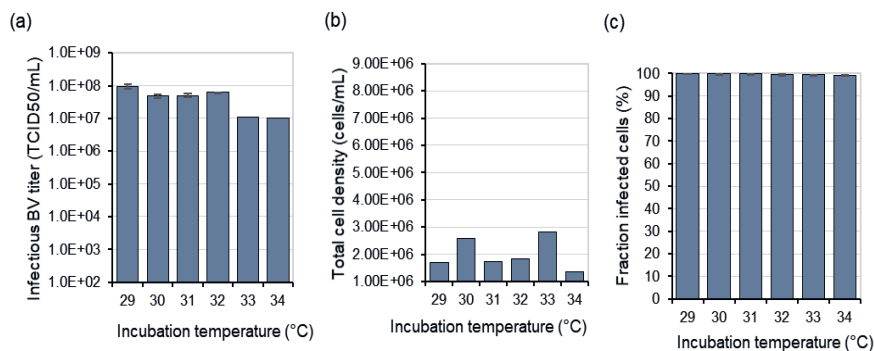
In this study, we used standard Sf9 and ExpiSf9 cells that have not been specifically adapted for growth at the elevated temperature of 34°C. Nonetheless, CHIKV VLPs were successfully produced and secreted into the culture fluid at this temperature. Although our novel BacFree BEVS is functional in non-adapted, commercial cell lines it might be beneficial for product yields to adapt a cell line for optimal protein expression production at the desired temperature (B. Fernandes et al., 2022).

Challenges in VLP purification from BV contaminants are common and solutions often go hand in hand with high cost or substantial product loss (Cervera et al., 2019; Cox, 2021; González-Domínguez et al., 2020; Vicente et al., 2011). The ability to reduce BV secretion in the upstream phase during recombinant protein production would lower the burden of BV contaminants during subsequent downstream processing. Lowering the amount of BV contaminants with several logarithmic scales provides a more beneficial ratio between product and contaminant and might further streamline the downstream process. The BacFree temperature-switch approach offers scalability and compatibility with the existing installed base and is also complementary to novel processing tools while preserving the inherent flexibility and speed that defines the BEVS. The BacFree expression system is an important step forward toward an optimal production platform for VLPs.

## Acknowledgments

We acknowledge Dr. Manli Wang (State Key Laboratory of Virology, Wuhan Institute of Virology) for sharing the Ac $\Delta$ gp41 bacmid. This research was supported by NWO Open Technology Program in Applied and Engineering Sciences (Project: “A baculovirus expression system free of contaminating baculovirus particles”).

## Supplementary figure



**Supplementary Figure 1.** Microbioreactor characterization of AcWT-VLP, GP41 WT in ExpiSf9 cells. ExpiSf9 cells were infected with the WT control virus at MOI=0.3. At 96 hpi, infectious BV titer (a), total cell density (b), and the percentage of infected cells (c) were determined. The average of two replicate infections is shown as bar graphs.



5

# Chapter 5

---

## Process intensification of the baculovirus expression vector system by high cell density infection at low multiplicity of infection using acoustic perfusion

---

Jort J. Altenburg<sup>1</sup>, Brenda E. Juarez-Garza<sup>1</sup>, Jelle van Keimpema<sup>1</sup>, Linda van Oosten<sup>2</sup>, Gorben P. Pijlman<sup>2</sup>, Monique M. van Oers<sup>2</sup>, René H. Wijffels<sup>1</sup>, Dirk E. Martens<sup>1</sup>

<sup>1</sup>Bioprocess Engineering, Wageningen University & Research, The Netherlands

<sup>2</sup>Laboratory of Virology, Wageningen University & Research, The Netherlands

*This chapter has been submitted to Biotechnology and Bioprocess Engineering*

### Abstract

The emergence of new viruses and existing pathogen spread necessitates efficient vaccine production methods. The baculovirus expression vector system (BEVS) is an efficient and scalable system for subunit and virus-like particle vaccine production and gene therapy. However, current production processes are often limited to low cell densities ( $1-4 \times 10^6$  cells/mL) in fed-batch mode. To improve the volumetric productivity of the BEVS, a medium exchange strategy was investigated. Screening experiments were performed to test baculovirus (expressing green fluorescent protein; GFP) infection and productivity of insect cell culture infected at high cell density ( $1-2 \times 10^7$  cells/mL), showing that infection at high cell density was possible with medium exchange. Next, duplicate perfusion runs with baculovirus infection were performed using a cell concentration upon infection (CCI) of  $1.2 \times 10^7$  cells/mL and a multiplicity of infection (MOI) of 0.01, reaching a maximum viable cell density of  $2.8 \times 10^7$  cells/mL and a maximum GFP production of 263 mg/L. The volumetric productivity of these perfusion runs was 4.8 times higher than for reference batch processes with a CCI of  $3 \times 10^6$  cells/mL and an MOI of 1. These results demonstrate that process intensification can be achieved for the BEVS by implementing perfusion, resulting in higher volumetric productivity.

## Introduction

Several viral outbreaks with epidemic and pandemic potential, most of which are zoonotic, have been witnessed in the last two decades (Shanmugaraj & Phoolcharoen, 2021). Examples include the 2002-2003 outbreak of SARS, the 2009 outbreak of H1N1 influenza (swine flu), the 2013-2016 outbreak of Ebola, and the 2019-2020 outbreak of COVID-19 caused by SARS-CoV-2. It is expected that the emergence of new infectious diseases will become more common due to social, environmental, and economic factors (Wolfe et al., 2007). Vaccines are the most effective medical intervention to combat global viral outbreaks (Domínguez-Andrés et al., 2020). To effectively contain a viral outbreak, the timely availability of vaccine material in sufficient amounts is crucial. Consequently, the ability to quickly develop and efficiently scale-up vaccine production processes is critical. The Baculovirus Expression Vector System (BEVS) allows the expression of foreign genes when infecting insect cells with a recombinant baculovirus. In this system, the baculovirus polyhedrin gene, which is expressed at a high level and is not essential for virus replication, is replaced by a gene of choice (Robert D Possee, 1988). The infection process and protein production using the BEVS is significantly influenced by the multiplicity of infection (MOI) and the cell concentration at infection (CCI). The MOI is the number of infectious baculoviruses per cell added to a culture (Carinhas et al., 2009). A high MOI ensures the immediate infection of all insect cells upon virus addition. Infecting at a high CCI may lead to substrate depletion and reduced protein production, while a low CCI results in limited protein production due to the small concentration of infected cells. With a high MOI approach, infection at the optimal CCI is possible, but a large amount of virus particles is needed (Maranga et al., 2003b). The use of a low MOI strategy results in at least a two-stage infection process and enables the use of smaller virus stocks. With a low MOI strategy and multiple infection cycles, the MOI, infection kinetics, and cell growth must be precisely known to determine the optimal CCI for reaching complete infection, while still, sufficient nutrients are present for maximum volumetric productivity. Unravelling the interplay between MOI and CCI is thus very important for a better understanding of the BEVS and the subsequent design of efficient infection strategies (Carinhas et al., 2009; Maranga et al., 2003b).

Batch culture is commonly used to produce recombinant proteins with baculovirus-infected insect cells although more recently perfusion culture has been applied for recombinant protein production using stable insect cell lines (Sequeira et al., 2018). The growth of insect cells and the maximum cell density for infection in a batch culture are usually limited by the nutrients in the cell culture medium,

which also limits the volumetric productivity (Zhang et al., 1998). Batch processes have low volumetric productivity because of a low optimal CCI and relatively long downtime of the equipment due to the short duration of a batch (Gallo-Ramírez et al., 2015). High-density perfusion processes are an attractive alternative to produce recombinant proteins due to the potential to increase volumetric productivity (Jäger, 1996). In a perfusion bioreactor, there is a continuous supply of fresh medium and removal of spent medium while the cells are retained in the bioreactor while gradually replacing the culture medium by using a cell retention device. In this way, the cells are continuously supplied with nutrients, while waste metabolites are continuously removed. This allows for reaching higher viable cell densities in the bioreactor. Moreover, the flow out of the reactor often contains the product and is already cell-free, simplifying the downstream processing (Dalm, 2007). Besides the cell-free harvest, often a small outflow with cells, called ‘the bleed’ is removed from the bioreactor to maintain cell viability (Dalm et al., 2004).

To achieve high volumetric productivity with the BEVS in a perfusion bioreactor, it is beneficial to acquire high cell densities during the production run, provided that the specific productivity remains constant. However, it has been observed that there is a reduction in specific productivity when infecting insect cells at cell densities above  $5 \times 10^6$  cells/mL (Bernal et al., 2009; Pijlman et al., 2020). This phenomenon is often referred to as the cell density effect. Potential explanations for this cell density effect are cells being in an unfavorable growth phase at the moment of infection, inhibition by accumulating waste metabolites, cell-to-cell contact inhibition, disruption in lipid biosynthesis, and the depletion of essential nutrients (Bernal et al., 2009; Ikonomidou et al., 2003; Lavado-García et al., 2022). Although the exact mechanisms behind are still unknown, the cell density effect has been prevented by a continuous supply of nutrients and/or the removal of inhibitory products (Caron et al., 1994; Chico & Jäger, 2000; Ikonomidou et al., 2003; Radford et al., 1997). Carinhas et al (2009) showed that medium exchange could overcome the cell density effect at high MOI but not at low MOI for the Sf9 cell line in SF900II serum-free medium. This previous research on the use of medium exchange or perfusion with the BEVS was performed with various cell lines and media types (including serum-containing medium) at relatively low cell densities and employed high MOIs for baculovirus infection. Until now, maximum reported CCIs for sf9 cells in batch mode are generally in the range of  $1-3.5 \cdot 10^6$  cells/mL and MOIs of  $>1$  (Lavado-García et al., 2022).

This study aimed to investigate whether it is possible to achieve high cell density protein production for the BEVS by using perfusion bioreactors infected at high CCI and low MOI. First, small-scale

screening experiments with ExpiSf9 insect cells in ExpiSf chemically defined medium were performed in shake flasks and spin tubes to determine the feasibility of baculovirus infection at high cell density and to see whether cell-specific productivity is maintained. Hereafter, the process was scaled-up to stirred tank bioreactors, and a low MOI perfusion strategy for the BEVS was applied using an acoustic cell retention device. Viable cell densities of  $25\text{-}28 \times 10^6$  cells/mL were achieved in two acoustic perfusion bioreactor runs that were highly reproducible. We showed that yield per cell is maintained at these high cell densities and bioreactor volumetric productivity was over 4.8-fold higher compared to reference batch processes.

## Materials & Methods

### Cell lines, media & virus stocks

The ExpiSf9 cell line (ThermoFisher) was used for all the experiments and the end-point dilution assays (EPDA). This cell line is a derivative of the *Spodoptera frugiperda* (Sf9) cell line that was adapted to grow on the chemically defined ExpiSf CD medium by Gibco (ThermoFisher, 2018). An *Autographa californica* multiple nucleopolyhedrovirus (AcMNPV) vector encoding two fluorescent markers was constructed. This virus (Ac-2FL) contains the eGFP open reading frame (ORF) behind the *Orchyia pseudotsugata* MNPV immediate-early 2 (OpIE-2) promoter as a marker for early infection (Massotte, 2003) and a mCherry ORF behind the polyhedrin promoter as a marker for very late gene expression, and hence, protein productivity. For the experiments involving protein quantification, an AcMNPV vector containing the GFP ORF behind the polyhedrin promoter was used (AcGFP). The recombinant baculoviruses were generated using the bac-to-bac expression system (Thermo Fisher). In short, *E. coli* cells containing the AcMNPV bacmid, and the transposition helper plasmid were transformed with pDest8-derived plasmids to introduce the marker genes into the baculovirus genome. Insect cells were then transfected with the recombinant bacmids using Expres2TR transfection reagent (Expres2ion Biotechnologies) to generate infectious baculovirus particles.

### Screening & bioreactor cultures

Screening experiments were performed by cultivating cells in 125 mL vent-capped PETG shake-flasks (Nalgene) with a working volume of 25 mL or by cultivating in 50 mL spin tubes (Sarstedt) with a working volume of 5 mL. The shake flasks were incubated in a Climo-Shaker ISF1-XC (Kuhner) at 27 °C with a shake velocity of 95 rpm. The spin tubes were mixed at 240 rpm on a Rotamax 120 (Heidolph) shaker placed within a Multitron (Infors HT) incubator at 27 °C. Medium exchange was

performed by centrifuging the cell suspension at 300g for 5 minutes. Medium exchange was started when a cell density of  $5\text{-}6 \times 10^6$  cells/mL was reached, and 30% of the medium was replaced once a day. After reaching a viable cell density (VCD) of  $11\text{-}12 \times 10^6$  cells/mL, 60% of the medium was replaced once a day (corresponding to an approximate continuous perfusion rate of 0.5 and 1.0 reactor volumes (RV)/day).

Bioreactor experiments were performed in 500 mL miniBio stirred tank bioreactors (Getinge) utilizing a my-Control bioreactor control system (Getinge). The reactor working volume of 300 mL was inoculated at a starting density of  $1.0 \times 10^6$  viable cells/mL. The temperature was controlled at 27°C using a Peltier heating/cooling system. The pH was not controlled but maintained between 5.6-6.2 by the buffering capacity of the medium. Dissolved oxygen was controlled at 30% of air saturation by supplying pure oxygen through an open hole sparger with a 2 mm internal diameter (Getinge). A single 25 mm marine impeller (Getinge) operated at 300 rpm provided agitation. Perfusion was initiated when the viable cell density reached  $4.0\text{-}7.0 \times 10^6$  viable cells/mL. The targeted cell-specific perfusion rate (CSPR) was 50 pL/cell/day. Cell retention was achieved by acoustic filtration using a 1L BioSep and APS 990 controller (Getinge). The controller was set at run/stop cycle times of 10 min/3s and a power level of 2W. The perfusion rate was set using a Watson-Marlow 205U (Watson-Marlow) peristaltic pump connected to the APS990 controller. In this way, the pump was paused during the stop cycle time. The recirculation flow was operated at 1.5 mL/min. The feed pump was controlled by the my-Control system and activated based on a level sensor to ensure a constant reactor volume. The off-gas flow was connected to a mass spectrometer (Thermo Fisher).

### Analytical methods

Cells were counted by trypan blue exclusion using a TC20 Automated Cell Counter (Bio-Rad) or by manual counting using DHC-F01 cell counting chambers (INCYTO). Infected cells were visualized by expression of GFP or mCherry detected by an IX71 fluorescent microscope (Olympus) or by a C6 Plus Flow Cytometer (BD Accuri). Bioreactor off-gas composition was measured with a mass spectrometer (Thermo Fisher). GFP concentrations were measured by comparing fluorescence to a GFP standard solution (Thermo Fisher). Fluorescence was quantified using an FLx800 micro-plate reader (BioTek) with a 485/528 excitation/emission filter. To determine intracellular GFP, 250  $\mu\text{L}$  lysis buffer (500 mM NaCl, 50 mM Tris(hydroxymethyl)methylamine (TRIS), 0.1% Triton X-100, pH 8) supplemented with 1mM Phenylmethylsulfonyl fluoride (PMSF) was added to 100  $\mu\text{L}$  of cell-containing sample fluid. This mixture was incubated on ice for 10 minutes and subsequently

centrifuged at 13000g for 10 minutes. The supernatant was stored at -20°C until further use. All baculovirus stocks were amplified in ExpiSf9 cells. The infectious viral titer of the produced baculovirus stocks and cell culture samples were determined by calculating the median 50% tissue culture infectious dose (TCID<sub>50</sub>) per mL via end-point dilution assay.

### Calculations

#### *Separation efficiency*

The separation efficiency (%) of the acoustic cell separator was calculated considering the total cell density in the reactor (TCD<sub>R</sub>, cells/mL) and the harvest flow (TCD<sub>H</sub>, cells/mL).

$$SE = \left(1 - \frac{TCD_H}{TCD_R}\right) \cdot 100 \quad (1)$$

#### *Cell specific perfusion rate (CSPR)*

The CSPR (m<sup>3</sup>/cell/day), is defined as the amount of medium supplied to a single viable cell per day and is given by:

$$CSPR = \frac{P}{VCD} \quad (2)$$

Where P is the perfusion rate (day<sup>-1</sup>), which is the total medium flow through the cell retention device (m<sup>3</sup>/day) divided by the reactor working volume (m<sup>3</sup>) and VCD is the viable cell density (cells/m<sup>3</sup>).

#### *Yield of product per cell (Y<sub>P/C</sub>)*

The yield of product per cell (µg/cell) is defined as:

$$Y_{P/C} = \frac{m_P}{IC_{MAX}} \quad (3)$$

Where m<sub>P</sub> is the total amount of product produced since the start of the process (µg) and IC<sub>max</sub> is the maximum number of infected cells reached in the reactor (cells).

#### *Yield of product per medium (Y<sub>P/M</sub>)*

The yield of product per medium (µg/mL) was calculated according to:

$$Y_{P/M} = \frac{m_P}{V_m} \quad (4)$$

Where  $V_m$  is the total amount of medium used (mL)

*Volumetric productivity (VP)*

The volumetric productivity (mg/L/day) is calculated according to:

$$VP = \frac{m_P}{t \cdot V_R} \quad (5)$$

Where  $t$  is the process duration (days) and  $V_R$  is the working volume of the reactor (L)

## Results and Discussion

### Baculovirus infection at high Sf9 cell densities

The loss in productivity occurring after infection of Sf9 cells above a certain cell density has been identified as a bottleneck for the BEVS (Carinhas et al., 2009; Caron et al., 1990; Pijlman et al., 2020). To test whether this bottleneck is due to nutrient limitation or inhibition of produced metabolites we applied an exchange strategy with ExpiSF CD medium to shake flask cultures. First, we determined in shake flasks whether non-infected cells can grow to higher cell densities. Two shake flasks cultivations without medium exchange and two shake flasks cultivations with medium exchange were performed. The maximum viable cell density of these non-infected cultures with medium exchange reached  $4.2 \times 10^7$  viable cells/mL, which is twice the maximum viable cell density reported in literature for this cell line (Yovcheva et al., 2018) and more than twice the viable cell density of  $1.8 \times 10^7$  cells/mL reached by the batch control culture without medium exchange (Figure 1A). This indicated that the maximum viable cell density can be increased by supplying additional nutrients required for the growth and maintenance of these cells and/or by removal of growth-inhibiting metabolites with the spent medium. For both cultures, the viability stayed above 80% during the entire run (Figure 1B).

Next, we determined whether complete infection can be achieved when cells are infected at high densities when applying medium exchange. For the infected shake flasks, a baculovirus encoding two fluorescent markers (Ac-2FL) was used, containing a gene for GFP located behind the immediate early OpIE2 promoter and a mCherry gene located behind the very late polyhedrin promoter. Infection was evaluated by measuring the percentages of GFP and mCherry fluorescent cells.

In batch mode, the optimal CCI for these cells is  $5-7 \times 10^6$  cells/mL when infected with an MOI of 5 (Yovcheva et al., 2018). Here, the cell density upon infection was chosen at  $1.2 \times 10^7$  cells/mL, twice the average recommended cell density for infection. The cells were infected with AcBac-2FL at an MOI of 0.01, allowing for continued growth of non-infected cells after infection. Four shake flasks were infected in total, two without medium exchange and two with medium exchange. The viable cell density of the infected shake flasks without medium exchange was similar to the uninfected batch control without medium exchange (Figure 1A). This was expected because infecting at low MOI requires more time to infect all cells. Cells continued to grow eventually reaching the maximum cell density for a batch culture of  $1.8 \times 10^7$  cells/mL before all cells were infected. Viability was maintained above 80%, which is comparable to that of the non-infected control (Figure 1B). The infected culture without medium exchange only reached very low levels

of green and red fluorescent cells, indicating that the infection was halted (Figures 1C & 1D). These experiments confirm that a CCI of  $1.2 \times 10^7$  cells/mL is above the optimal CCI for a batch process without medium exchange and a low MOI.

The infected shake flasks with medium exchange had comparable growth to the control with medium exchange until 20 hours (Figure 1A). This was expected since the low MOI of 0.01 requires multiple infection cycles before all cells are infected, allowing for continued cell growth. The maximum viable cell density of  $1.6 \times 10^7$  viable cells/mL was reached at 48 hours post infection (hpi). This is considerably lower than the maximum density in the non-infected control with medium exchange indicating a stop of cell growth due to baculovirus infection. In contrast to the other conditions, the infected shake flasks with medium exchange showed a drop in viable cell density between 100-120 hpi and had a significant reduction in viability, reaching around 45% of viable cells after 120 hpi. A reduction in viable cell concentration and viability is expected when insect cells undergo baculovirus infection. Fluorescence measurements indicated an efficient infection for the shake flasks with medium exchange, with infection percentages of 100% based on the early expression of eGFP (Figure 1C) and 93% based on the late expression of mCherry (Figure 1D). This demonstrated that medium exchange enabled baculovirus infection of all cells in the culture at high cell densities while using a low MOI.

A comparison between eGFP and mCherry expression showed that eGFP started to be detected at 22 hpi, while mCherry was seen after 46 hours. The difference in time of expression is expected because the eGFP gene is behind the immediate early baculovirus promoter OpIE-2 and the mCherry gene is behind the very late polyhedrin promoter. In summary, these experiments showed that medium exchange allowed for complete baculovirus infection at high cell densities when infecting with a low MOI.

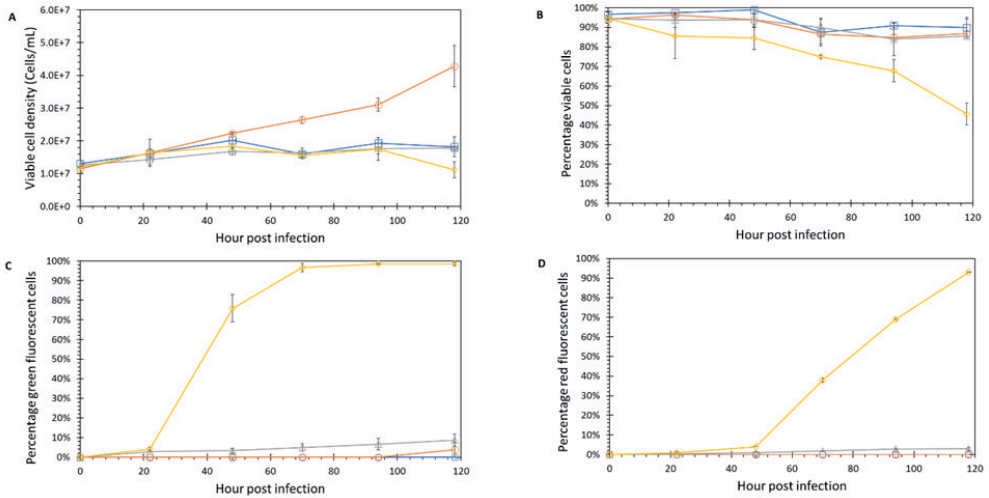


**Figure 1.** Time-course profiles of shake flask Sf9 cultures infected with baculovirus at high cell densities. The control Sf9 culture was grown without medium exchange or baculovirus infection (□). A second control was grown with medium exchange but without baculovirus infection (○). The infected shake flasks were infected with the Ac-2FL baculovirus, expressing eGFP from the immediate early OpIE2 promoter and mCherry from the very late polyhedrin promoter. Cells were infected at  $12 \times 10^6$  viable cells/mL at an MOI of 0.01 baculovirus/cell. Infected shake flasks either had; no medium exchange (△) or daily medium exchange (◇). (A) Viable cell densities. (B) Percentage of viable cells. (C) Percentage of cells containing early expressed eGFP. (D) Percentage of cells containing late expressed mCherry. The data shown are averages of duplicate runs, and error bars represent the distance to the minimum and maximum value. Data are shown starting from  $12 \times 10^6$  viable cells/mL, which was the moment the cells were infected.

**Productivity at high cell densities with medium exchange.**

Next, we studied whether the product yield per cell could be maintained when infecting cells at higher densities while applying medium exchange. High cell-density baculovirus infections were performed using spin tubes. The cells were infected at an MOI of 0.1 (since an MOI of 1 would require too much volume to be added) with AcGFP, and GFP production was quantified by fluorescence intensity measurements. The experiment included a control without medium exchange that was infected at a low cell density of  $4 \times 10^6$  cells/mL, which is around or just below the optimal CCI for these conditions, and two experimental cultures with 60% medium exchange per day that were infected at higher densities of respectively  $1.1 \times 10^7$  cells/mL and  $2.0 \times 10^7$  cells/mL. Since cells were infected with an MOI of 0.1, the viable cell density continued to increase after infection (Figure 2A). For the control flasks infected at  $4 \times 10^6$  cells/mL the maximum cell density reached was around  $7.1 \times 10^6$  cells/mL, a 79% increase compared to the initial cell density at the moment of infection. Similarly, the cell density increased for the cultures infected at  $1.1 \times 10^7$  cells/mL and  $2.0 \times 10^7$  cells/mL. However, the increase in cell density after infection was reduced to 39% and 1.5%, respectively. The viability after infection dropped more drastically for the cultures infected at  $1.1 \times 10^7$  cells/mL and  $2.0 \times 10^7$  cells/mL compared to the control culture that was infected at  $4 \times 10^6$  cells/mL (Figure 2B). At 8 days post-infection, the viability of the control culture was around 30%, while the viabilities for the cultures infected at  $1.1 \times 10^7$  cells/mL and  $2.0 \times 10^7$  cells/mL were 6% and 12%, respectively. Both the reduced growth and faster drop in viability could indicate nutrient or oxygen limitation. While at  $4 \times 10^6$  cells/mL the cells were still growing exponentially, at  $1.1 \times 10^7$  cells/mL and  $2.0 \times 10^7$  cells/mL the cells no longer grew exponentially, and the specific growth decreased with increasing cell density. Exposing the cells to a sufficiently high medium exchange rate is important to maintain cell growth (Schulze et al., 2021). To compare the productivity the total concentration (intracellular and extracellular) of GFP was measured (Figure 2C). GFP was first detected on day 1 post-infection which is expected when using an MOI of 0.1 and the GFP gene expressed from the polyhedrin promoter. The culture infected at  $1.1 \times 10^7$  cells/mL showed a similar GFP production pattern compared to the control culture and maximum GFP concentration levelled off at around 200 mg/L compared to 100 mg/L for the control. The culture infected at  $2.0 \times 10^7$  cells/mL had lower GFP production in the beginning compared to the other two cultures. Moreover, GFP concentrations did not reach a plateau value and were still increasing until 8 days post-infection. Possibly, at these high cell densities, insufficient medium exchange rates slowed down GFP production. The total amount of GFP produced at day 8 increased with the increase of the cell density upon infection (Figure 2C). The yield per cell (YP/c) reached by the culture infected at

$1.1 \times 10^7$  cells/mL was slightly lower than the control infected at  $4 \times 10^6$  cells/mL, while the YP/c reached by the culture infected at  $2.0 \times 10^7$  cells/mL was slightly higher than the control (Figure 2D). Viable cell density for the culture infected at  $2.0 \times 10^7$  cells/mL was maintained but did not increase after infection. This could explain the higher YP/c values for this CCI as less nutrients were used for cell division. High MOI infections could reduce the uncertainty related to additional infection cycles and give a clearer picture of the maximum CCI. However, this is not always possible at these high cell densities due to the large volume of virus stock required to infect at high MOI and high CCI. Calculated YP/c values were in the same order of magnitude for all CCIs, which indicates that the yield of recombinant product per cell can be maintained when infecting at high cell density using medium exchange for this cell line and medium. In addition, low MOI infections seem possible. This provides a good basis for the application of medium exchange and/or perfusion strategies in combination with low MOI infection on larger scale to intensify production.

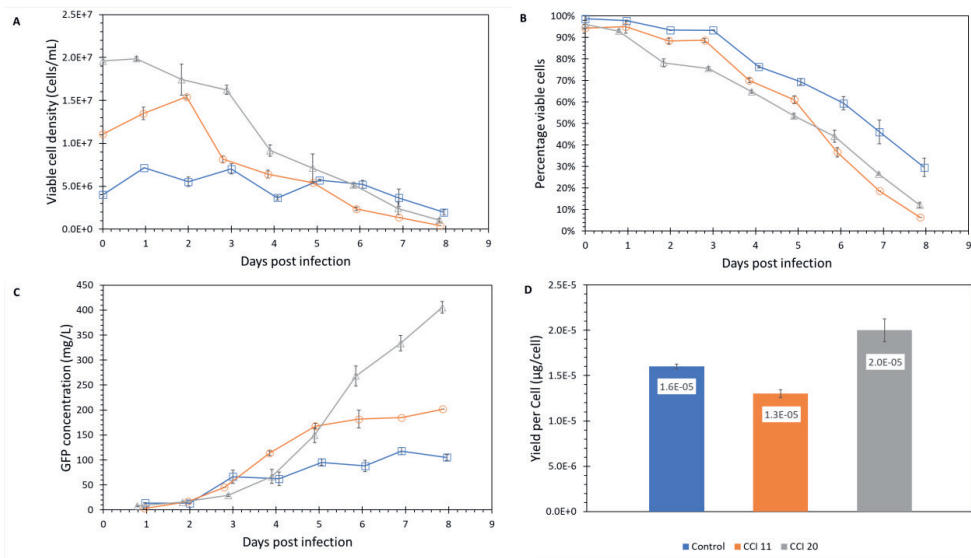


**Figure 2.** Productivity screening in Sf9 spin tubes at different CCIs. Spinner tubes were infected at an MOI of 0.1 at CCIs of  $4 \times 10^6$  viable cells/mL ( $\square$ ),  $1.1 \times 10^7$  viable cells/mL ( $\circ$ ), and  $2.0 \times 10^7$  viable cells/mL ( $\triangle$ ). Medium exchange was performed once per day for CCIs  $1.1 \times 10^7$  viable cells/mL, and  $2.0 \times 10^7$  viable cells/mL. The cells were infected with an AcGFP baculovirus. Data shown are averages of duplicate runs and error bars represent the distance to the minimum and maximum value. (A) Viable cell densities. (B) Viability. (C) GFP concentration. (D) Yield of product per cell ( $Y_{p/c}$ ) of infected cultures with an MOI of 0.1 in spin tubes.

### Cell growth characterization in a perfusion bioreactor

To scale up and test a medium exchange strategy with low MOI infection, an acoustic cell retention system was used to enable perfusion cultivation in bench top stirred-tank bioreactors.

First, Sf9 insect cell growth was characterized in this perfusion system without baculovirus infection. The culture was started in batch mode with an inoculation density of  $1.0 \times 10^6$  viable cells/mL. Perfusion was started at 2 days post-inoculation at 0.5 RV/day. The perfusion rate was further increased to 1 RV/day from day 5 onwards. On day 7, a bleed rate of 0.2 RV/day was applied to maintain viability (Dalm et al., 2004). The separation efficiency of the Mini BioSep was  $> 95\%$  during most of the run (Figure 3). The cell-specific perfusion rate (CSPR) indicates the amount of medium supplied per cell per day via perfusion and must be above a certain value to prevent nutrient limitation. The CSPR during the run was between 31-77 pL/cell/day, with an average of 50 pL/cell/day (Figure 3). While the minimum CSPR for these cells is not known, a value of 50 pL/cell/day is often used for CHO cell cultivations (Schulze et al., 2021) although lower CSPR values have been reported for stable insect cell lines (Fernandes et al., 2022). Starting on day 4, viability dropped from 95% to 80%. During this period, the CSPR dropped to 30-40 pL/cell/day and growth rates shifted from exponential to linear. In the end, a maximum viable cell density of  $3.8 \times 10^7$  cells/mL was reached. It is possible that the CSPR was too low to maintain exponential growth and reach higher cell densities. This could also have caused the decrease in viability. Moreover, since the acoustic cell retention device retains live and dead cells, dead cells may still accumulate in the reactor despite applying reactor bleed. This could have further impacted the viability during the run. Lastly, the gas flow needed to supply sufficient oxygen increased to extremely high values (0.5-1 vvm, data not shown) and the shear associated with these high gas flow rates could have affected cell growth and viability. An open hole sparger generating larger 2-3 mm bubbles was used here. Switching to a porous sparger generating smaller bubbles might reduce the need for excessive gas flow rates needed for oxygenation of the cell culture and reduce shear. Overall, these results indicated a medium exchange strategy could be scaled-up to bioreactors using an acoustic perfusion system to achieve ExpiSf9 cell concentrations of up to  $3.8 \times 10^7$  viable cells/mL.

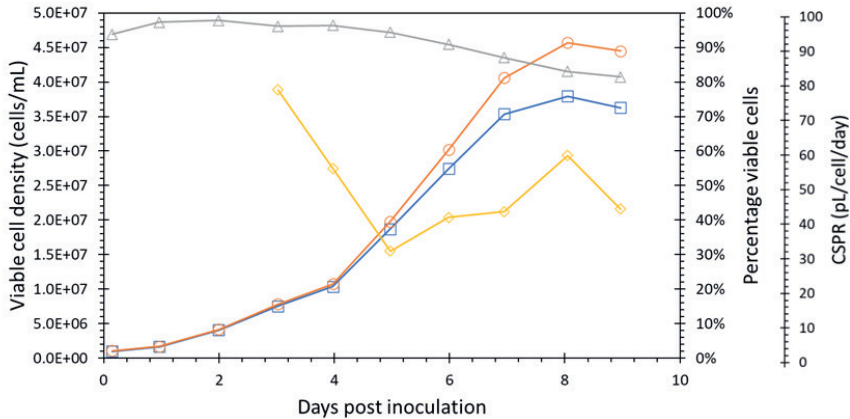


**Figure 3.** Sf9 cell growth characterization in a perfusion bioreactor. Viable ( $\square$ ) and total ( $\circ$ ) cell densities, percentage of viable cells ( $\triangle$ ), and CSPR ( $\diamond$ ) during a bioreactor run without baculovirus infection. Perfusion mode was started on day 2.

## BEVS performance in perfusion bioreactors

### *Cell growth and viability*

We next investigated whether efficient baculovirus infection was possible at high cell density in perfusion bioreactors. Based on the cell growth characterization in the perfusion bioreactor with healthy ExpiSf9 cells, two additional perfusion runs were performed in 500 mL stirred tank reactors using acoustic cell retention. Both perfusion runs were inoculated with a seeding density of  $1.0 \times 10^6$  viable cells/mL. Perfusion was started at 3 days post-inoculation with a target CSPR of 50 pL/cell/day since lower CSPRs appeared to slow down cell growth. The perfusion cultures were infected at 4 days post-inoculation. Previous experiments showed that infection was still possible at  $2 \times 10^7$  viable cells/mL. A doubling in cell concentrations was observed when using an MOI of 0.01. Therefore, the targeted CCI was  $1 \times 10^7$  viable cells/mL. Concentrations at infection were  $1-1.2 \times 10^7$  viable cells/mL for run 1 and 2, respectively, and both bioreactors were infected with AcGFP at low MOI (0.01). At 6-7 days post-inoculation (corresponding to 2-3 days post-infection) cell growth stopped, indicating complete infection, and the maximum viable cell density was reached (Figure 4A). Maximum viable cell densities were very comparable for both runs ( $2.5-2.8 \times 10^7$  viable cells/mL). Both cell cultures doubled more than once in cell density after infecting with low MOI. Assuming BV release between 12-124 hours the continued growth for about 2 days indicates that about two infection cycles were needed to reach complete infection. Maximum viable cell densities were substantially higher than those reached in batch mode (Table 1). Both runs were terminated at below 10% viability (Figure 4B). The viability of both runs started

decreasing more rapidly from day 3 post-infection. The viability of run 1 dropped slightly earlier than that of run 2, which may indicate a faster infection rate in run 1. Also, the lower CSPR in run 1 (Figure 4A) may have contributed to the earlier decrease in viability by causing nutrient limitation and an increase in death rate. The goal was to maintain a CSPR above 50 pL/cell/day. For run 1, the CSPR decreased below the aimed minimal value several times, with a minimum of 37 pL/cell/day. For run 2, the CSPR never dropped below 50 pL/cell/day, with a minimum of 55 pL/cell/day. Online viable biomass measurement coupled to the bioreactor feeding rate can avoid such fluctuations in CSPR (Carvell & Dowd, 2006; Dowd et al., 2003). Glucose concentrations were analyzed and remained higher than 55mM (data not shown) and thus did not appear to be limited during the run. However, the limitation of other nutrients, such as cysteine (Radford et al., 1997), could not be ruled out. Screening for optimal CSPR values should be performed to get more insight in the impact of nutrient availability on cell culture performance. Cell retention within the reactor is crucial during perfusion to minimize the loss of cells through the harvest flow. The separation efficiency of the acoustic cell retention device was always higher than 90% and >94% during the first days of perfusion (Figure 4D) for both runs. However, after baculovirus infection, the liquid in the acoustic chamber was occasionally opaque, indicating poor separation. The separation efficiencies demonstrated a downhill trend towards the end of the culture (Figure 4D). This is likely caused by a change in the morphology of the insect cells after baculovirus infection and during cell death. Since acoustic cell separation is based on particle size and physical properties of the cells, changing cell morphology can affect cell separation (Ding et al., 2014).

### *Development of baculovirus infection*

eGFP fluorescence was used to determine the percentage of cells infected with Ac-2FL. Cell growth stopped around 2 days post infection (dpi), indicating all cells were infected. This is in accordance with the moment GFP expression becomes visible about 3 days post infection or 1 day after most of the cells became infected (Figure 4B). Infection slowed down after the percentage of infected cells reached 60-70% around day 8 (4 dpi). This was unexpected, as in batch cultures a continuous rapid increase toward almost 100% infected cells is achieved.

This could be due to a decrease in the release of budded viruses. At day 7 (2 dpi) the infectious titers were  $1 \times 10^7$  and  $1 \times 10^6$  TCID<sub>50</sub>/mL for run 1 and 2, respectively, meaning that the MOIs were lower than 1 and not sufficient to infect all cells. On day 8, final baculovirus titers of  $3.5\text{-}5 \times 10^7$  TCID<sub>50</sub>/mL were reached giving an MOI between 1 and 2, which would result in about 60-80% infection. Based on the final titers reached and the maximum infected cell density a value of 2

budded viruses released per cell is calculated, which confirms the slower infection. However, the release of 2 BV per cell does not agree with the rapid initial increase in infection. Possibly the number of BVs released per cell decreases during the run. This could be related to the high cell density, which was seen to reduce the virus binding efficiency, potentially due to cell-cell interactions resulting in clumping (Power et al., 1996). Some cell clumping was observed in both reactor runs. Increasing the agitation speed could reduce clumping, although higher agitation rates can negatively impact cell growth (Kioukia et al., 1996). Furthermore, baculovirus expression is influenced by the cell cycle phase upon infection (Saito et al., 2002). It has been demonstrated that infection during the G<sub>1</sub> and S phases results in faster and higher protein expression and that cells arrested in the G<sub>2</sub> phase of the cell cycle are less susceptible to baculovirus infection (Lynn & Hink, 1978). Specific growth rates were lower in both cultures after day 3 just before infection. This may have resulted in the accumulation of cells in the G<sub>2</sub> phase and thus a slower infection progression in part of the cells. However, measurement of cell cycle distribution is difficult in infected culture due to interference of baculovirus DNA. Another reason could be that the viability started to drop rapidly around day 8. Dead cells were excluded from the analysis and consequently the percentage of cells not yet showing green fluorescence will increase due to the loss of infected cells from the measurement which could explain the slow increase in the percentage of GFP-containing cells after this point. Finally, virus stability could be lower later in the culture due to changing conditions in the medium or cells, possibly related to the lower viability.

The virus titers showed a similar profile for both runs (Figure 4C). Starting at 2 days post-infection, titers increased until maximum infectious titers of  $3.5\text{-}5.0 \times 10^7$  TCID<sub>50</sub>/mL were reached at day 8. Furthermore, the increase is slightly later for run 2 as compared to run 1, which agrees with the later decrease in viability observed earlier. This could be caused by the slightly higher CCI in the first run or slight differences in MOI, which further demonstrates the relationship between CCI and MOI for the timing of the run.

#### *Volumetric productivity*

After infection with Ac-GFP, total GFP concentrations increased from 3-4 days post-infection, and this is in line with the detection of GFP inside the cells around day 3 post-infection. Maximum concentrations of 230-280 mg/L were reached at 6 days post-infection (Figure 4C). The GFP concentration increased no further 6 days post-infection due to the low cell viability. A very small number of cells could still be producing GFP at this point, but their cell number and duration of production were insufficient to further increase the detected GFP concentrations. The GFP yield

per cell was very comparable for both perfusion runs (Table 1). Comparison with batch reference runs infected with the same baculovirus construct showed that yield per cell was even improved by 2-fold for the perfusion cultures (Table 1). Volumetric productivity, however, was 3-5 fold higher when infecting at high cell density using perfusion. The average product yield per medium was dependent on the run time. A shorter run time improved the volumetric productivity and the product yield per medium (Table 1). Decreasing or stopping the perfusion flow towards the end of the culture can further improve product yield per medium and reduce medium consumption. In conclusion, this data demonstrates the potential for rapid scale-up and process intensification of the baculovirus expression vector system by using perfusion to infect insect cells at high cell densities and low MOI.

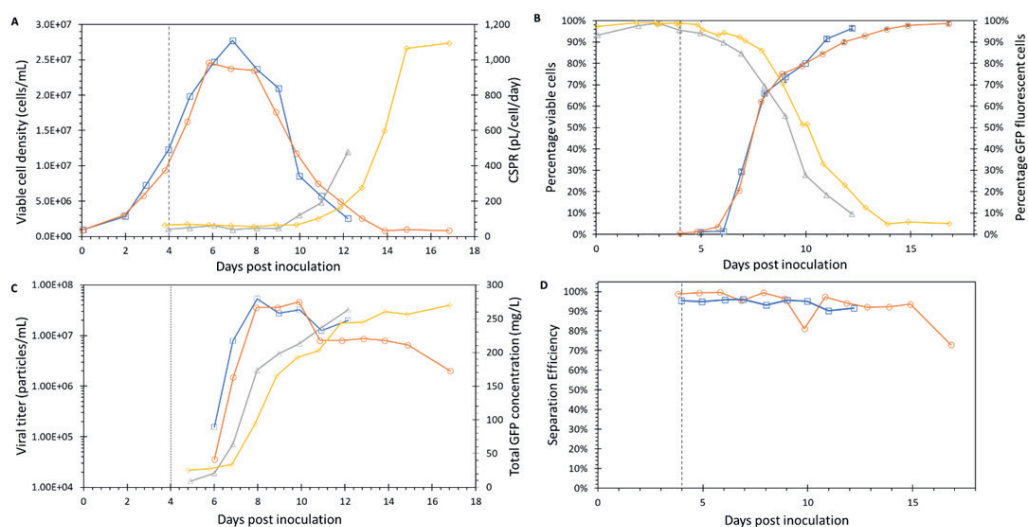


**Figure 4.** BEVS performance in perfusion bioreactors. Two perfusion runs were performed, the reactors were started in batch mode and perfusion was started on day 3. Insect cells were infected with baculovirus on day 4 indicated by the dashed lines. Run 1 lasted until day 12 and run 2 was extended until day 17. (A) Viable cell densities for run 1 (□), and run 2 (○), and CSPR for run 1 (△), and run 2 (◇). (B) Percentage of viable cells for run 1 (△), run 2 (◇), and percentage of GFP fluorescent cells for run 1 (□), and run 2 (○). (C) Viral titer for run 1 (□) and run 2 (○) and total GFP concentration for run 1 (△) and run 2 (◇). (D) Acoustic separator efficiency for run 1 (□) and run 2 (○).

**Table 1.** GFP productivity comparison between two perfusion runs with baculovirus infection versus a batch run. For run 2, two termination time points were included to indicate the effect on volumetric productivity and medium use.  $\pm$  Values indicate the standard measurement errors.

	MOI	Run time (days)	Maximum viable cell density (cells/mL)	Product yield per cell ( $\mu\text{g}/\text{cell}$ )	Volumetric productivity ( $\text{mg}/\text{L}/\text{day}$ )	Yield of product per medium ( $\mu\text{g}/\text{mL}$ )
Run 1	0.01	12.2	$2.77 \times 10^7$	$1.01 \times 10^{-5}$	$23 \pm 1.9$	$28 \pm 2.3$
Run 2	0.01	16.8	$2.46 \times 10^7$	$1.01 \times 10^{-5}$	$14.8 \pm 1.2$	$15.7 \pm 1.3$
Run 2 shortened	0.01	11.9	$2.46 \times 10^7$	$9.87 \times 10^{-6}$	$20.5 \pm 1.7$	$22.5 \pm 1.9$
Batch reference	1	3.8	$4.0 \times 10^6$	$4.23 \times 10^{-6}$	$4.51 \pm 0.4$	$16.9 \pm 1.4$

## Conclusion

Process intensification was achieved for the baculovirus expression vector system by implementing perfusion to infect stirred-tank bioreactors at high CCI and low MOI. The investigated strategy used a low MOI of 0.01 to infect insect cells with baculovirus at viable cell densities of  $1.0\text{-}1.2 \times 10^7$  cells/mL. By using an acoustic perfusion device to allow for medium exchange and cell retention, the cell density effect was overcome and densities of  $2.5\text{-}2.8 \times 10^7$  viable cells/mL were achieved in two perfusion bioreactor runs that showed high reproducibility. The recombinant protein yield per cell was maintained at high cell densities and bioreactor volumetric productivity was up to 4.8-fold higher compared to batch processes. Process optimization to reduce total cultivation time or reach even higher cell densities may further increase volumetric productivity. A low MOI strategy allows for the use of small virus stocks, which can be generated more efficiently and quickly than larger stocks. This can save time and resources and reduce the risk of contamination. Implementing this perfusion strategy for the BEVS reduces the time for scale-up and could increase the production capacity of existing production facilities.

### Acknowledgments

We thank Fred van den End, Sebastiaan Haemers, Snezana Gagic, and Wendy Evers (Wageningen University & Research) for their technical assistance. We also thank Tom van Arragon, Martijn Kreukniet, and Timo Keijzer (Geringe) for their support in using the acoustic cell retention device. This publication is part of the BACFREE project with project number 16762 of the Open Technology Programme which is (partly) financed by the Dutch Research Council (NWO).



6

# **Chapter 6**

---

**General discussion**

## **Introduction**

The Baculovirus Expression Vector System (BEVS) has several advantages over other expression systems. The time needed for process development and to produce material for clinical studies is relatively short. Since only modification of the baculovirus vector is needed, it allows for the use of a single well-characterized cell line and production process to produce any protein. This eliminates the need for the time-consuming tasks of developing, qualifying, and obtaining regulatory approval for a new cell line as well as developing the production process for each protein. Expression levels are high due to the strong polyhedrin and/or p10 promoters and the BEVS is flexible as it can accommodate a wide range of proteins, including difficult-to-express and complex proteins. It also allows for the expression of multiple genes simultaneously. The baculovirus genome is relatively easy to manipulate, facilitating the insertion of target genes and other genetic modifications to optimize protein expression (Van Oers et al., 2015). One drawback of the system is that the cells lyse at the end of the process due to infection, i.e., it is a transient process. Thus, continuous production is not possible in a single reactor system. Furthermore, for products that are excreted (e.g., viral glycoprotein subunits, certain VLPs), the moment of harvesting is very important for optimal product concentrations and low levels of host cell components due to cell lysis. A second drawback is the release of budded viruses (BVs) during the production process, which can be costly and difficult to remove depending on the type of final product (Cervera et al., 2019; M. M. J. Cox, 2021; Vicente et al., 2011).

At this moment, twelve BEVS-derived products have been approved for use, including four human vaccines several human therapeutics, and five veterinary vaccines (Hong et al., 2022) and many more products are in development as described in **Chapter 1**. The short development time between target identification and having a production process for clinical trials and commercial production makes the BEVS a particularly attractive technology to produce vaccines to combat new infectious diseases as reported in **Chapter 2**. Besides vaccines, the BEVS is increasingly used to produce gene therapy vectors after BEVS-derived Glybera (an adeno-associated virus gene therapy against lipoprotein lipase deficiency) became the first approved gene therapy product. FluBlok was the first human vaccine produced with the BEVS. Licensure of these frontrunner BEVS-derived products for humans have paved a regulatory pathway, reducing regulatory uncertainty.

The number of products on the market that are produced with the BEVs is still limited and the BEVS is mainly used to produce proteins on a small scale for research purposes. Therefore, BEVS production processes still are relatively underdeveloped compared to other industrial-established counterparts like Chinese Hamster Ovary (CHO) cell culture processes for monoclonal antibody production. The following are aspects that could be investigated to further improve BEVS bioprocessing:

1. Besides the product also budded viruses are released, which for pharmaceutical applications must be removed during downstream processing (DSP), which may result in significant loss of product depending on the type of product. Thus, the development of BV-free processes is important.
2. Production processes can be further optimized using for example fed batch and perfusion approaches.

3. Many of the small-scale processes use a high multiplicity of infection (MOI). However, at industrial scales, the use of low MOIs is preferred since this requires less viral seed production, and results in less dilution of the medium at the moment of infection. Thus, when developing intensified or BV-free processes the use of low MOI should be included.
4. Finally, the amount of online monitoring in the BEVS is still limited and should be improved to determine for example optimal infection moments and time of harvest

## 1. Budded virus-free production

Baculoviruses possess a limited host range, primarily targeting specific insects. They are widely regarded as safe biological pesticides that do not pose any adverse effects on plants, mammals, birds, fish, or non-target insects (Y. C. Hu, 2005). Individuals encounter baculoviruses regularly through the consumption of fresh vegetables (McWilliam, 2006). The budded viruses (BVs) are enveloped nucleocapsid particles containing a single copy of the baculoviral double-stranded DNA genome and are responsible for cell-to-cell spread within the insect and in cultured insect cells. BVs have adjuvant activity, if not removed or inactivated they have the potential to contribute markedly to the immunogenicity of VLP-based vaccines (Hervas-Stubbs et al., 2007). Nevertheless, BVs can pose theoretical safety risks as residual BVs may enter mammalian cells and some baculovirus promoters may be active in these cells. This could trigger undesired immune responses induced by contaminating baculoviral DNA or protein (Kenoutis et al., 2006; Marek et al., 2011; Murges et al., 1997; Ono et al., 2014). While the risks associated with baculovirus are small, the use and presence of baculoviruses in production can raise public health concerns, particularly in the case of vaccine production. Baculovirus-free production helps to avoid such concerns and ensures that the public has confidence in the safety of the final product. Compliance with regulatory guidelines is essential for obtaining regulatory approval and ensuring the product meets the necessary standards for commercialization. A major consideration for regulatory agencies when evaluating a novel cell substrate is the potential to harbor adventitious agents that could threaten patient safety. Residual DNA in the final product should be limited as much as possible from a safety and regulatory point of view (FDA, 2010). Through budded virus-free production, manufacturers can simplify the regulatory review process, focusing on other critical aspects of product quality and efficacy. This streamlined review process can lead to time savings in the overall approval timeline. Moreover, budded virus-free production helps mitigate manufacturing delays by minimizing the risk of contamination-related setbacks.

In principle, BVs can be removed in DSP. However, for some products like VLPs, this is difficult. The size, charge and density of BVs are often similar to that of secreted or enveloped VLPs, making downstream purification challenging and often resulting in decreased product yields (Cervera et al., 2019; Puente-Massaguer et al., 2022; Vicente et al., 2011). Product streams containing VLPs must undergo either chemical inactivation treatments to eliminate baculovirus infectivity or undergo multiple downstream processing steps that could potentially impact the amount and quality of the resulting VLPs (Roldão et al., 2010). This problem can be solved by

developing Baculovirus-free production processes, reducing losses in product yield and quality, and lowering the overall cost of production.

Baculovirus-free expression systems have been constructed by deletion of the essential baculovirus genes gp64 (Chaves et al., 2018), vp80 (Marek et al., 2011), or lef-5 (D. Hu et al., 2023). The deletion of these baculovirus genes results in the inability of viral propagation in conventional cell lines. BV amplification for seed production is achieved by developing a cell line that stably expresses the deleted gene in trans complementing the missing protein. However, such trans-complementing cell lines pose the risks of instability of the transgene expression and the ability of the baculovirus to regain the deleted gene. Recently, a CRISPR-Cas-based approach was developed to mediate the disruption of genes essential for BV formation, which relies on a CRISPR-Cas-expressing cell line (Bruder & Aucoin, 2023). In both above-mentioned approaches, two cell lines are needed for production where viral propagation is done in a separate production process in the complemented cell line to produce the seed for the final production process. The recombinant protein production is next done using this seed with another non-complemented cell line where a high MOI must be used for efficient VLP production.

In transient transfection, the target gene is introduced into insect cells without the use of a baculovirus vector, but for instance by use of a plasmid, thereby eliminating the risk of budded virus contamination. This method allows for rapid protein expression. Advantages include the avoidance of baculovirus vectors and the prevention of budded virus contamination. However, disadvantages include potential variability in transfection efficiency, difficulties in scaling up, and the need for optimization, as the transient expression may result in lower protein yields compared to the use of baculovirus vectors (Radner et al., 2012).

The need for two cell lines is not ideal for a production process. Furthermore, the need to infect the final production at high MOI is also sub-optimal, since it requires the production of large numbers of BV particles and thus large bioreactor systems. Therefore, the ideal BV-free system should use one virus strain and one cell line and allow for low MOI processes. A low MOI process ensures that smaller virus stocks can be used in the production process, leading to significant cost and time savings. Using the same cell line and baculovirus constructs throughout the process simplifies the production process from start to finish. Such a baculovirus-free production system should still exhibit flexibility to accommodate evolving demands without compromising recombinant protein yield or process robustness. Furthermore, it should be easily scalable and seamlessly integrated within existing production facilities. Lastly, an ideal system should comply with existing regulatory requirements to make the approval process more streamlined and faster.

For this reason, we developed a novel temperature-sensitive baculovirus expression system with an upstream reduction of baculovirus contaminants (BacFree) in **Chapter 4**. In this inducible system, BV production can be switched off during the production process. By introducing an isoleucine-to-threonine mutation in residue 317 (I317T) of GP41 a temperature-sensitive phenotype was observed. BV production appeared normal at 23.5°C (permissive temperature) but a single-cell infection was observed at 32.5°C (non-permissive temperature) (Lee & Miller, 1979; Olszewski & Miller, 1997). We investigated if the point mutation in GP41 I317T could

form the basis for a BEVS with a temperature-inducible shutdown of BV production to aid the production of chikungunya enveloped virus-like particles (CHIKV VLPs). For this system, a single cell line and virus strain are needed. At standard cultivation temperatures (27-28°C) virus propagation can take place while VLP production without BV release occurs at elevated temperatures (34°C). We showed that by using this temperature-sensitive baculovirus a 100-fold reduction in residual BV titer could be achieved after increasing the temperature. With this approach, low MOI processes are now also possible. Both low and high MOI processes were scalable to stirred-tank bioreactors. The next step is to assess the overall process robustness and productivity for this strategy. This approach eliminates the need for stable cell line development and allows for flexibility in the use of cell lines and MOIs. The reduced residual BV titer could reduce the burden of DSP purification steps and make regulatory approval more streamlined.

While the BacFree system is promising, further improvements are necessary to make the system more relevant for implementation on a commercial scale. To start, the productivity at elevated temperatures should be characterized better, and if possible, improved to ensure adequate process yield. While western blot analysis of secreted VLPs did not indicate reduced yields, production at higher temperatures has been shown to lower the yield of simpler, non-secreted proteins like green fluorescent protein (GFP). This could be an indication that the higher temperatures are not optimal for the protein production machinery inside the insect cell. Insect cells also seemed more vulnerable at elevated temperatures, as cell viability decreased at a faster rate compared to the standard temperature of 27-28°C. Lower productivity at elevated temperatures could potentially be solved in three ways; First, if this is related to the functioning of the insect cell, an adaptation of cells to higher temperatures could be beneficial. Maintaining high viability could prolong the production phase leading to higher protein yields. Second, if it is baculovirus related, modifying the baculovirus or viral promoters to maintain expression at elevated temperatures might be needed. Third, changing the temperature sensitivity of the baculovirus to be non-permissive at lower temperatures could circumvent problems related to elevated temperatures. From a commercial-scale perspective, heating requirements will be lower, and the required time to reach the setpoint after the temperature shift will be shorter. Complementary to these approaches are process intensification methods to achieve improved process yield and time savings. The proposed system can benefit from process intensification since it is still easily adaptable for various products and compatible with existing production capacity as will be discussed further on.

When using a low MOI infection strategy, only a small subset of the cells is infected initially, and multiple infection cycles are needed to infect all cells in the bioreactor. Such a low MOI infection strategy is advantageous in terms of virus stock requirements and offers a potentially shorter process development and production timelines, as less time-consuming virus titer assays are needed, and virus expansion steps are required. A good example of this is shown in **Chapter 2** where a low MOI infection strategy was used to produce SARS-CoV2-S1 subunits. Since a low MOI was used, newly generated P1 baculovirus stocks could immediately be used to infect bioreactors after the infectious titer was determined. However, in low MOI processes, infection, the release of BVs, and recombinant protein production do not occur synchronously for all cells, leading to increased process variation and complexity compared to high MOI processes. For the BacFree strategy, it becomes more difficult to determine the moment of temperature shift when

using a low MOI. Choosing the optimal moment is critical to obtain lower residual BV titers, as witnessed in **Chapter 4**. Online monitoring proved to be a helpful tool for determining the moment to shift the temperature.

Adequate process characterization is particularly important to ensure efficient process development and application of low MOI infection processes on a commercial scale. Process modeling would enhance the process understanding of such processes and benefit prediction and decision-making during process development. Besides quantitative characterization, such models would benefit from a better mechanistic understanding of the infection process and temperature sensitivity. Online monitoring, as described in more detail in **Chapter 3**, could aid in decision-making, tracking the state of the cell culture in real time, and further increasing process understanding. Data generated by online monitoring can be used as input for process modeling. Data from the high-resolution measurements and additional parameters that are measured can lead to new insights into underlying mechanisms or detect temporary process deviations that are otherwise unnoticed when using solely offline methods.

Besides improved process characterization and productivity, the production of BV particles could be further reduced. While a 100-fold reduction in BV titers was achieved, residual infectious BV titers were still in the order of  $10^5$  TCID<sub>50</sub>/mL and easily detectable by end-point dilution assays. Complete budded virus-free production might be challenging, especially when using low MOI infection strategies without washing steps, as residual BVs from earlier infection cycles might still be present. However, further reduction of residual BV titers would increase the product-to-BV ratio and provide an even better starting point for subsequent downstream processing.

The proposed strategy using a temperature-sensitive baculovirus is promising, since it reduces residual BV titers while allowing for the use of a low MOI and only one cell line and one baculovirus construct throughout the process. It is also easily adaptable for different products and implementable within existing production facilities. Before such a system can be cost-effective for commercial-scale applications, improvements must be made. Firstly, productivity should be characterized and where possible improved by either increasing protein yield at elevated temperature or reducing the non-permissive temperature. Second, further reduction of residual BV titers is desirable to improve industrial relevance. Lastly, optimization and characterization of the potentially elegant but complex temperature inducible low MOI BacFree strategy are required to reduce process variation and achieve a sufficient level of process robustness for application on larger industrial scales.

## 2. Proces intensification

Recently mRNA and adenovirus-based vaccines have been at the forefront of the fight against the covid-19 pandemic, and this has led to an acceleration in the development of the technology and increased interest from academia and industry, which is also reflected in the significant increase in investments (Florio et al., 2023). However, it has become evident that production-related challenges (such as Janssen's perfusion method versus Oxford-AstraZeneca's batch method) and storage conditions (requiring ultra-low temperatures of -80°C versus standard refrigeration at 4°C) play a crucial role in determining their ultimate success (Joe et al., 2023). For instance, the BEVS has several advantages compared to current mRNA technology such as a lower storage

temperatures of the final product, compatibility with currently installed production capacity and the ability to produce proteins with post-translational modifications. Further improvement and increased understanding of the BEVS is necessary to keep the platform relevant for tackling future global health challenges.

Process intensification could play a crucial role in enhancing the BEVS manufacturing platform, aiming to increase productivity, efficiency, and sustainability. Broadly, process intensification involves implementing various strategies, including the implementation of innovative technologies, advanced control systems, optimization, and automation to improve process performance. The main objectives of process intensification for BEVS manufacturing are:

1. **Cost Reduction:** For certain products, e.g., veterinary vaccines, a reduction of production costs is necessary since margins are low. Process intensification can lower costs by improving productivity, reducing raw material consumption, and minimizing waste and energy usage.
2. **Time reduction:** Production and development times should be as short as possible while the process should be robust yielding consistent product quality. This is essential to avoid delays due to unnecessary loss of batches during production and make process development and scale-up more straightforward and less time-consuming.
3. **Increased Capacity:** Process intensification allows manufacturers to enhance production capacity by producing more goods in less time using the same equipment. By improving the efficiency of manufacturing processes, manufacturers can meet increasing product demands without requiring significant additional capital investments.

The ideal BEVS platform process should have a high volumetric productivity, while still allowing for flexibility in adaptation to various products. High volumetric productivities allow for smaller production bioreactors, decreasing the size requirements of new or currently installed production capacity. Process intensification has the potential to establish improved production standards for the BEVS.

Process intensification has received considerable attention in the biopharmaceutical field in the past years and a vast array of strategies, tools, and platforms has been developed. Some examples of process intensification that are currently employed are the use of continuous processing strategies, such as perfusion (Tona et al., 2023), process miniaturization and automation through the use of miniaturized and automated bioreactor systems (Bhambure et al., 2011), and process integration through the use of multifunctional equipment and merging of multiple unit operations in a single device (Rathore et al., 2018). However, most applications are about processes with Chinese Hamster Ovary (CHO) cells, the workhorse of the biopharmaceutical industry (Strube et al., 2018). For the BEVS, known process intensification efforts have been limited. Most BEVS processes are still batch processes operated at relatively low cell densities and with limited online process monitoring.

The complexity of the BEVS makes process intensification challenging. Due to the lytic nature of the BEVS and associated issues with the stability of the baculovirus (Tramper et al., 1990), continuous production is difficult (van Lier et al., 1992; Van Lier et al., 1994). Scaling up from

laboratory scale to larger production scales is complicated due to maintaining consistent infection parameters, viral titer, and overall process control. Despite these challenges, ongoing research is focused on process intensification for the baculovirus expression system as there is a lot to gain:

1. Low MOI processes can reduce the necessary production capacity, as fewer bioreactors are needed for virus seed production.
2. Seed train intensification, e.g., N-1 perfusion, can shorten total bioprocessing time from the thaw of the working cell bank vial to the final harvest of the product as fewer seed expansion steps are needed and high cell density inoculations are possible.
3. Perfusion, fed-batch, or intensified fed-batch processes could increase the volumetric productivity of existing production facilities, by increasing yield per cell or total cell densities during bioprocessing.
4. Process analytical technology and modeling can improve process understanding, and allow for predictive capabilities and advanced process control, thereby shortening development times and enabling early detection of process deviations.

### 2.1 Intensification of the production step

Batch culture is commonly used to produce recombinant proteins with the BEVS. High-density perfusion processes are an attractive alternative to produce recombinant proteins due to the potential to increase volumetric productivity (Jäger, 1996). In a perfusion bioreactor, there is a continuous supply of fresh medium and removal of spent medium while the cells are retained in the bioreactor and the culture medium is gradually replaced by using a cell retention device. In this way, the cells are continuously supplied with nutrients and waste metabolites are continuously removed. This allows for reaching higher viable cell densities in the bioreactor. However, it has been observed that there is a reduction in specific productivity when infecting insect cells at cell densities above  $5 \times 10^6$  cells/mL (Bernal et al., 2009; Pijlman et al., 2020). This effect could be prevented by a continuous supply of nutrients and/or the removal of inhibitory products (Caron et al., 1994; Chico & Jäger, 2000; Ikonomidou et al., 2003; Radford et al., 1997). Carinhas et al (2009) showed that medium exchange could overcome the cell density effect at high MOI but not at low MOI for the Sf9 cell line in SF900II serum-free medium. In **Chapter 5** we reported the possibilities of using perfusion cultivation to enhance the volumetric productivity of a BEVS production process using a low MOI strategy. It was shown that medium exchange allowed for a higher cell density at infection (CCI) even when using a low MOI. It was possible to achieve complete baculovirus infection with CCIs up to  $20 \times 10^6$  viable cells/ using an MOI of 0.01 TCID<sub>50</sub>/cell when applying medium exchange, indicating that there is potential to improve maximum cell densities. Compared to the benchmark process, using a CCI of  $2.0 \times 10^6$  viable cells/mL and an MOI of 1 TCID<sub>50</sub>/cell, the volumetric productivity of the perfusion process infected at  $12 \times 10^6$  viable cells/mL with an MOI of 0.01 TCID<sub>50</sub>/cell was about 5 times higher. This shows that process intensification through perfusion and/or medium exchange is possible with the current BEVS system even when using low MOIs.

Limitations were also identified, namely oxygen supply and a slower rate of infection compared to high MOI processes infected at lower CCIs. Sparging-associated shear is a common and well-

studied cause of cell death. High cell density cultures require a high oxygen supply. The accompanying high oxygen flows could be a limitation to the achievable maximum cell density and cause excessive shear stress in the bioreactor. Sparging with smaller bubbles is advantageous as required oxygen flows will be significantly lower (Figure 1). However, in batch cultivation, it was observed that sparging with small oxygen bubbles using a porous sparger had a detrimental effect on cell viability and maximum cell densities. Most commercial media contain Pluronic to protect against sparging-associated shear stress. It was found that by adding more Pluronic, maximum cell densities and viability were comparable or even higher in cultures sparged with porous spargers compared to the reference process using an open hole sparger (Figure). Thus, it is expected that the use of a porous sparger complemented with the addition of extra Pluronic will be beneficial when working with a high cell density insect culture and might further improve the volumetric productivity.

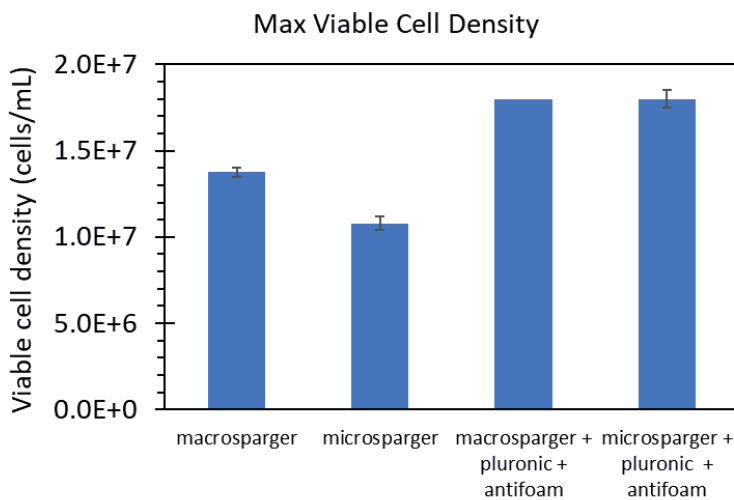


**Figure 1.** Maximum achieved viable cell densities for expisf9 batch cultures in bioreactors. Oxygen was either supplied through open hole sparging (macrosparger) or porous sparging (microsparger). For some conditions, Pluronic and antifoam were added to reduce sparging-associated shear stress. Error bars represent duplicate measurement values.

During the perfusion process, slow rates of baculovirus infection were observed, prolonging the process unnecessarily. This problem must be tackled to make BEVS perfusion a viable strategy. Virus stability is an issue, working with stable viruses that quickly replicate and produce large amounts of new viruses in subsequent infection cycles is essential. Selecting robust viral strains that have been engineered for their stability and high replication rates is essential. Optimizing infection conditions is another key aspect. Factors such as cell density, the multiplicity of infection (MOI), incubation time, and culture conditions should be systematically optimized to promote efficient viral replication. Through controlled experimentation, optimal conditions can be identified that maximize viral replication while ensuring cell viability and product quality. As stated, vector design and engineering can also play a significant role in improving virus stability and replication. By modifying the viral genome or expression cassette, factors such as promoter

strength and gene copy number can be optimized to influence viral replication and increase genome stability. This can lead to higher virus yields in subsequent infection cycles. Furthermore, host cell engineering can be employed to improve compatibility with viral replication machinery. Modifying host cell factors critical for viral entry, replication, or assembly can enhance the host-virus interaction, resulting in more efficient viral replication and increased production of baculoviruses.

## 2.2 Addition of 2-hydroxybutyrate and butyrate to insect cell cultures

Short-chain fatty acids are known to enhance protein synthesis in mammalian cell culture (Cherlet & Marc, 2000; Hendrick et al., 2001). Using such compounds in insect cell culture can be beneficial to improve the production of baculovirus particles, or boost the production of recombinant protein yield (Yovcheva et al., 2018). We found that the addition of butyrate or 2-hydroxybutyrate to the culture improved both protein yield and baculovirus production (Figure 2). Moreover, it was found that the addition of 2-hydroxybutyrate did not arrest growth of the cell culture, allowing a continuation of cell growth after addition and therefore making it more compatible with low MOI infection strategies. This contrasted with the addition of butyrate which arrested the cell in the G1 phase after addition (Figure 3). The perfusion process as reported in **Chapter 5** could benefit from the addition of such compounds, as it could improve the observed slow infection rate. The mechanisms behind the positive effects of 2-hydroxybutyrate addition to insect cell cultures are not completely clear. It could act as an alternative energy source, play a role in maintaining cellular redox balance, modulate intracellular signaling pathways, impact cell physiology, or interact with cellular metabolism (Krebs, 1967; Liu et al., 2019; Newman & Verdin, 2014; Puchalska & Crawford, 2017; Rashighi & Harris, 2017). While the exact mechanisms occurring after the addition of ketone bodies such as 2-hydroxybutyrate are still unknown, its use in insect cell culture looks promising to achieve higher protein yield, faster infection kinetics, and maintenance of cell viability.

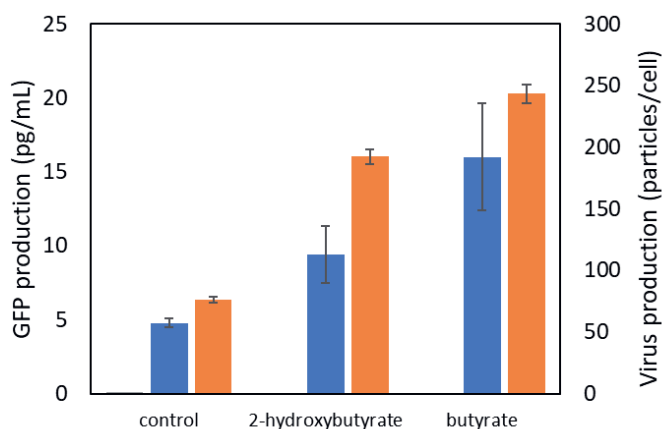


**Figure 2.** Effect of 2-hydroxybutyrate or butyrate addition on GFP production (blue) and virus particle production (orange). Cells were infected at a CCI of  $2 \cdot 10^6$  viable cells/mL and an MOI of 0.01 ivp/cell. Either 2-hydroxybutyrate or butyrate was added immediately after infection, for the control condition only baculovirus was added. Error bars represent duplicate measurement values (blue) or standard deviation (orange).

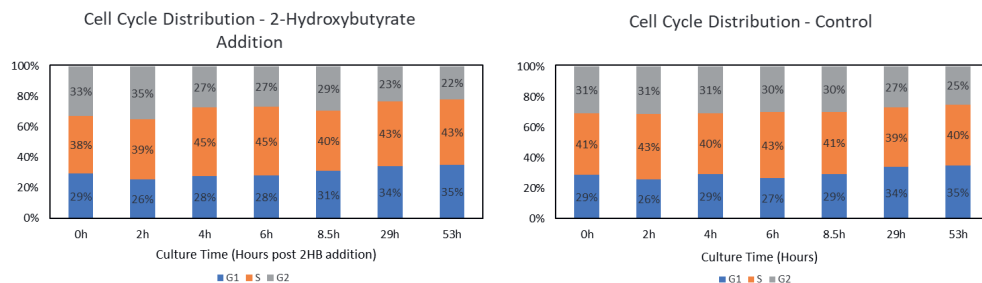


**Figure 3.** Cell cycle distribution after 2-hydroxybutyrate addition (left) and control without addition (right).

### 2.3 Process miniaturization

Process miniaturization is another effective tool to achieve process intensification, especially concerning process development for the BEVS, as it improves high-throughput data generation. At times when a rapid response to disease outbreaks is needed, and timelines for process development are limited, such tools can be instrumental in achieving considerable time savings. Due to the high throughput nature of such systems, large datasets can be generated in a short amount of time and with minimal resources. For instance, during the process development of the SARS-CoV2-S1 production process, as reported in **Chapter 2**, we utilized a 24-well plate microbioreactor (Figure 4) to screen for optimal pH before scaling up the process. This tool allowed us to screen a range of 8 different pH setpoints simultaneously and in triplicate using only one operator. In **Chapter 4** the non-permissive temperature for the temperature shift strategy was determined in the same way.

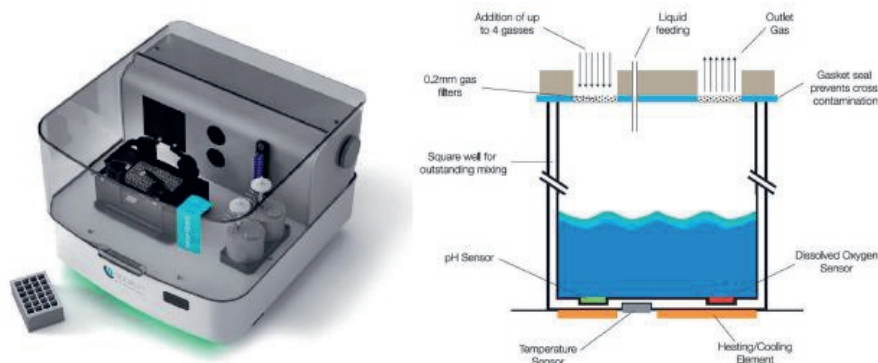


**Figure 4.** 24-well plate screening microbioreactor with a schematic representation of an individual well.

However, one should consider the differences in hydrodynamics, mass transfer, and mixing characteristics between small-scale and large-scale systems can affect process performance and productivity. It is essential to carefully assess the scalability of results obtained from miniaturized

bioreactors. Time-savings achieved by high throughput parallel processing using such systems can be wasted by delays from scale-up issues. The smaller volumes and limited accessibility can make it difficult to obtain representative samples for analysis, which may affect the accuracy of data interpretation and process understanding. Miniaturized bioreactors are more susceptible to operational variability and fluctuations. Even slight changes in operating conditions or procedural errors can have a more significant impact on the culture environment and process performance due to the smaller volume. This increased variability may require stricter process control measures and careful interpretation of results. Miniaturized bioreactor systems often require specific technical expertise for their operation, maintenance, and data analysis. Operators need to be familiar with the principles, operations, and workflows of these specialized systems. Acquiring and maintaining the necessary expertise may require additional training and investment. Nevertheless, having access to effective process miniaturization tools can speed up process development significantly. The ability to test at smaller scales greatly simplifies parallel testing. Flexibility is improved as it becomes easier to adjust process variables, experimental conditions and optimize operating conditions. Automation of such miniaturized processes allows for a single operator to generate large datasets that would otherwise require a team of skilled operators. Automation not only saves time and resources but also ensures consistent data collection and analysis, leading to more reliable insights and decision-making.

### 3. Online monitoring

Online monitoring has the capability to generate high-resolution data in (near) real-time. This can be used to (1) control process parameters within tight boundaries, (2) detect process deviations early allowing rapid process intervention or shut down, (3) make decisions in managing the process, e.g. when to add virus, change the temperature or harvest, and (4) obtain more insight in process dynamics to increase process understanding. With this in mind, online monitoring has many potential applications for the BEVS due to the lytic nature of the system and the associated complex interplay between parameters such as MOI, CCI, and TOH.

Currently, several physical probes are available to allow online measurements of biomass, such as dielectric spectroscopy and light scattering. Dielectric spectroscopy measures viable biomass based on biomass capacitance, whereas light scattering methods measure total biomass (Carvell & Dowd, 2006; Kiviharju et al., 2007; Ude et al., 2014). These methods are well suited for measuring cell biomass; however, they cannot directly measure the viability or infection stage of a single cell. Image-based cell culture monitoring is a more direct approach, where cells can be visualized individually to extract both the cell density and information on the state of the cells. An example of such an online imaging tool is online double digital differential holographic microscopy (D<sup>3</sup>HM) (Janicke et al., 2017; Rappaz et al., 2014). With this technique, the cell density is measured as well as a large number of optical parameters among which cell diameter and circularity, as well as quantitative parameters associated with the light phase and light intensity of each cell.

### Online double digital differential holographic microscopy (D3HM)

In **Chapter 3** we reported the real-time online monitoring of insect cell proliferation and baculovirus infection using double digital differential holographic microscopy and machine learning. D3HM allowed us to obtain information on the state of the cell culture at the individual cell level by capturing holographic images of the cells. These holographic pictures allowed for direct calculation of the cell concentration and analysis of a large set of optical cell parameters that can be linked to the state of the cell. For example, upon baculovirus infection, distinct changes in cell morphology occur such as cell enlargement and changes in the granularity of the cell (Kamen et al., 1996; Schopf et al., 1990; Taticek & Shuler, 1997). Specific optical changes also occur if the cell loses viability. Changes in measured optical parameters were then linked to the infection state and viability by a machine-learning model (Figure 5). After training the machine algorithm with a training data set, the cell density, cell viability, cell diameter, and the fraction of infected cells could be accurately determined for a variety of bioreactor processes. These high-resolution time-series profiles gave more insight into the state of the cell culture inside the bioreactor. Infected cells could be detected earlier compared to offline methods and the effect of process interventions such as feeding became distinguishable. Limited data sets (2-3 runs) are needed to train the initial machine-learning model. Each newly generated data set can be used to improve the machine learning algorithms and can be used retroactively by re-calculating old data sets. The variety of cell parameters computed by the microscope potentially contains a wealth of information on the biological state of the cells. Linking these parameters to cell physiology could lead to further insights into the state of the cell culture.

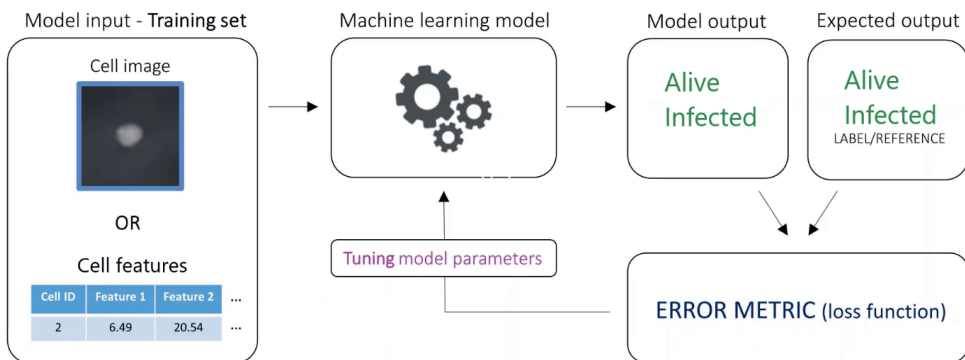


**Figure 5.** Workflow for training the machine learning model to detect alive and dead cells.

Real-time tracking of viral infection dynamics allows better insights into the progress of the infection, optimal harvest timing, and culture viability. In **Chapter 2** a D3HM online microscope was used to help determine the optimal harvest moment of SARS-CoV2-S1 protein. In **Chapter 5** we reported the use of the D3HM microscope to determine the optimal moment of temperature shift when using a low MOI strategy. Currently, online D3HM depends on the continuous circulation of cell culture through the flow chamber of the online microscope. When the bioreactor working volume is large, the experienced effects on oxygen transfer (due to the

permeability of the tubing) and cell viability (due to shear stress) are negligible. However, when using low working volumes >500 mL, the continuous circulation of cell culture fluid has detrimental effects on cell viability. Therefore, the minimum working volume has to be taken into account when using online D3HM.

### **D3HM for virus titer determination**

Since D3HM enables label-free detection of infected cells, this technique could potentially be used to develop an improved virus titer assay. Currently, infectious BV titers are often determined using end-point dilution assays which take up to seven days to read out the result. Other methods include expensive analyzers or cumbersome staining methods. Faster analysis of infectious titers and accurate characterization of virus uptake and release enable a more systematic and efficient Quality by Design implementation. Using D3HM for this purpose could potentially be a huge benefit in terms of time savings and would allow for faster determination of infectious titers. Such a method would also be more suitable for high-throughput analysis compared to end-point dilution assays and consume significantly fewer resources making it a viable option for smaller-scale laboratories. A major challenge of this method is the detection of slight changes in infection percentages. It is essential to detect these slight changes to effectively predict the progression and timelines of baculovirus infection. Despite being faster and less labor-intensive compared to methods commonly used, the proposed method would still involve a 24-hour delay between sampling and infectious titer determination. Information on infectious titers is essential to optimize infection conditions, control the virus-cell ratio, and improve process reproducibility and consistency. An ideal method would be to measure virus titers online or in near real-time. Since infectious titers and MOI are a big source of variability in a production process, near real-time measurements of these parameters would allow more accurate process control. This, in turn, leads to improved process intensification by reducing process development time, minimizing batch failures, and enhancing overall product quality.

### **Conclusion**

Baculovirus-free production can improve process yield and make regulatory approval more streamlined. The proposed BacFree strategy works in existing production facilities and is compatible with low MOI strategies, diminishing the need for large virus seed production. Further reductions in residual BV titers and better characterization of productivity at elevated temperatures are necessary to establish the proposed BacFree strategy as an industry standard.

The BEVS can benefit significantly from process intensification. Through perfusion, high cell-density infections can be performed at low MOI to improve volumetric productivity. This enables manufacturers to meet product demand without requiring significant additional capital investments. The proposed perfusion strategy could be optimized further, by improving viral infection kinetics to shorten production time and optimizing for optimal CCI. Combination with the proposed BacFree strategy could improve product yield, while simultaneously reducing residual BV titers.

Online D3HM has the capability to generate high-resolution data of BEVS bioreactor processes in (near) real-time. This can be used to control process parameters, detect process deviations

early, and make decisions in managing the process, for instance when to add the baculovirus, change the temperature, or harvest. The variety of cell parameters computed by the microscope potentially hides a wealth of information on the biological state of the cells. Linking these parameters to cell physiology could lead to further insights into the state of the cell culture.

So far, the BEVS has been a particularly attractive technology to produce vaccines and gene therapy vectors. Predicting which technology will have the most significant long-term impact remains challenging. The prevailing consensus suggests that multiple production platforms should coexist, considering that the adoption of each technology is driven by a cost-benefit analysis. For the BEVS to remain a viable alternative to other technologies and effectively address current and future global health issues, it must continuously undergo substantial optimization, characterization, and improvement. This way, its full potential can be harnessed to tackle various health challenges worldwide.

## References

1. Addetia, A., Crawford, K. H. D., Dingens, A., Zhu, H., Roychoudhury, P., Huang, M. L., Jerome, K. R., Bloom, J. D., & Greninger, A. L. (2020). Neutralizing antibodies correlate with protection from SARS-CoV-2 in humans during a fishery vessel outbreak with a high attack rate. *Journal of Clinical Microbiology*, 58(11). <https://doi.org/10.1128/JCM.02107-20>
2. Altenburg, J. J., Klaverdijk, M., Cabosart, D., Desmecht, L., Brunekreeft-Terlouw, S. S., Both, J., Tegelbeckers, V. I. P., Willekens, M. L. P. M., van Oosten, L., Hick, T. A. H., van der Aalst, T. M. H., Pijlman, G. P., van Oers, M. M., Wijffels, R. H., & Martens, D. E. (2022). Real-time online monitoring of insect cell proliferation and baculovirus infection using digital differential holographic microscopy and machine learning. *Biotechnology Progress*, e3318. <https://doi.org/10.1002/BTPR.3318>
3. Angelo, M. G., Zima, J., Tavares Da Silva, F., Baril, L., & Arellano, F. (2014). Post-licensure safety surveillance for human papillomavirus-16/18-AS04-adjuvanted vaccine: More than 4years of experience. In *Pharmacoepidemiology and Drug Safety* (Vol. 23, Issue 5, pp. 456–465). John Wiley and Sons Ltd. <https://doi.org/10.1002/pds.3593>
4. Anurag S Rathore, & Helen Winkle. (2009). Quality-by-design approach. *Nature Biotechnology*, 27(1), 26–34. <https://doi.org/10.1038/nbt0109-26>
5. Arunachalam, P. S., Walls, A. C., Golden, N., Atyeo, C., Fischinger, S., Li, C., Aye, P., Navarro, M. J., Lai, L., Edara, V. V., Röltgen, K., Rogers, K., Shirreff, L., Ferrell, D. E., Wrenn, S., Pettie, D., Kraft, J. C., Miranda, M. C., Kepl, E., ... Pulendran, B. (2021). Adjuvanting a subunit COVID-19 vaccine to induce protective immunity. *Nature*, 1–6. <https://doi.org/10.1038/s41586-021-03530-2>
6. Azali, M. A., Mohamed, S., Harun, A., Hussain, F. A., Shamsuddin, S., & Johan, M. F. (2022). Application of Baculovirus Expression Vector system (BEV) for COVID-19 diagnostics and therapeutics: a review. *Journal of Genetic Engineering and Biotechnology*, 20(1). <https://doi.org/10.1186/s43141-022-00368-7>
7. Bachmann, M. F., & Jennings, G. T. (2010). Vaccine delivery: a matter of size, geometry, kinetics and molecular patterns. *Nature Reviews Immunology* 2010 10:11, 10(11), 787–796. <https://doi.org/10.1038/nri2868>
8. Bachmann, M. F., Mohsen, M. O., Zha, L., Vogel, M., & Speiser, D. E. (2021). SARS-CoV-2 structural features may explain limited neutralizing-antibody responses. *Npj Vaccines*, 6(1), 1–5. <https://doi.org/10.1038/s41541-020-00264-6>
9. Baden, L. R., El Sahly, H. M., Essink, B., Kotloff, K., Frey, S., Novak, R., Diemert, D., Spector, S. A., Roupheal, N., Creech, C. B., McGettigan, J., Khetan, S., Segall, N., Solis, J., Brosz, A., Fierro, C., Schwartz, H., Neuzil, K., Corey, L., ... Zaks, T. (2021). Efficacy and safety of the mRNA-1273 SARS-CoV-2 vaccine. *New England Journal of Medicine*, 384(5), 403–416. <https://doi.org/10.1056/nejmoa2035389>
10. Bernal, V., Carinhas, N., Yokomizo, A. Y., Carrondo, M. J. T., & Alves, P. M. (2009). Cell density effect in the baculovirus-insect cells system: A quantitative analysis of energetic

- metabolism. *Biotechnology and Bioengineering*, 104(1), 162-180.  
<https://doi.org/10.1002/bit.22364>
11. Bhambure, R., Kumar, K., & Rathore, A. S. (2011). High-throughput process development for biopharmaceutical drug substances. *Trends in Biotechnology*, 29(3), 127-135.  
<https://doi.org/10.1016/j.tibtech.2010.12.001>
  12. Boezen, D., Ali, G., Wang, M., Wang, X., van der Werf, W., Vlak, J. M., & Zwart, M. P. (2022). Empirical estimates of the mutation rate for an alphabaculovirus. *PLOS Genetics*, 18(6), e1009806. <https://doi.org/10.1371/journal.pgen.1009806>
  13. Braunagel, S. C., Parr, R., Belyavskiy, M., & Summers, M. D. (1998). *Autographa californica* nucleopolyhedrovirus infection results in Sf9 cell cycle arrest at G2/M phase. *Virology*, 244(1), 195-211. <https://doi.org/10.1006/viro.1998.9097>
  14. Brouwer, P. J. M., Antanasijevic, A., Berndsen, Z., Yasmeen, A., Fiala, B., Bijl, T. P. L., Bontjer, I., Bale, J. B., Sheffler, W., Allen, J. D., Schorcht, A., Burger, J. A., Camacho, M., Ellis, D., Cottrell, C. A., Behrens, A. J., Catalano, M., del Moral-Sánchez, I., Ketas, T. J., ... Sanders, R. W. (2019). Enhancing and shaping the immunogenicity of native-like HIV-1 envelope trimers with a two-component protein nanoparticle. *Nature Communications*, 10(1). <https://doi.org/10.1038/s41467-019-12080-1>
  15. Brown, M., Crawford, A. M., & Faulkner, P. (1979). Genetic analysis of a baculovirus, *Autographa californica* nuclear polyhedrosis virus I. Isolation of temperature-sensitive mutants and assortment into complementation groups. *Journal of Virology*, 31(1), 190-198. <https://doi.org/10.1128/JVI.31.1.190-198.1979>
  16. Bruder, M. R., & Aucoin, M. G. (2023). Evaluation of virus-free manufacture of recombinant proteins using CRISPR-mediated gene disruption in baculovirus-infected insect cells. *Vaccines*, 11(2), 225. <https://doi.org/10.3390/vaccines11020225>
  17. Brune, K. D., Leneghan, D. B., Brian, I. J., Ishizuka, A. S., Bachmann, M. F., Draper, S. J., Biswas, S., & Howarth, M. (2016). Plug-and-Display: decoration of virus-like particles via isopeptide bonds for modular immunization. *Scientific Reports*, 6(1), 1-13.  
<https://doi.org/10.1038/srep19234>
  18. Buckland, B., Boulanger, R., Fino, M., Srivastava, I., Holtz, K., Khramtsov, N., McPherson, C., Meghrou, J., Kubera, P., & Cox, M. M. J. (2014). Technology transfer and scale-up of the Flublok® recombinant hemagglutinin (HA) influenza vaccine manufacturing process. *Vaccine*, 32(42), 5496-5502. <https://doi.org/10.1016/j.vaccine.2014.07.074>
  19. Byun, S., Hecht, V. C., & Manalis, S. R. (2015). Article Characterizing Cellular Biophysical Responses to Stress by Relating. *Biophysj*, 109(8), 1565-1573.  
<https://doi.org/10.1016/j.bpj.2015.08.038>
  20. Carinhas, N., Bernal, V., Oliveira, R., & Alves, P. M. (2009). Baculovirus production for gene therapy : the role of cell density , multiplicity of infection and medium exchange. 1041-1049. <https://doi.org/10.1007/s00253-008-1727-4>
  21. Caron, A. W., Archambault, J., & Massie, B. (1990). High-level recombinant protein production in bioreactors using the baculovirus-insect cell expression system.

- Biotechnology and Bioengineering, 36(11), 1133–1140.  
<https://doi.org/10.1002/bit.260361108>
22. Caron, A. W., Tom, R. L., Kamen, A. A., & Massie, B. (1994). Baculovirus expression system scaleup by perfusion of high-density Sf-9 cell cultures. *Biotechnology and Bioengineering*, 43(9), 881–891. <https://doi.org/10.1002/BIT.260430907>
  23. Carrillo, J., Izquierdo-Useros, N., Ávila-Nieto, C., Pradenas, E., Clotet, B., & Blanco, J. (2021). Humoral immune responses and neutralizing antibodies against SARS-CoV-2; implications in pathogenesis and protective immunity. *Biochemical and Biophysical Research Communications*, 538, 187–191. <https://doi.org/10.1016/j.bbrc.2020.10.108>
  24. Carstens, E. B., Chan, H., Yu, H., Williams, G. V., & Casselman, R. (1994). Genetic analyses of temperature-sensitive mutations in baculovirus late expression factors. *Virology*, 204(1), 323–337. <https://doi.org/10.1006/VIRO.1994.1537>
  25. Carvalho, T., Krammer, F., & Iwasaki, A. (2021). The first 12 months of COVID-19: a timeline of immunological insights. In *Nature Reviews Immunology* (Vol. 21, Issue 4, pp. 245–256). Nature Research. <https://doi.org/10.1038/s41577-021-00522-1>
  26. Carvell, J. P., & Dowd, J. E. (2006). On-line measurements and control of viable cell density in cell culture manufacturing processes using radio-frequency impedance. *Cytotechnology*, 50(1–3), 35–48. <https://doi.org/10.1007/s10616-005-3974-x>
  27. Cervera, L., Gòdia, F., Tarrés-Freixas, F., Aguilar-Gurrieri, C., Carrillo, J., Blanco, J., & Gutiérrez-Granados, S. (2019). Production of HIV-1-based virus-like particles for vaccination: achievements and limits. *Applied Microbiology and Biotechnology*, 103(18), 7367–7384. <https://doi.org/10.1007/s00253-019-10038-3>
  28. Cervera, L., Gòdia, F., Tarrés-Freixas, F., Aguilar-Gurrieri, C., Carrillo, J., Blanco, J., & Gutiérrez-Granados, S. (2019). Production of HIV-1-based virus-like particles for vaccination: achievements and limits. *Applied Microbiology and Biotechnology*, 103(18), 7367–7384. <https://doi.org/10.1007/s00253-019-10038-3>
  29. Chaves, L. C. S., Ribeiro, B. M., & Blissard, G. W. (2018). Production of GP64-free virus-like particles from baculovirus-infected insect cells. *Journal of General Virology*, 99(2), 265–274. <https://doi.org/10.1099/jgv.0.001002>
  30. Cherlet, M., & Marc, A. (2000). Stimulation of monoclonal antibody production of hybridoma cells by butyrate: Evaluation of a feeding strategy and characterization of cell behaviour. *Cytotechnology*, 32(1), 17–29. <https://doi.org/10.1023/A:1008069523163>
  31. Chico, E., & Jäger, V. (2000). Perfusion culture of baculovirus-infected BTI-Tn-5B1-4 insect cells: A method to restore cell-specific  $\beta$ -trace glycoprotein productivity at high cell density. *Biotechnology and Bioengineering*, 70(5), 574–586. [https://doi.org/10.1002/1097-0290\(20001205\)70:5<574::AID-BIT12>3.0.CO;2-Q](https://doi.org/10.1002/1097-0290(20001205)70:5<574::AID-BIT12>3.0.CO;2-Q)
  32. Chisti, Y. (2000). Animal-cell damage in sparged bioreactors. *Trends in Biotechnology*, 18(10), 420–432. [https://doi.org/10.1016/S0167-7799\(00\)01474-8](https://doi.org/10.1016/S0167-7799(00)01474-8)
  33. Chun, J., Cho, Y., Park, K. H., Choi, H., Cho, H., Lee, H. J., Jang, H., Kim, K. H., Oh, Y. K., & Kim, Y. B. (2019). Effect of fc fusion on folding and immunogenicity of middle east

- respiratory syndrome coronavirus spike protein. *Journal of Microbiology and Biotechnology*, 29(5), 813–819. <https://doi.org/10.4014/jmb.1903.03043>
34. Coutard, B., Valle, C., de Lamballerie, X., Canard, B., Seidah, N. G., & Decroly, E. (2020). The spike glycoprotein of the new coronavirus 2019-nCoV contains a furin-like cleavage site absent in CoV of the same clade. *Antiviral Research*, 176(February), 104742. <https://doi.org/10.1016/j.antiviral.2020.104742>
35. Cox, M. (2017). Modern technology: The preferred biosecurity strategy? In *Vaccine* (Vol. 35, Issue 44, pp. 5949–5950). <https://doi.org/10.1016/j.vaccine.2017.03.048>
36. Cox, M. M. J. (2021). Innovations in the insect cell expression system for industrial recombinant vaccine antigen production. *Vaccines*, 9(12), 1504. <https://doi.org/10.3390/vaccines9121504>
37. Cox, M. M. J., & Hashimoto, Y. (2011). A fast track influenza virus vaccine produced in insect cells. *Journal of Invertebrate Pathology*, 107(SUPPL.), S31–S41. <https://doi.org/10.1016/j.jip.2011.05.003>
38. Cox, M. M. J., Izikson, R., Post, P., & Dunkle, L. (2015). Safety, efficacy, and immunogenicity of Flublok in the prevention of seasonal influenza in adults. *Therapeutic Advances in Vaccines*, 3(4), 97–108. <https://doi.org/10.1177/2051013615595595>
39. Dalm, M. (2007). **ACOUSTIC PERFUSION PROCESSES FOR HYBRIDOMA CULTURES: Viability, cell cycle and metabolic analysis.** [Ph.D. Thesis]. Wageningen University & Research, The Netherlands.
40. Dalm, M. C. F., Cuijten, S. M. R., Van Grunsven, W. M. J., Tramper, J., & Martens, D. E. (2004). Effect of feed and bleed rate on hybridoma cells in an acoustic perfusion bioreactor: Part I. Cell density, viability, and cell-cycle distribution. *Biotechnology and Bioengineering*, 88(5), 547–557. <https://doi.org/10.1002/bit.20287>
41. De Vincenzo, R., Conte, C., Ricci, C., Scambia, G., & Capelli, G. (2014). Long-term efficacy and safety of human papillomavirus vaccination. In *International Journal of Women's Health* (Vol. 6, pp. 999–1010). Dove Medical Press Ltd. <https://doi.org/10.2147/IJWH.S50365>
42. Ding, X., Peng, Z., Lin, S. C. S., Geri, M., Li, S., Li, P., Chen, Y., Dao, M., Suresh, S., & Huang, T. J. (2014). Cell separation using tilted-angle standing surface acoustic waves. *Proceedings of the National Academy of Sciences of the United States of America*, 111(36), 12992–12997. <https://doi.org/10.1073/pnas.1413325111>
43. Domínguez-Andrés, J., van Crevel, R., Divangahi, M., & Netea, M. G. (2020). Designing the next generation of vaccines: Relevance for future pandemics. *MBio*, 11(6), 1–16. <https://doi.org/10.1128/mBio.02616-20>
44. Dowd, J. E., Jubb, A., Kwok, K. E., & Piret, J. M. (2003). Optimization and control of perfusion cultures using a viable cell probe and cell specific perfusion rates. *Cytotechnology*, 42(1), 35–45. <https://doi.org/10.1023/A:1026192228471>
45. Esposito, D., Mehalko, J., Drew, M., Snead, K., Wall, V., Taylor, T., Frank, P., Denson, J. P., Hong, M., Gulten, G., Sadtler, K., Messing, S., & Gillette, W. (2020). Optimizing high-

- yield production of SARS-CoV-2 soluble spike trimers for serology assays. *Protein Expression and Purification*, 174. <https://doi.org/10.1016/j.pep.2020.105686>
46. Fan, X., Cao, D., Kong, L., & Zhang, X. (2020). Cryo-EM analysis of the post-fusion structure of the SARS-CoV spike glycoprotein. *Nature Communications*, 11(1). <https://doi.org/10.1038/s41467-020-17371-6>
47. FDA. (2010). *Guidance for Industry Cell Characterization and Qualification of Cell Substrates and Other Biological Materials Used in the Production of Viral Vaccines for Infectious Disease Indications*. FDA Guidance for Industry, February, 1–50. <https://www.fda.gov/downloads/BiologicsBloodVaccines/GuidanceComplianceRegulatoryInformation/Guidances/Vaccines/UCM202439.pdf>
48. Felberbaum, R. S. (2015). The baculovirus expression vector system: A commercial manufacturing platform for viral vaccines and gene therapy vectors. *Biotechnology Journal*, 10(5), 702–714. <https://doi.org/10.1002/biot.201400438>
49. Fernandes, B., Correia, R., Alves, P. M., & Roldão, A. (2022). Intensifying continuous production of Gag-HA VLPs at high cell density using stable insect cells adapted to low culture temperature. *Frontiers in Bioengineering and Biotechnology*, 10, 1. <https://doi.org/10.3389/fbioe.2022.917746>
50. Fernandes, F., Teixeira, A. P., Carinhas, N., Carrondo, M. J. T., & Alves, P. M. (2013). Insect cells as a production platform of complex virus-like particles. In *Expert Review of Vaccines* (Vol. 12, Issue 2, pp. 225–236). <https://doi.org/10.1586/erv.12.153>
51. Fougereux, C., Goksøyr, L., Idorn, M., Soroka, V., Myeni, S. K., Dagil, R., Janitzek, C. M., Søgaard, M., Aves, K.-L., Horsted, E. W., Erdoğan, S. M., Gustavsson, T., Dorosz, J., Clemmensen, S., Fredsgaard, L., Thrane, S., Vidal-Calvo, E. E., Khalifé, P., Hulen, T. M., ... Sander, A. F. (2021). Capsid-like particles decorated with the SARS-CoV-2 receptor-binding domain elicit strong virus neutralization activity. *Nature Communications*, 12(1), 324. <https://doi.org/10.1038/s41467-020-20251-8>
52. Fredsgaard, L., Goksøyr, L., Thrane, S., Aves, K. L., Theander, T. G., & Sander, A. F. (2021). Head-to-head comparison of modular vaccines developed using different capsid virus-like particle backbones and antigen conjugation systems. *Vaccines*, 9(6), 539. <https://doi.org/10.3390/vaccines9060539>
53. Frishman, D., & Argos, P. (1995). Knowledge-based protein secondary structure assignment. *Proteins: Structure, Function, and Bioinformatics*, 23(4), 566–579. <https://doi.org/10.1002/prot.340230412>
54. Fuenmayor, J., Gòdia, F., & Cervera, L. (2017). Production of virus-like particles for vaccines. *New Biotechnology*, 39, 174–180. <https://doi.org/10.1016/j.nbt.2017.07.010>
55. Gallo-Ramírez, L. E., Nikolay, A., Genzel, Y., & Reichl, U. (2015). Bioreactor concepts for cell culture-based viral vaccine production. *Expert Review of Vaccines*, 14(9), 1181–1195. <https://doi.org/10.1586/14760584.2015.1067144>
56. Goepfert, P. A., Fu, B., Chabanon, A.-L., Bonaparte, M. I., Davis, M. G., Essink, B. J., Frank, I., Haney, O., Janosczyk, H., Keefer, M. C., Koutsoukos, M., Kimmel, M. A.,

- Masotti, R., Savarino, S. J., Schuerman, L., Schwartz, H., Sher, L. D., Smith, J., Tavares-Da-Silva, F., ... de Bruyn, G. (2021). Safety and immunogenicity of SARS-CoV-2 recombinant protein vaccine formulations in healthy adults: interim results of a randomised, placebo-controlled, phase 1-2, dose-ranging study. *The Lancet Infectious Diseases*. [https://doi.org/10.1016/s1473-3099\(21\)00147-x](https://doi.org/10.1016/s1473-3099(21)00147-x)
57. Gomes, A. R., Byregowda, S. M., Veeregowda, B. M., & Balamurugan, V. (2016). An Overview of Heterologous Expression Host Systems for the Production of Recombinant Proteins. *Advances in Animal and Veterinary Sciences*, 4(4), 346–356. <https://doi.org/10.1016/j.revmic.2007.02.006>
58. González-Domínguez, I., Puente-Massaguer, E., Cervera, L., & Gòdia, F. (2020). Quality assessment of virus-like particles at single particle level: A comparative study. *Viruses*, 12(2), 223. <https://doi.org/10.3390/v12020223>
59. Gordon, J. D., & Carstens, E. B. (1984). Phenotypic characterization and physical mapping of a temperature-sensitive mutant of *Autographa californica* nuclear polyhedrosis virus defective in DNA synthesis. *Virology*, 138(1), 69–81. [https://doi.org/10.1016/0042-6822\(84\)90148-X](https://doi.org/10.1016/0042-6822(84)90148-X)
60. Guebre-Xabier, M., Patel, N., Tian, J. H., Zhou, B., Maciejewski, S., Lam, K., Portnoff, A. D., Massare, M. J., Frieman, M. B., Piedra, P. A., Ellingsworth, L., Glenn, G., & Smith, G. (2020). NVX-CoV2373 vaccine protects cynomolgus macaque upper and lower airways against SARS-CoV-2 challenge. *Vaccine*, 38(50), 7892–7896. <https://doi.org/10.1016/J.VACCINE.2020.10.064>
61. Guo, R., Zhang, Y., Liang, S., Xu, H., Zhang, M., & Li, B. (2010). Sodium butyrate enhances the expression of baculovirus-mediated sodium/iodide symporter gene in A549 lung adenocarcinoma cells. *Nuclear Medicine Communications*, 31(10), 916–921. <https://doi.org/10.1097/MNM.0b013e328333dedd7>
62. Gupta, R., Arora, K., Roy, S. S., Joseph, A., Rastogi, R., Arora, N. M., & Kundu, P. K. (2023). Platforms, advances, and technical challenges in virus-like particles-based vaccines. *Frontiers in Immunology*, 14. <https://doi.org/10.3389/FIMMU.2023.1123805>
63. Harrison, R. L., & Jarvis, D. L. (2006). Protein N-glycosylation in the baculovirus-insect cell expression system and engineering of insect cells to produce “mammalianized” recombinant glycoproteins. In *Advances in Virus Research* (Vol. 68, pp. 159–191). Academic Press. [https://doi.org/10.1016/S0065-3527\(06\)68005-6](https://doi.org/10.1016/S0065-3527(06)68005-6)
64. Haun, B. K., Lai, C. Y., Williams, C. A., Wong, T. A. S., Lieberman, M. M., Pessaint, L., Andersen, H., & Lehrer, A. T. (2020). CoVaccine HTTM Adjuvant Potentiates Robust Immune Responses to Recombinant SARS-CoV-2 Spike S1 Immunization. *Frontiers in Immunology*, 11, 2780. <https://doi.org/10.3389/fimmu.2020.599587>
65. Heitz, F., Nay, C., & Guenet, C. (1997). Expression of functional human muscarinic M2 receptors in different insect cell lines. *Journal of Receptor and Signal Transduction Research*, 17(1–3), 305–317. <https://doi.org/10.3109/10799899709036611>

66. Hendrick, V., Winnepeninckx, P., Abdelkafi, C., Vandeputte, O., Cherlet, M., Marique, T., Renemann, G., Loa, A., Kretzmer, G., & Werenne, J. (2001). Increased productivity of recombinant tissular plasminogen activator (t-PA) by butyrate and shift of temperature: A cell cycle phases analysis. *Cytotechnology*, 36(1-3), 71-83.  
<https://doi.org/10.1023/A:1014088919546>
67. Hervás-Stubbs, S., Rueda, P., Lopez, L., & Leclerc, C. (2007). Insect Baculoviruses Strongly Potentiate Adaptive Immune Responses by Inducing Type I IFN. *The Journal of Immunology*, 178(4), 2361-2369. <https://doi.org/10.4049/jimmunol.178.4.2361>
68. Hoffmann, M., Kleine-Weber, H., Schroeder, S., Krüger, N., Herrler, T., Erichsen, S., Schiergens, T. S., Herrler, G., Wu, N. H., Nitsche, A., Müller, M. A., Drosten, C., & Pöhlmann, S. (2020). SARS-CoV-2 cell entry depends on ACE2 and TMPRSS2 and is blocked by a clinically proven protease inhibitor. *Cell*, 181(2), 271-280.e8.  
<https://doi.org/10.1016/j.cell.2020.02.052>
69. Hong, M., Li, T., Xue, W., Zhang, S., Cui, L., Wang, H., Zhang, Y., Zhou, L., Gu, Y., Xia, N., & Li, S. (2022). Genetic engineering of baculovirus-insect cell system to improve protein production. *Frontiers in Bioengineering and Biotechnology*, 10(September), 1-15.  
<https://doi.org/10.3389/fbioe.2022.994743>
70. Hopkins, R. F., & Esposito, D. (2009). A rapid method for titrating baculovirus stocks using the Sf-9 Easy Titer cell line. *BioTechniques*, 47(3), 785-788.  
<https://doi.org/10.2144/000113238>
71. Hu, D., Xie, X., Zhang, T., Yu, Y., Xu, Z., Zhang, Y., & Liu, Q. (2023). A lef5-deficient baculovirus expression system with no virion contamination and promoting secretion. *Journal of Biotechnology*, 365, 20-28. <https://doi.org/10.1016/j.jbiotec.2023.01.013>
72. Hu, D., Xie, X., Zhang, T., Yu, Y., Xu, Z., Zhang, Y., & Liu, Q. (2023). A lef5-deficient baculovirus expression system with no virion contamination and promoting secretion. *Journal of Biotechnology*, 365(November 2022), 20-28.  
<https://doi.org/10.1016/j.jbiotec.2023.01.013>
73. Hu, Y. C. (2005). Baculovirus as a highly efficient expression vector in insect and mammalian cells. *Acta Pharmacologica Sinica*, 26(4), 405-416.  
<https://doi.org/10.1111/j.1745-7254.2005.00078.x>
74. Hua, Z., & Hou, B. (2013). TLR signaling in B-cell development and activation. In *Cellular and Molecular Immunology* (Vol. 10, Issue 2, pp. 103-106). Nature Publishing Group.  
<https://doi.org/10.1038/cmi.2012.61>
75. Huang, N., Wu, W., Yang, K., Passarelli, A. L., Rohrmann, G. F., & Clem, R. J. (2011). Baculovirus Infection Induces a DNA Damage Response That Is Required for Efficient Viral Replication. *Journal of Virology*, 85(23), 12547-12556.  
<https://doi.org/10.1128/jvi.05766-11>
76. Ikonomidou, L., Schneider, Y. J., & Agathos, S. N. (2003). Insect cell culture for industrial production of recombinant proteins. *Applied Microbiology and Biotechnology*, 62(1), 1-20. <https://doi.org/10.1007/s00253-003-1223-9>

77. Jäger, V. (1996). Perfusion bioreactors for the production of recombinant proteins in insect cells. 191–198. [https://doi.org/10.1007/0-306-46850-6\\_16](https://doi.org/10.1007/0-306-46850-6_16)
78. Janakiraman, V., Forrest, W. F., Chow, B., & Seshagiri, S. (2006). A rapid method for estimation of baculovirus titer based on viable cell size. *Journal of Virological Methods*, 132(1–2), 48–58. <https://doi.org/10.1016/J.JVIROMET.2005.08.021>
79. Janicke, B., Kårnsnäs, A., Egelberg, P., & Alm, K. (2017). Label-free high temporal resolution assessment of cell proliferation using digital holographic microscopy. *Cytometry Part A*, 91(5), 460–469. <https://doi.org/10.1002/cyto.a.23108>
80. Janitzek, C. M., Matondo, S., Thrane, S., Nielsen, M. A., Kavishe, R., Mwakalinga, S. B., Theander, T. G., Salanti, A., & Sander, A. F. (2016). Bacterial superglue generates a full-length circumsporozoite protein virus-like particle vaccine capable of inducing high and durable antibody responses. *Malaria Journal*, 15(1), 1–9. <https://doi.org/10.1186/s12936-016-1574-1>
81. Joe, C. C. D., Chopra, N., Nestola, P., Niemann, J., & Douglas, A. D. (2023). Rapid-response manufacturing of adenovirus-vectored vaccines. *Nature Biotechnology*, 41(March), 314–316. <https://doi.org/10.1038/s41587-023-01682-2>
82. Juraszek, J., Rutten, L., Blokland, S., Bouchier, P., Voorzaat, R., Ritschel, T., Bakkers, M. J. G., Renault, L. L. R., & Langedijk, J. P. M. (2021). Stabilizing the closed SARS-CoV-2 spike trimer. *Nature Communications*, 12(1), 1–8. <https://doi.org/10.1038/s41467-020-20321-x>
83. Kamen, A. A., Bédard, C., Tom, R., Perret, S., & Jardin, B. (1996). On-line monitoring of respiration in recombinant-baculovirus infected and uninfected insect cell bioreactor cultures. *Biotechnology and Bioengineering*, 50(1), 36–48. [https://doi.org/10.1002/\(SICI\)1097-0290\(19960405\)50:1<36::AID-BIT5>3.0.CO;2-2](https://doi.org/10.1002/(SICI)1097-0290(19960405)50:1<36::AID-BIT5>3.0.CO;2-2)
84. Kato, T., Takami, Y., Kumar Deo, V., & Park, E. Y. (2019). Preparation of virus-like particle mimetic nanovesicles displaying the S protein of Middle East respiratory syndrome coronavirus using insect cells. *Journal of Biotechnology*, 306(September), 177–184. <https://doi.org/10.1016/j.jbiotec.2019.10.007>
85. Ke, Z., Oton, J., Qu, K., Cortese, M., Zila, V., McKeane, L., Nakane, T., Zivanov, J., Neufeldt, C. J., Cerikan, B., Lu, J. M., Peukes, J., Xiong, X., Kräusslich, H. G., Scheres, S. H. W., Bartenschlager, R., & Briggs, J. A. G. (2020). Structures and distributions of SARS-CoV-2 spike proteins on intact virions. *Nature*, 588(7838), 498–502. <https://doi.org/10.1038/s41586-020-2665-2>
86. Keech, C., Albert, G., Cho, I., Robertson, A., Reed, P., Neal, S., Pledsted, J. S., Zhu, M., Cloney-Clark, S., Zhou, H., Smith, G., Patel, N., Frieman, M. B., Haupt, R. E., Logue, J., McGrath, M., Weston, S., Piedra, P. A., Desai, C., ... Glenn, G. M. (2020). Phase 1-2 trial of a SARS-CoV-2 recombinant spike protein nanoparticle vaccine. *New England Journal of Medicine*, 383(24), 2320–2332. <https://doi.org/10.1056/nejmoa2026920>
87. Kenoutis, C., Efrose, R. C., Swevers, L., Lavdas, A. A., Gaitanou, M., Matsas, R., & Iatrou, K. (2006). Baculovirus-Mediated Gene Delivery into Mammalian Cells Does Not Alter

- Their Transcriptional and Differentiating Potential but Is Accompanied by Early Viral Gene Expression. *Journal of Virology*, 80(8), 4135–4146.  
<https://doi.org/10.1128/jvi.80.8.4135-4146.2006>
88. Kiehl, T. R., Shen, D., Khattak, S. F., Jian Li, Z., & Sharfstein, S. T. (2011). Observations of cell size dynamics under osmotic stress. *Cytometry Part A*, 79 A(7), 560–569.  
<https://doi.org/10.1002/cyto.a.21076>
89. Kioukia, N., Nienow, A. W., Al-Rubeai, M., & Emery, A. N. (1996). Influence of agitation and sparging on the growth rate and infection of insect cells in bioreactors and a comparison with hybridoma culture. *Biotechnology Progress*, 12(6), 779–785.  
<https://doi.org/10.1021/bp9600703>
90. Kirchdoerfer, R. N., Wang, N., Pallesen, J., Wrapp, D., Turner, H. L., Cottrell, C. A., Corbett, K. S., Graham, B. S., McLellan, J. S., & Ward, A. B. (2018). Stabilized coronavirus spikes are resistant to conformational changes induced by receptor recognition or proteolysis. *Scientific Reports*, 8(1), 1–11. <https://doi.org/10.1038/s41598-018-34171-7>
91. Kiviharju, K., Salonen, K., Moilanen, U., Meskanen, E., Leisola, M., & Eerikäinen, T. (2007). On-line biomass measurements in bioreactor cultivations: Comparison study of two on-line probes. *Journal of Industrial Microbiology and Biotechnology*, 34(8), 561–566.  
<https://doi.org/10.1007/s10295-007-0233-5>
92. Kost, T. (1999). Recombinant baculoviruses as expression vectors for insect and mammalian cells. *Current Opinion in Biotechnology*, 10(5), 428–433.  
[https://doi.org/10.1016/S0958-1669\(99\)00005-1](https://doi.org/10.1016/S0958-1669(99)00005-1)
93. Kost, T. A., Condreay, J. P., & Jarvis, D. L. (2005). Baculovirus as versatile vectors for protein expression in insect and mammalian cells. *Nature Biotechnology*, 23(5), 567–575.  
<https://doi.org/10.1038/nbt1095>
94. Krebs, H. A. (1967). The redox state of nicotinamide adenine dinucleotide in the cytoplasm and mitochondria of rat liver. *Advances in Enzyme Regulation*, 5(C), 409–434.  
[https://doi.org/10.1016/0065-2571\(67\)90029-5](https://doi.org/10.1016/0065-2571(67)90029-5)
95. Kumari, P., Rothan, H. A., Natekar, J. P., Stone, S., Pathak, H., Strate, P. G., Arora, K., Brinton, M. A., & Kumar, M. (2021). Neuroinvasion and encephalitis following intranasal inoculation of sars-cov-2 in k18-hacc2 mice. *Viruses*, 13(1), 132.  
<https://doi.org/10.3390/v13010132>
96. Lan, J., Ge, J., Yu, J., Shan, S., Zhou, H., Fan, S., Zhang, Q., Shi, X., Wang, Q., Zhang, L., & Wang, X. (2020). Structure of the SARS-CoV-2 spike receptor-binding domain bound to the ACE2 receptor. *Nature*, 581(7807), 215–220. <https://doi.org/10.1038/s41586-020-2180-5>
97. Lavado-García, J., Pérez-Rubio, P., Cervera, L., & Gòdia, F. (2022). The cell density effect in animal cell-based bioprocessing: Questions, insights and perspectives. *Biotechnology Advances*, 60(March). <https://doi.org/10.1016/j.biotechadv.2022.108017>
98. Lee, H. H., & Miller, L. K. (1979). Isolation, Complementation, and Initial Characterization of Temperature-Sensitive Mutants of the Baculovirus *Autographa*

- californica Nuclear Polyhedrosis Virus . *Journal of Virology*, 31(1), 240–252.  
<https://doi.org/10.1128/jvi.31.1.240-252.1979>
99. Li, J., Ulitzky, L., Silberstein, E., Taylor, D. R., & Viscidi, R. (2013). Immunogenicity and protection efficacy of monomeric and trimeric recombinant SARS coronavirus spike protein subunit vaccine candidates. *Viral Immunology*, 26(2), 126–132.  
<https://doi.org/10.1089/vim.2012.0076>
100. Li, L., Fierer, J. O., Rapoport, T. A., & Howarth, M. (2014). Structural analysis and optimization of the covalent association between SpyCatcher and a peptide tag. *Journal of Molecular Biology*, 426(2), 309–317. <https://doi.org/10.1016/j.jmb.2013.10.021>
101. Li, T., Zheng, Q., Yu, H., Wu, D., Xue, W., Xiong, H., Huang, X., Nie, M., Yue, M., Rong, R., Zhang, S., Zhang, Y., Wu, Y., Wang, S., Zha, Z., Chen, T., Deng, T., Wang, Y., Zhang, T., ... Xia, N. (2020). SARS-CoV-2 spike produced in insect cells elicits high neutralization titres in non-human primates. *Emerging Microbes and Infections*, 9(1), 2076–2090. <https://doi.org/10.1080/22221751.2020.1821583>
102. Li, Y., Shen, S., Hu, L., Deng, F., Vlak, J. M., Hu, Z., Wang, H., & Wang, M. (2018). The functional oligomeric state of tegument protein GP41 is essential for baculovirus budded virion and occlusion-derived virion assembly. *Journal of Virology*, 92(12), 2083–2100. <https://doi.org/10.1128/JVI.02083-17>
103. Liang, J. G., Su, D., Song, T. Z., Zeng, Y., Huang, W., Wu, J., Xu, R., Luo, P., Yang, X., Zhang, X., Luo, S., Liang, Y., Li, X., Huang, J., Wang, Q., Huang, X., Xu, Q., Luo, M., Huang, A., ... Liang, P. (2021). S-Trimer, a COVID-19 subunit vaccine candidate, induces protective immunity in nonhuman primates. *Nature Communications*, 12(1), 1–12.  
<https://doi.org/10.1038/s41467-021-21634-1>
104. Liu, C., Mendonça, L., Yang, Y., Gao, Y., Shen, C., Liu, J., Ni, T., Ju, B., Liu, C., Tang, X., Wei, J., Ma, X., Zhu, Y., Liu, W., Xu, S., Liu, Y., Yuan, J., Wu, J., Liu, Z., ... Zhang, P. (2020). The architecture of inactivated SARS-CoV-2 with postfusion spikes revealed by cryo-EM and cryo-ET. *Structure*, 28(11), 1218–1224.e4.  
<https://doi.org/10.1016/j.str.2020.10.001>
105. Liu, J.-C., & Maruniak, J. E. (1995). Nucleotide sequence and transcriptional analysis of the gp41 gene of *Spodoptera frugiperda* nuclear polyhedrosis virus. *Journal of General Virology*, 76(6), 1443–1450. <https://doi.org/10.1099/0022-1317-76-6-1443>
106. Liu, K., Li, F., Sun, Q., Lin, N., Han, H., You, K., Tian, F., Mao, Z., Li, T., Tong, T., Geng, M., Zhao, Y., Gu, W., & Zhao, W. (2019). P53 B-Hydroxybutyrylation Attenuates P53 Activity. *Cell Death and Disease*, 10(3). <https://doi.org/10.1038/s41419-019-1463-y>
107. López-Sagaseta, J., Malito, E., Rappuoli, R., & Bottomley, M. J. (2016). Self-assembling protein nanoparticles in the design of vaccines. In *Computational and Structural Biotechnology Journal* (Vol. 14, pp. 58–68). Elsevier B.V.  
<https://doi.org/10.1016/j.csbj.2015.11.001>
108. Luckow, V. A., & Summers, M. D. (1988). Trends in the development of baculovirus expression vectors. *Bio/Technology*, 6(1), 47–55. <https://doi.org/10.1038/nbt0188-47>

109. Lynn, D. E., & Hink, W. F. (1978). Infection of synchronized TN-368 cell cultures with alfalfa looper nuclear polyhedrosis virus. *Journal of Invertebrate Pathology*, 32(1), 1–5. [https://doi.org/10.1016/0022-2011\(78\)90167-2](https://doi.org/10.1016/0022-2011(78)90167-2)
110. Maranga, L., Brazão, T. F., & Carrondo, M. J. T. (2003). Virus-like particle production at low multiplicities of infection with the baculovirus insect cell system. *Biotechnology and Bioengineering*, 84(2), 245–253. <https://doi.org/10.1002/bit.10773>
111. Maranga, L., Brazao, T. F., & Carrondo, M. J. T. (2003a). Virus-like particle production at low multiplicities of infection with the baculovirus insect cell system. *Biotechnology and Bioengineering*, 84(2), 245–253. <https://doi.org/10.1002/bit.10773>
112. Marek, M., Van Oers, M. M., Devaraj, F. F., Vlak, J. M., & Merten, O. W. (2011). Engineering of baculovirus vectors for the manufacture of virion-free biopharmaceuticals. *Biotechnology and Bioengineering*, 108(5), 1056–1067. <https://doi.org/10.1002/bit.23028>
113. Massotte, D. (2003). G protein-coupled receptor overexpression with the baculovirus-insect cell system: A tool for structural and functional studies. *Biochimica et Biophysica Acta - Biomembranes*, 1610(1), 77–89. [https://doi.org/10.1016/S0005-2736\(02\)00720-4](https://doi.org/10.1016/S0005-2736(02)00720-4)
114. McLachlin, J. R., & Miller, L. K. (1994). Identification and characterization of vlf-1, a baculovirus gene involved in very late gene expression. *Journal of Virology*, 68(12), 7746–7756. <https://doi.org/10.1128/JVI.68.12.7746-7756.1994>
115. McWilliam, A. (2006). Environmental Impact of Baculoviruses. Food and Agriculture Organization FAO, 1–34. [www.fao.org/teca/system/files/R7299\\_FTR\\_anx3.pdf](http://www.fao.org/teca/system/files/R7299_FTR_anx3.pdf) [Consulta: noviembre de 2012]
116. Metz, S. W., Gardner, J., Geertsema, C., Le, T. T., Vlak, J. M., Suhrbier, A., Goh, L., & Pijlman, G. P. (2013). Effective chikungunya virus-like particle vaccine produced in insect cells. *PLoS Neglected Tropical Diseases*, 7(3), e2124. <https://doi.org/10.1371/journal.pntd.0002124>
117. Metz, S. W., Martina, B. E., van den Doel, P., Geertsema, C., Osterhaus, A. D., Vlak, J. M., & Pijlman, G. P. (2013). Chikungunya virus-like particles are more immunogenic in a lethal AG129 mouse model compared to glycoprotein E1 or E2 subunits. *Vaccine*, 31(51), 6092–6096. <https://doi.org/10.1016/j.vaccine.2013.09.045>
118. Miconai, A., Wien, F., Bulyáki, É., Kun, J., Moussong, É., Lee, Y. H., Goto, Y., Réfrégiers, M., & Kardos, J. (2018). BeStSel: A web server for accurate protein secondary structure prediction and fold recognition from the circular dichroism spectra. *Nucleic Acids Research*, 46(W1), W315–W322. <https://doi.org/10.1093/nar/gky497>
119. Miconai, A., Wien, F., Kernya, L., Lee, Y. H., Goto, Y., Réfrégiers, M., & Kardos, J. (2015). Accurate secondary structure prediction and fold recognition for circular dichroism spectroscopy. *Proceedings of the National Academy of Sciences of the United States of America*, 112(24), E3095–E3103. <https://doi.org/10.1073/pnas.1500851112>
120. Miller, L. K., Trimarchi, R. E., Browne, D., & Pennock, G. D. (1983). A temperature-sensitive mutant of the baculovirus *Autographa californica* Nuclear polyhedrosis virus

- defective in an early function required for further gene expression. *Virology*, 126(1), 376-380. [https://doi.org/10.1016/0042-6822\(83\)90487-7](https://doi.org/10.1016/0042-6822(83)90487-7)
121. Mittal, M., Banerjee, M., Lua, L. H., & Rathore, A. S. (2022). Current status and future challenges in transitioning to continuous bioprocessing of virus-like particles. *Journal of Chemical Technology & Biotechnology*, 97(9), 2376-2385. <https://doi.org/10.1002/jctb.6821>
122. Mohsen, M. O., & Bachmann, M. F. (2022). Virus-like particle vaccinology, from bench to bedside. *Cellular & Molecular Immunology*, 19(9), 993-1011. <https://doi.org/10.1038/s41423-022-00897-8>
123. Mohsen, M. O., Gomes, A. C., Vogel, M., & Bachmann, M. F. (2018). Interaction of viral capsid-derived virus-like particles (VLPs) with the innate immune system. In *Vaccines* (Vol. 6, Issue 3, p. 37). MDPI AG. <https://doi.org/10.3390/vaccines6030037>
124. Moore, J. P., & Klasse, P. J. (2020). COVID-19 vaccines: “Warp speed” needs mind melds, not warped minds. *Journal of Virology*, 94(17). <https://doi.org/10.1128/jvi.01083-20>
125. Moreau, G. B., Burgess, S. L., Sturek, J. M., Donlan, A. N., Petri, W. A., & Mann, B. J. (2020). Evaluation of K18-hACE2 mice as a model of SARS-CoV-2 infection. *American Journal of Tropical Medicine and Hygiene*, 103(3), 1215-1219. <https://doi.org/10.4269/ajtmh.20-0762>
126. Murges, D., Kremer, A., & Knebel-Mörsdorf, D. (1997). Baculovirus transactivator IEL1 is functional in mammalian cells. *Journal of General Virology*, 78(6), 1507-1510. <https://doi.org/10.1099/0022-1317-78-6-1507>
127. Nagy, A., & Alhatlani, B. (2021). An overview of current COVID-19 vaccine platforms. In *Computational and Structural Biotechnology Journal* (Vol. 19, pp. 2508-2517). Elsevier B.V. <https://doi.org/10.1016/j.csbj.2021.04.061>
128. Newman, J. C., & Verdin, E. (2014).  $\beta$ -hydroxybutyrate: Much more than a metabolite. *Diabetes Research and Clinical Practice*, 106(2), 173-181. <https://doi.org/10.1016/j.diabres.2014.08.009>
129. Oker-Blom, C., Orellana, A., & Keinänen, K. (1996). Highly efficient production of GFP and its derivatives in insect cells for visual in vitro applications. *FEBS Letters*, 389(3), 238-243. [https://doi.org/10.1016/0014-5793\(96\)00593-5](https://doi.org/10.1016/0014-5793(96)00593-5)
130. Olszewski, J., & Miller, L. K. (1997). A role for baculovirus GP41 in budded virus production. *Virology*, 233(2), 292-301. <https://doi.org/10.1006/viro.1997.8612>
131. Ono, C., Ninomiya, A., Yamamoto, S., Abe, T., Wen, X., Fukuhara, T., Sasai, M., Yamamoto, M., Saitoh, T., Satoh, T., Kawai, T., Ishii, K. J., Akira, S., Okamoto, T., & Matsuura, Y. (2014). Innate Immune Response Induced by Baculovirus Attenuates Transgene Expression in Mammalian Cells. *Journal of Virology*, 88(4), 2157-2167. <https://doi.org/10.1128/jvi.03055-13>
132. Pais, D. A. M., Galvão, P. R. S., Kryzhanska, A., Barbau, J., Isidro, I. A., & Alves, P. M. (2020). Holographic imaging of insect cell cultures: Online non-invasive monitoring of

- adeno-associated virus production and cell concentration. *Processes*, 8(4).  
<https://doi.org/10.3390/PR8040487>
133. Pallesen, J., Wang, N., Corbett, K. S., Wrapp, D., Kirchdoerfer, R. N., Turner, H. L., Cottrell, C. A., Becker, M. M., Wang, L., Shi, W., Kong, W. P., Andres, E. L., Kettenbach, A. N., Denison, M. R., Chappell, J. D., Graham, B. S., Ward, A. B., & McLellan, J. S. (2017). Immunogenicity and structures of a rationally designed prefusion MERS-CoV spike antigen. *Proceedings of the National Academy of Sciences of the United States of America*, 114(35), E7348–E7357. <https://doi.org/10.1073/pnas.1707304114>
134. Palomares, L. A., Pedroza, J. C., & Ramírez, O. T. (2001). Cell size as a tool to predict the production of recombinant protein by the insect-cell baculovirus expression system. *Biotechnology Letters*, 23(5), 359–364.  
<https://doi.org/10.1023/A:1005688417525/METRICS>
135. Partington, S., Yu, H., Lu, A., & Carstens, E. B. (1990). Isolation of temperature sensitive mutants of *Autographa californica* nuclear polyhedrosis virus: Phenotype characterization of baculovirus mutants defective in very late gene expression. *Virology*, 175(1), 91–102.  
[https://doi.org/10.1016/0042-6822\(90\)90189-X](https://doi.org/10.1016/0042-6822(90)90189-X)
136. Peng, Y., Song, J., Lu, J., & Chen, X. (2007). The histone deacetylase inhibitor sodium butyrate inhibits baculovirus-mediated transgene expression in Sf9 cells. *Journal of Biotechnology*, 131(2), 180–187. <https://doi.org/10.1016/j.jbiotec.2007.06.009>
137. Pidre, M. L., Arriás, P. N., Amorós Morales, L. C., & Romanowski, V. (2023). The Magic Staff: A Comprehensive Overview of Baculovirus-Based Technologies Applied to Human and Animal Health. *Viruses*, 15(1). <https://doi.org/10.3390/v15010080>
138. Pijlman, G. P. (2015). Enveloped virus-like particles as vaccines against pathogenic arboviruses. *Biotechnology Journal*, 10(5), 659–670.  
<https://doi.org/10.1002/biot.201400427>
139. Pijlman, G. P., Grose, C., Hick, T. A. H. H., Breukink, H. E., van den Braak, R., Abbo, S. R., Geertsema, C., van Oers, M. M., Martens, D. E., & Esposito, D. (2020). Relocation of the attTn7 Transgene Insertion Site in Bacmid DNA Enhances Baculovirus Genome Stability and Recombinant Protein Expression in Insect Cells. *Viruses*, 12(12), 1448.  
<https://doi.org/10.3390/v12121448>
140. Polack, F. P., Thomas, S. J., Kitchin, N., Absalon, J., Gurtman, A., Lockhart, S., Perez, J. L., Pérez Marc, G., Moreira, E. D., Zerbini, C., Bailey, R., Swanson, K. A., Roychoudhury, S., Koury, K., Li, P., Kalina, W. V., Cooper, D., Frenck, R. W., Hammitt, L. L., ... Gruber, W. C. (2020). Safety and efficacy of the BNT162b2 mRNA covid-19 vaccine. *New England Journal of Medicine*, 383(27), 2603–2615. <https://doi.org/10.1056/nejmoa2034577>
141. Possee, R. D., Chambers, A. C., Graves, L. P., Aksular, M., & King, L. A. (2020). Recent developments in the use of baculovirus expression vectors. *Current Issues in Molecular Biology*, 34, 215–230. <https://doi.org/10.21775/cimb.034.215>

142. Power, J. F., Reid, S., Greenfield, P. F., & Nielsen, L. K. (1996). The kinetics of baculovirus adsorption to insect cells in suspension culture. *Cytotechnology*, 21(2), 155–163. <https://doi.org/10.1007/BF02215665>
143. Puchalska, P., & Crawford, P. A. (2017). Multi-dimensional Roles of Ketone Bodies in Fuel Metabolism, Signaling, and Therapeutics. *Cell Metabolism*, 25(2), 262–284. <https://doi.org/10.1016/j.cmet.2016.12.022>
144. Puente-Massaguer, E., González-Domínguez, I., Strobl, F., Grabherr, R., Striedner, G., Lecina, M., & Gòdia, F. (2022). Bioprocess characterization of virus-like particle production with the insect cell baculovirus expression system at nanoparticle level. *Journal of Chemical Technology and Biotechnology*, 97(9), 2456–2465. <https://doi.org/10.1002/jctb.7105>
145. Pyle, L. E., Barton, P., Fujiwara, Y., Mitchell, A., & Fidge, N. (1995). Secretion of biologically active human proapolipoprotein A-I in a baculovirus-insect cell system: Protection from degradation by protease inhibitors. *Journal of Lipid Research*, 36(11), 2355–2361. [https://doi.org/10.1016/s0022-2275\(20\)39716-9](https://doi.org/10.1016/s0022-2275(20)39716-9)
146. Radford, K. M., Reid, S., & Greenfield, P. F. (1997). Substrate limitation in the Baculovirus Expression Vector System. *Biotechnology and Bioengineering*, 56(1), 32–44. [https://doi.org/10.1002/\(SICI\)1097-0290\(19971005\)56:1<32::AID-BIT4>3.0.CO;2-W](https://doi.org/10.1002/(SICI)1097-0290(19971005)56:1<32::AID-BIT4>3.0.CO;2-W)
147. Radner, S., Celie, P. H. N., Fuchs, K., Sieghart, W., Sixma, T. K., & Stornaiuolo, M. (2012). Transient transfection coupled to baculovirus infection for rapid protein expression screening in insect cells. *Journal of Structural Biology*, 179(1), 46–55. <https://doi.org/10.1016/j.jsb.2012.04.013>
148. Ramachandran, A., Bashyam, M. D., Viswanathan, P., Ghosh, S., Kumar, M. S., & Hasnain, S. E. (2001). The bountiful and baffling baculovirus: The story of polyhedrin transcription. *Current Science*, 81(8), 998–1010.
149. Rappaz, B., Breton, B., Shaffer, E., & Turcatti, G. (2014). Digital Holographic Microscopy: A Quantitative Label-Free Microscopy Technique for Phenotypic Screening. *Combinatorial Chemistry & High Throughput Screening*, 17(1), 80–88. <https://doi.org/10.2174/13862073113166660062>
150. Rashighi, M., & Harris, J. E. (2017). 乳鼠心肌提取 HHS Public Access. *Physiology & Behavior*, 176(3), 139–148. <https://doi.org/10.1053/j.gastro.2016.08.014>.CagY
151. Rathore, A. S., Kateja, N., & Kumar, D. (2018). Process integration and control in continuous bioprocessing. *Current Opinion in Chemical Engineering*, 22, 18–25. <https://doi.org/10.1016/j.coche.2018.08.005>
152. Ribeiro, B. M., Hutchinson, K., & Miller, L. K. (1994). A mutant baculovirus with a temperature-sensitive IE-1 transregulatory protein. *Journal of Virology*, 68(2), 1075–1084. <https://doi.org/10.1128/JVI.68.2.1075-1084.1994>
153. Robert D Possee. (1988). Baculoviruses as gene expression vectors. *Annual Review of Microbiology*, 42, 177–199. <https://doi.org/10.1146/annurev.mi.42.100188.001141>

154. Roldão, A., Mellado, M. C. M., Castilho, L. R., Carrondo, M. J. T., & Alves, P. M. (2010). Virus-like particles in vaccine development. *Expert Review of Vaccines*, 9(10), 1149–1176. <https://doi.org/10.1586/erv.10.115>
155. Rosinski, M., Reid, S., & Nielsen, L. K. (2000). Osmolarity effects on observed insect cell size after baculovirus infection are avoided using growth medium for sample dilution. *Biotechnology Progress*, 16(5), 782–785. <https://doi.org/10.1021/bp000083n>
156. Sadoff, J., Gray, G., Vandebosch, A., Cárdenas, V., Shukarev, G., Grinsztejn, B., Goepfert, P. A., Truyers, C., Fennema, H., Spiessens, B., Offergeld, K., Scheper, G., Taylor, K. L., Robb, M. L., Treanor, J., Barouch, D. H., Stoddard, J., Ryser, M. F., Marovich, M. A., ... Douoguih, M. (2021). Safety and efficacy of single-dose Ad26.COV2.S vaccine against COVID-19. *New England Journal of Medicine*. <https://doi.org/10.1056/nejmoa2101544>
157. Saito, T., Dojima, T., Toriyama, M., & Park, E. Y. (2002). The effect of cell cycle on GFPuv gene expression in the baculovirus expression system. *Journal of Biotechnology*, 93(2), 121–129. [https://doi.org/10.1016/S0168-1656\(01\)00398-4](https://doi.org/10.1016/S0168-1656(01)00398-4)
158. Sander, L., & Harrysson, Æ. A. (2007). Using cell size kinetics to determine optimal harvest time for *Spodoptera frugiperda* and *Trichoplusia ni* BTI-TN-5B1-4 cells infected with a baculovirus expression vector system expressing enhanced green fluorescent protein. 35–48. <https://doi.org/10.1007/s10616-007-9064-5>
159. Schiller, J., & Lowy, D. (2018). Explanations for the high potency of HPV prophylactic vaccines. *Vaccine*, 36(32), 4768–4773. <https://doi.org/10.1016/j.vaccine.2017.12.079>
160. Schopf, B., Howaldt, M. W., & Bailey, J. E. (1990). DNA distribution and respiratory activity of *Spodoptera frugiperda* populations infected with wild-type and recombinant *Autographa californica* nuclear polyhedrosis virus. *Journal of Biotechnology*, 15(1–2), 169–185. [https://doi.org/10.1016/0168-1656\(90\)90059-K](https://doi.org/10.1016/0168-1656(90)90059-K)
161. Schrauf, S., Tschismarov, R., Tauber, E., & Ramsauer, K. (2020). Current Efforts in the Development of Vaccines for the Prevention of Zika and Chikungunya Virus Infections. *Frontiers in Immunology*, 11(April), 1–20. <https://doi.org/10.3389/fimmu.2020.00592>
162. Schulze, M., Lemke, J., Pollard, D., Wijffels, R. H., Matuszczyk, J., & Martens, D. E. (2021). Automation of high CHO cell density seed intensification via online control of the cell specific perfusion rate and its impact on the N-stage inoculum quality. *Journal of Biotechnology*, 335(February), 65–75. <https://doi.org/10.1016/j.jbiotec.2021.06.011>
163. Sedova, E. S., Shcherbinin, D. N., Migunov, A. I., Smirnov, Y. A., Logunov, D. Y., Shmarov, M. M., Tsybalova, L. M., Naroditskiĭ, B. S., Kiselev, O. I., & Gintsburg, A. L. (2012). Recombinant Influenza Vaccines. *Acta Naturae*, 4(4), 17–27. <https://doi.org/10.32607/20758251-2012-4-4-17-27>
164. Sequeira, D. P., Correia, R., Carrondo, M. J. T., Roldão, A., Teixeira, A. P., & Alves, P. M. (2018). Combining stable insect cell lines with baculovirus-mediated expression for multi-HA influenza VLP production. *Vaccine*, 36(22), 3112–3123. <https://doi.org/10.1016/j.vaccine.2017.02.043>

165. Shang, J., Wan, Y., Luo, C., Ye, G., Geng, Q., Auerbach, A., & Li, F. (2020). Cell entry mechanisms of SARS-CoV-2. *Proceedings of the National Academy of Sciences of the United States of America*, 117(21), 11727–11734. <https://doi.org/10.1073/pnas.2003138117>
166. Shang, J., Ye, G., Shi, K., Wan, Y., Luo, C., Aihara, H., Geng, Q., Auerbach, A., & Li, F. (2020). Structural basis of receptor recognition by SARS-CoV-2. *Nature*, 581(7807), 221–224. <https://doi.org/10.1038/s41586-020-2179-y>
167. Shanmugaraj, B., & Phoolcharoen, W. (2021). Addressing demand for recombinant biopharmaceuticals in the COVID-19 era. *Asian Pacific Journal of Tropical Medicine*, 14(2), 49–51. <https://doi.org/10.4103/1995-7645.306736>
168. Shinde, V., Bhikha, S., Hoosain, Z., Archary, M., Bhorat, Q., Fairlie, L., Lalloo, U., Masilela, M. S. L., Moodley, D., Hanley, S., Fouche, L., Louw, C., Tameris, M., Singh, N., Goga, A., Dheda, K., Grobbelaar, C., Kruger, G., Carrim-Ganey, N., ... Madhi, S. A. (2021). Efficacy of NVX-CoV2373 Covid-19 Vaccine against the B.1.351 Variant. *New England Journal of Medicine*, 384(20), 1899–1909. <https://doi.org/10.1056/nejmoa2103055>
169. Shippam-Brett, C. E., Willis, L. G., & Theilmann, D. A. (2001). Analysis of sequences involved in IE2 transactivation of a baculovirus immediate-early gene promoter and identification of a new regulatory motif. *Virus Research*, 75(1), 13–28. [https://doi.org/10.1016/S0168-1702\(00\)00253-7](https://doi.org/10.1016/S0168-1702(00)00253-7)
170. Smith, G. E., Fraser, M. J., & Summers, M. D. (1983). Molecular Engineering of the *Autographa californica* Nuclear Polyhedrosis Virus Genome: Deletion Mutations Within the Polyhedrin Gene. *Journal of Virology*, 46(2), 584–593. <https://doi.org/10.1128/jvi.46.2.584-593.1983>
171. Socher, E., Conrad, M., Heger, L., Paulsen, F., Sticht, H., Zunke, F., & Arnold, P. (2021). Mutations in the B.1.1.7 SARS-CoV-2 spike protein reduce receptor-binding affinity and induce a flexible link to the fusion peptide. *Biomedicines*, 9(5), 525. <https://doi.org/10.3390/biomedicines9050525>
172. Stiles, B., & Wood, H. A. (1983). A study of the glycoproteins of *Autographa californica* nuclear polyhedrosis virus (AcNPV). *Virology*, 131(1), 230–241. [https://doi.org/10.1016/0042-6822\(83\)90548-2](https://doi.org/10.1016/0042-6822(83)90548-2)
173. Strube, J., Ditz, R., Kornecki, M., Huter, M., Schmidt, A., Thiess, H., & Zobel-Roos, S. (2018). Process intensification in biologics manufacturing. *Chemical Engineering and Processing - Process Intensification*, 133(September), 278–293. <https://doi.org/10.1016/j.cep.2018.09.022>
174. Stuiblé, M., Gervais, C., Lord-Dufour, S., Perret, S., L'Abbé, D., Schrag, J., St-Laurent, G., & Durocher, Y. (2021). Rapid, high-yield production of full-length SARS-CoV-2 spike ectodomain by transient gene expression in CHO cells. *Journal of Biotechnology*, 326, 21–27. <https://doi.org/10.1016/j.jbiotec.2020.12.005>
175. Sui, Y., Bekele, Y., & Berzofsky, J. A. (2021). Potential SARS-CoV-2 immune correlates of protection in infection and vaccine immunization. In *Pathogens* (Vol. 10, Issue 2, pp. 1–11). MDPI AG. <https://doi.org/10.3390/pathogens10020138>

176. Targovnik, A. M., Simonin, J. A., Mc Callum, G. J., Smith, I., Cuccovia Warlet, F. U., Nugnès, M. V., Miranda, M. V., & Belaich, M. N. (2021). Solutions against emerging infectious and noninfectious human diseases through the application of baculovirus technologies. In *Applied Microbiology and Biotechnology* (Vol. 105, Issues 21–22, pp. 8195–8226). Springer. <https://doi.org/10.1007/s00253-021-11615-1>
177. Tatischev, R. A., & Shuler, M. L. (1997). Effect of elevated oxygen and glutamine levels on foreign protein production at high cell densities using the insect cell-baculovirus expression system. *Biotechnology and Bioengineering*, 54(2), 142–152. [https://doi.org/10.1002/\(SICI\)1097-0290\(19970420\)54:2<142::AID-BIT6>3.0.CO;2-L](https://doi.org/10.1002/(SICI)1097-0290(19970420)54:2<142::AID-BIT6>3.0.CO;2-L)
178. Taylor, K., Nguyen, A., & Stéphenne, J. (2009). The need for new vaccines. *Vaccine*, 27(SUPPL.6), 3–8. <https://doi.org/10.1016/j.vaccine.2009.10.014>
179. Thrane, S., Janitzek, C. M., Matondo, S., Resende, M., Gustavsson, T., de Jongh, W. A., Clemmensen, S., Roeffen, W., van de Vegte Bolmer, M., van Gemert, G. J., Sauerwein, R., Schiller, J. T., Nielsen, M. A., Theander, T. G., Salanti, A., & Sander, A. F. (2016). Bacterial superglue enables easy development of efficient virus-like particle based vaccines. *Journal of Nanobiotechnology*, 14(1), 30. <https://doi.org/10.1186/s12951-016-0181-1>
180. Tian, J. H., Patel, N., Haupt, R., Zhou, H., Weston, S., Hammond, H., Logue, J., Portnoff, A. D., Norton, J., Guebre-Xabier, M., Zhou, B., Jacobson, K., Maciejewski, S., Khatoon, R., Wisniewska, M., Moffitt, W., Kluepfel-Stahl, S., Ekechukwu, B., Papin, J., ... Smith, G. (2021). SARS-CoV-2 spike glycoprotein vaccine candidate NVX-CoV2373 immunogenicity in baboons and protection in mice. *Nature Communications*, 12(1). <https://doi.org/10.1038/s41467-020-20653-8>
181. Tona, R. M., Shah, R., Middaugh, K., Steve, J., Marques, J., Roszell, B. R., & Jung, C. (2023). Process intensification for lentiviral vector manufacturing using tangential flow depth filtration. *Molecular Therapy - Methods & Clinical Development*, 29(June), 93–107. <https://doi.org/10.1016/j.omtm.2023.02.017>
182. Treanor, J. J., Schiff, G. M., Hayden, F. G., Brady, R. C., Hay, C. M., Meyer, A. L., Holden-Wiltse, J., Liang, H., Gilbert, A., & Cox, M. (2007). Safety and immunogenicity of a baculovirus-expressed hemagglutinin influenza vaccine: A randomized controlled trial. *Journal of the American Medical Association*, 297(14), 1577–1582. <https://doi.org/10.1001/jama.297.14.1577>
183. Ude, C., Schmidt-Hager, J., Findeis, M., John, G. T. homa., Scheper, T., & Beutel, S. (2014). Application of an online-biomass sensor in an optical multisensory platform prototype for growth monitoring of biotechnical relevant microorganism and cell lines in single-use shake flasks. *Sensors (Basel, Switzerland)*, 14(9), 17390–17405. <https://doi.org/10.3390/s140917390>
184. van Lier, F. L. J., van der Meijs, W. C. J., Grobben, N. G., Olie, R. A., Vlak, J. M., & Tramper, J. (1992). Continuous  $\beta$ -galactosidase production with a recombinant baculovirus insect-cell system in bioreactors. *Journal of Biotechnology*, 22(3), 291–298. [https://doi.org/10.1016/0168-1656\(92\)90147-2](https://doi.org/10.1016/0168-1656(92)90147-2)

185. Van Lier, F. L. J., Van Duijnhoven, C. F. G., De Vaan, M. M. J. A. C. M., Vlak, J. M., & Tramper, J. (1994). Continuous  $\beta$ -Galactosidase Production in Insect Cells with a p10 Gene Based Baculovirus Vector in a Two-Stage Bioreactor System. *Biotechnology Progress*, 10(1), 60–64. <https://doi.org/10.1021/bp00025a007>
186. van Oers, M. M. (2011). Opportunities and challenges for the baculovirus expression system. *Journal of Invertebrate Pathology*, 107(SUPPL.), S3–S15. <https://doi.org/10.1016/j.jip.2011.05.001>
187. Van Oers, M. M., Pijlman, G. P., & Vlak, J. M. (2015). Thirty years of baculovirus-insect cell protein expression: From dark horse to mainstream technology. In *Journal of General Virology* (Vol. 96, Issue 1, pp. 6–23). <https://doi.org/10.1099/vir.0.067108-0>
188. van Oosten, L., Altenburg, J. J., Fougeroux, C., Geertsema, C., van den End, F., Evers, W. A. C., Westphal, A. H., Lindhoud, S., van den Berg, W., Swarts, D. C., Deurhof, L., Suhrbier, A., Le, T. T., Torres Morales, S., Myeni, S. K., Kikkert, M., Sander, A. F., de Jongh, W. A., Dagil, R., ... Pijlman, G. P. (2021). Two-Component Nanoparticle Vaccine Displaying Glycosylated Spike S1 Domain Induces Neutralizing Antibody Response against SARS-CoV-2 Variants. *MBio*. <https://doi.org/10.1128/mbio.01813-21>
189. Vicente, T., Roldão, A., Peixoto, C., Carrondo, M. J. T. T., & Alves, P. M. (2011). Large-scale production and purification of VLP-based vaccines. *Journal of Invertebrate Pathology*, 107(SUPPL.), S42–S48. <https://doi.org/10.1016/j.jip.2011.05.004>
190. Vicente, T., Roldão, A., Peixoto, C., Carrondo, M. J. T., & Alves, P. M. (2011). Large-scale production and purification of VLP-based vaccines. *Journal of Invertebrate Pathology*, 107(SUPPL.), S42–S48. <https://doi.org/10.1016/j.jip.2011.05.004>
191. Walls, A. C., Fiala, B., Schäfer, A., Wrem, S., Pham, M. N., Murphy, M., Tse, L. V., Shehata, L., O'Connor, M. A., Chen, C., Navarro, M. J., Miranda, M. C., Pettie, D., Ravichandran, R., Kraft, J. C., Ogohara, C., Palser, A., Chalk, S., Lee, E. C., ... King, N. P. (2020). Elicitation of potent neutralizing antibody responses by designed protein nanoparticle vaccines for SARS-CoV-2. *Cell*, 183(5), 1367–1382.e17. <https://doi.org/10.1016/j.cell.2020.10.043>
192. Walls, A. C., Park, Y.-J., Tortorici, M. A., Wall, A., McGuire, A. T., & Veesler, D. (2020). Structure, function, and antigenicity of the SARS-CoV-2 spike glycoprotein. *Cell*, 1–12. <https://doi.org/10.1016/j.cell.2020.02.058>
193. Wang, D., Baudys, J., Bundy, J. L., Solano, M., Keppel, T., & Barr, J. R. (2020). Comprehensive analysis of the glycan complement of SARS-CoV-2 spike proteins using signature ions-triggered electron-transfer/higher-energy collisional dissociation (ET<sub>h</sub>CD) mass spectrometry. *Analytical Chemistry*, 92(21), 14730–14739. <https://doi.org/10.1021/acs.analchem.0c03301>
194. Wang, Q., Zhang, Y., Wu, L., Niu, S., Song, C., Zhang, Z., Lu, G., Qiao, C., Hu, Y., Yuen, K. Y., Wang, Q., Zhou, H., Yan, J., & Qi, J. (2020). Structural and functional basis of SARS-CoV-2 entry by using human ACE2. *Cell*, 181(4), 894–904.e9. <https://doi.org/10.1016/j.cell.2020.03.045>

195. Wang, Y., Wang, L., Cao, H., & Liu, C. (2020). SARS-CoV-2 S1 is superior to the RBD as a COVID-19 subunit vaccine antigen. *Journal of Medical Virology*, July 2020, 892–898. <https://doi.org/10.1002/jmv.26320>
196. Wang, Z., Schmidt, F., Weisblum, Y., Muecksch, F., Barnes, C. O., Finkin, S., Schaefer-Babajew, D., Cipolla, M., Gaebler, C., Lieberman, J. A., Oliveira, T. Y., Yang, Z., Abernathy, M. E., Huey-Tubman, K. E., Hurley, A., Turroja, M., West, K. A., Gordon, K., Millard, K. G., ... Nussenzweig, M. C. (2021). mRNA vaccine-elicited antibodies to SARS-CoV-2 and circulating variants. *Nature*, 592(7855), 616–622. <https://doi.org/10.1038/s41586-021-03324-6>
197. Weidner, T., Druzinec, D., Mühlmann, M., Buchholz, R., & Czermak, P. (2017). The components of shear stress affecting insect cells used with the baculovirus expression vector system. *Zeitschrift Fur Naturforschung - Section C Journal of Biosciences*, 72(9–10), 429–439. <https://doi.org/10.1515/znc-2017-0066>
198. Whitford, M., & Faulkner, P. (1992a). A structural polypeptide of the baculovirus *Autographa californica* nuclear polyhedrosis virus contains O-linked N-acetylglucosamine. *Journal of Virology*, 66(6), 3324–3329. <https://doi.org/10.1128/jvi.66.6.3324-3329.1992>
199. Whitford, M., & Faulkner, P. (1992b). Nucleotide sequence and transcriptional analysis of a gene encoding gp41, a structural glycoprotein of the baculovirus *Autographa californica* nuclear polyhedrosis virus. *Journal of Virology*, 66(8), 4763–4768. <https://doi.org/10.1128/jvi.66.8.4763-4768.1992>
200. Wiegmann, V., Martinez, C. B., & Baganz, F. (2020). Using a parallel micro-cultivation system (micro-matrix) as a process development tool for cell culture applications. In *Methods in Molecular Biology* (Vol. 2095, pp. 69–81). Humana, New York, NY. [https://doi.org/10.1007/978-1-0716-0191-4\\_5](https://doi.org/10.1007/978-1-0716-0191-4_5)
201. Wolfe, N. D., Dunavan, C. P., & Diamond, J. (2007). Origins of major human infectious diseases. *Nature*, 447(7142), 279–283. <https://doi.org/10.1038/nature05775>
202. Wrapp, D., Wang, N., Corbett, K. S., Goldsmith, J. A., Hsieh, C.-L., Abiona, O., Graham, B. S., & McLellan, J. S. (2020). Cryo-EM structure of the 2019-nCoV spike in the prefusion conformation. *Science*, 367(6483), 1260–1263. <https://doi.org/10.1126/science.abb2507>
203. Wrobel, A. G., Benton, D. J., Xu, P., Roustan, C., Martin, S. R., Rosenthal, P. B., Skehel, J. J., & Gamblin, S. J. (2020). SARS-CoV-2 and bat RaTG13 spike glycoprotein structures inform on virus evolution and furin-cleavage effects. *Nature Structural and Molecular Biology*, 27(8), 763–767. <https://doi.org/10.1038/s41594-020-0468-7>
204. Wu, Y., Huang, X., Yuan, L., Wang, S., Zhang, Y., Xiong, H., Chen, R., Ma, J., Qi, R., Nie, M., Xu, J., Zhang, Z., Chen, L., Wei, M., Zhou, M., Cai, M., Shi, Y., Zhang, L., Yu, H., ... Xia, N. (2021). A recombinant spike protein subunit vaccine confers protective immunity against SARS-CoV-2 infection and transmission in hamsters. *Science Translational Medicine*, 13(606), eabg1143. <https://doi.org/10.1126/scitranslmed.abg1143>

205. Yovcheva, M., Thompson, K., Barnes, S., Irvin, K., Cross, M., Lucki, N., Chiou, H., & Zmuda, J. F. (2018). High-Titer Recombinant Protein Production. *Genetic Engineering & Biotechnology News*, 38(13), 20–21. <https://doi.org/10.1089/gen.38.13.08>
206. Yu, J., Tostanosk, L. H., Peter, L., Mercad, N. B., McMahan, K., Mahrokha, S. H., Nkolol, J. P., Liu, J., Li, Z., Chandrashekar, A., Martine, D. R., Loos, C., Atyeo, C., Fischinger, S., Burk, J. S., Slei, M. D., Chen, Y., Zuiani, A., Lelis, F. J. N., ... Barou, D. H. (2020). DNA vaccine protection against SARS-CoV-2 in rhesus macaques. *Science*, 369(6505), 806–811. <https://doi.org/10.1126/science.abc6284>
207. Yue, Q., Yu, Q., Yang, Q., Xu, Y., Guo, Y., Blissard, G. W., & Li, Z. (2017). Distinct roles of cellular ESCRT-I and ESCRT-III proteins in efficient entry and egress of budded virions of *Autographa californica* multiple nucleopolyhedrovirus. *Journal of Virology*, 92(1), 1–35. <https://doi.org/10.1128/jvi.01636-17>
208. Zakeri, B., Fierer, J. O., Celik, E., Chittock, E. C., Schwarz-Linek, U., Moy, V. T., & Howarth, M. (2012). Peptide tag forming a rapid covalent bond to a protein, through engineering a bacterial adhesin. *Proceedings of the National Academy of Sciences of the United States of America*, 109(12), E690–E697. <https://doi.org/10.1073/pnas.1115485109>
209. Zhang, B., Chao, C. W., Tsybovsky, Y., Abiona, O. M., Hutchinson, G. B., Moliva, J. I., Olia, A. S., Pegu, A., Phung, E., Stewart-Jones, G. B. E., Verardi, R., Wang, L., Wang, S., Werner, A., Yang, E. S., Yap, C., Zhou, T., Mascola, J. R., Sullivan, N. J., ... Kwong, P. D. (2020). A platform incorporating trimeric antigens into self-assembling nanoparticles reveals SARS-CoV-2-spike nanoparticles to elicit substantially higher neutralizing responses than spike alone. *Scientific Reports*, 10(1). <https://doi.org/10.1038/s41598-020-74949-2>
210. Zhang, J., Collins, A., Chen, M., Knyazev, I., & Gentz, R. (1998). High-density perfusion culture of insect cells with a biosep ultrasonic filter. *Biotechnology and Bioengineering*, 59(3), 351–359. [https://doi.org/10.1002/\(SICI\)1097-0290\(19980805\)59:3<351::AID-BIT11>3.0.CO;2-H](https://doi.org/10.1002/(SICI)1097-0290(19980805)59:3<351::AID-BIT11>3.0.CO;2-H)
211. Zhao, L., Ren, T. H., & Wang, D. D. (2012). Clinical pharmacology considerations in biologics development. *Acta Pharmacologica Sinica*, 33(11), 1339–1347. <https://doi.org/10.1038/aps.2012.51>
212. Zhou, P., Yang, X. Lou, Wang, X. G., Hu, B., Zhang, L., Zhang, W., Si, H. R., Zhu, Y., Li, B., Huang, C. L., Chen, H. D., Chen, J., Luo, Y., Guo, H., Jiang, R. Di, Liu, M. Q., Chen, Y., Shen, X. R., Wang, X., ... Shi, Z. L. (2020). A pneumonia outbreak associated with a new coronavirus of probable bat origin. *Nature*, 579(7798), 270–273. <https://doi.org/10.1038/s41586-020-2012-7>
213. Zhou, Z., Post, P., Chubet, R., Holtz, K., McPherson, C., Petric, M., & Cox, M. (2006). A recombinant baculovirus-expressed S glycoprotein vaccine elicits high titers of SARS-associated coronavirus (SARS-CoV) neutralizing antibodies in mice. *Vaccine*, 24(17), 3624–3631. <https://doi.org/10.1016/j.vaccine.2006.01.059>



# Summary

### Summary

A growing world population in combination with a growth in welfare and the fact that populations become older causes an increase in age and welfare related diseases resulting in problems for our healthcare system. Deforestation, climate change and increased mobility indirectly causes emergence and spread of new (e.g., SARS-Cov-2) and existing viral diseases (e.g., West-Nile and Zika fever). All this results in a rise in the demand for vaccines and new medicines. The development of new treatments is also necessary for conditions like cancer and autoimmune diseases and is aided by an increased understanding of disease mechanisms. Many of these treatments comprise complex recombinant proteins, such as viral capsid proteins and monoclonal antibodies. The baculovirus expression vector system (BEVS) is a fast and versatile system for producing such recombinant proteins. It utilizes insect cells infected with genetically modified baculoviruses to express the target proteins. The BEVS has shown promise in rapidly developing vaccines during disease outbreaks and as a production platform for novel gene therapy treatments. To remain competitive in the vaccine and gene therapy space and sufficiently accommodate future needs, the BEVS should be optimized, improved, and further developed to improve (large-scale) biomanufacturing capacity for clinical applications. The aim of this project was to study and address problem associated with the co-production of contaminating budded virus (BV) particles and improve BEVS process yield. To achieve this, the study pursued a dual purpose: firstly, to establish budded virus-free production by utilizing a temperature-sensitive baculovirus mutant, and secondly, to develop a scalable perfusion process employing a low multiplicity of infection (MOI).

The COVID-19 pandemic proved to be an important catalyst for the rapid development and approval of novel vaccines. In **Chapter 2** the development, production, and pre-clinical testing of a nanoparticle vaccine against SARS-CoV-2 is reported. Using the BEVS, we produced (1) the full-length spike protein, (2) a secreted form of a prefusion-stabilized spike, and (3) a secreted form of the SARS-CoV-2 S1 domain and next purified these proteins. We formulated the secreted S as an adjuvanted subunit vaccine and tested the protection of K18-hACE2 mice from a SARS-CoV-2 challenge. We also fused the S1 domain to the split-protein tag and displayed this on AP205 virus-like particles (VLPs). Mice vaccinated with the S1-VLP vaccine had strong immune responses and neutralizing antibodies against both the Wuhan SARS-CoV-2 and the UK/B.1.1.7 variant (VOC-202012/01) that was predominant in Europe.

Obtaining real-time monitoring of cell culture status during bioreactor cultivation and production yields significant advantages in enhancing the understanding of the BEVS and timely control of the production process like the moment of temperature increase and moment of harvest. In **Chapter 3** we report the training and evaluation of a machine-learning model to monitor insect cell proliferation and baculovirus infection in bioreactors using online double-differential digital holographic microscopy (D3HM). We found that with a limited training set the microscope and machine learning algorithm could predict cell concentrations, viability, and infection percentage for different viral constructs, MOIs, and process conditions in bioreactor insect culture. The high

time resolution (0.5h) of the online measurements enabled the detection of small events or process deviations, such as cell growth arrest due to the addition of butyrate to the culture, which would have otherwise been missed by manual sampling. Using online monitoring techniques opens up new possibilities for advanced process control and increases process understanding.

Removing residual baculovirus contaminants from VLP products is a major challenge for the BEVS and may result in a significant loss of valuable product. In **Chapter 4**, we investigate if the temperature-sensitive mutation in the baculovirus protein GP41 could be the basis for a BEVS with an inducible shutdown of BV production to aid the production of chikungunya virus (CHIKV) VLPs. For this, the I317T mutation in GP41 was implemented in a baculovirus bacmid vector at the polyhedrin locus and under the p10 promoter. Using a micro-bioreactor screening system, it was found that increasing temperatures to 34°C shortly after baculovirus infection at high MOI significantly decreased BV titers while VLP production and insect cell viability were maintained. This strategy was successfully scaled up to stirred-tank bioreactors and a 100-fold reduction in final BV titers was achieved for both high and low MOI infection strategies. For the low MOI strategy, online monitoring of cell diameter was an effective tool for determining the optimal timing of the temperature shift. The proposed novel temperature-sensitive baculovirus expression vector system with upstream reduction of baculovirus contaminants (BacFree) can/will lower downstream processing requirements and associated product loss during baculovirus removal, while still being scalable and compatible with existing production strategies.

**Chapter 5** focuses on development of a scalable perfusion process to improve product yield and volumetric productivity with the BEVS. Bioreactor perfusion was implemented to allow high-cell density infection of insect cells. We used a low MOI of 0.01 to infect insect cells with baculovirus at viable cell densities of  $1.0\text{-}1.2 \times 10^7$  cells/mL. By using an acoustic perfusion device to allow for medium exchange and cell retention, sufficient nutrients were supplied and/or toxic metabolites removed to allow for continued growth and proper progression of the infection. Cell concentrations of  $2.5\text{-}2.8 \times 10^7$  viable cells/mL were achieved in two perfusion bioreactor runs that showed high reproducibility. The recombinant protein yield per cell was maintained at high cell densities and bioreactor volumetric productivity was up to 4.8-fold higher compared to batch processes. Implementing this perfusion strategy for the BEVS allows for production on a smaller scale, which would also reduce the time needed for scale-up to the production reactor or could increase the production capacity of existing production facilities. Further optimization to reach higher volumetric productivities is possible. In addition, the system can be combined with the BacFree technology described in chapter 4 to reduce final BV titers.

In **Chapter 6**, we discussed the obtained results and their implications for the BEVS, and we considered additional aspects that could be potentially advantageous for the system. Firstly, exploring further improvements of the BacFree strategy, potentially combined with a low MOI perfusion strategy, to reduce final BV titers and improve volumetric productivity simultaneously. Secondly, investigating the use of microbubbles for oxygen sparging (microsparging) to improve oxygen transfer and reduce gas flows into the reactor, especially in the context of perfusion

processes. Thirdly, examining the potential benefits of incorporating short-chain fatty acids into the cell culture, with butyrate and 2-hydroxybutyrate showing promise as candidates to enhance protein yield and virus production. Lastly, exploring high-throughput, rapid, and label-free methods for baculovirus quantification, such as D3HM technology or utilizing electrical parameters like capacitance. This would be highly beneficial for BEVS process development, in particular for low MOI processes. Collectively, these measures are anticipated to reinforce the position of the BEVS as a robust platform technology for the efficient production of therapeutic proteins, to effectively combat current and future global or local health challenges.





# Samenvatting

### Samenvatting

Een groeiende wereldbevolking, een groeiende welvaart en het feit dat bevolkingen ouder worden, leidt tot een toename van leeftijds- en welvaart gerelateerde ziekten, resulterend in een grotere druk op ons gezondheidssysteem. Ontbossing, klimaatverandering en een toenemende mobiliteit van mensen veroorzaken indirect het ontstaan en de verspreiding van nieuwe (bijv. SARS-Cov-2) en bestaande virale ziekten (bijv. West-Nile en Zika koorts). De ontwikkeling van nieuwe behandelingen is daarnaast noodzakelijk voor bestaande aandoeningen zoals kanker en auto-immuunziekten, geholpen door een beter begrip van ziektemechanismen. Dit alles leidt tot een stijgende vraag naar vaccins en nieuwe geneesmiddelen. Veel van deze behandelingen bestaan uit complexe recombinante eiwitten, zoals virale capsid-eiwitten en monoklonale antilichamen. Het baculovirus expressievector systeem (BEVS) is een snel en veelzijdig systeem voor de productie van dergelijke recombinante eiwitten. Het maakt gebruik van insectencellen die zijn geïnfecteerd met genetisch gemodificeerde baculovirussen om de gewenste recombinante eiwitten tot expressie te brengen. Het BEVS is met name geschikt bij de snelle ontwikkeling van vaccins tijdens ziekte-uitbraken en als productieplatform voor nieuwe gentherapiebehandelingen. Om toekomstige behoeften voldoende te kunnen accommoderen, moet het BEVS worden geoptimaliseerd, verbeterd en verder ontwikkeld om zo de productiecapaciteit voor klinische toepassingen te verbeteren. Het doel van deze studie was om te onderzoeken hoe de vorming van verontreinigend bijproduct in de vorm van budded virus (BV) deeltjes vermeden kon worden en of de productopbrengst van het BEVS-proces verder verbeterd kon worden. Om dit te bereiken, had de studie een tweeledige opzet: ten eerste, om eiwitproductie vrij van budded virus tot stand te brengen door gebruik te maken van een temperatuurgevoelige baculovirus mutant, en ten tweede, om een schaalbaar perfusieproces te ontwikkelen met een lage multiplicitéit van infectie (MOI).

De COVID-19-pandemie bleek een belangrijke katalysator te zijn voor de snelle ontwikkeling en goedkeuring van nieuwe vaccins. In **Hoofdstuk 2** wordt de ontwikkeling, productie en preklinische test van een nanopartikelvaccin tegen SARS-CoV-2 gerapporteerd. Met behulp van het BEVS produceerden we (1) het volledige spike-eiwit, (2) een uitgescheiden vorm van een prefusiestabiliseerde spike en (3) een uitgescheiden vorm van het S1-domein van SARS-CoV-2 en zuiverden vervolgens deze eiwitten. We formuleerden de uitgescheiden S als een geadjuveerd subeenheid-proteïnevaccin en testten de bescherming van K18-hACE2 muizen tegen een SARS-CoV-2 infectie. We fuseerden ook het S1-domein met de split-proteïnetag en toonden dit op AP205 virusachtige deeltjes (VLPs). Muizen die werden ingeënt met het S1-VLP-vaccin vertoonden sterke immuunreacties en neutraliserende antilichamen tegen zowel het Wuhan SARS-CoV-2 als de UK/B.1.1.7-variant (VOC-202012/01) die in Europa overheersend was.

Het verkrijgen van real-time informatie van celkweken tijdens productie in bioreactoren biedt aanzienlijke voordelen voor het verbeteren van het begrip van het BEVS en de tijdige controle van het productieproces, zoals het moment van temperatuurverhoging en het oogstmoment. In

**Hoofdstuk 3** rapporteren we over de training en evaluatie van een machine learning model om de groei van insectencellen en de infectie met baculovirussen in bioreactoren te monitoren met behulp van online double-differential digital holographic microscopy (D<sup>3</sup>HM). We zagen dat met een beperkte trainingsset van data, de microscoop en het machine learning algoritme de cel concentraties, levensvatbaarheid en infectiepercentage konden voorspellen voor verschillende virale constructies, MOIs en procescondities in bioreactorkweken van insectencellen. De hoge frequentie (elke 30 minuten) van de online metingen maakte het mogelijk om kleine gebeurtenissen of procesafwijkingen, zoals celgroei-arrest als gevolg van de toevoeging van boterzuur aan de cultuur, te detecteren. Dit soort kleine afwijkingen zouden door het nemen van alleen handmatige monsters zijn gemist. Het gebruik van online monitorings technieken opent nieuwe mogelijkheden voor geavanceerde procesbeheersing en verhoogt het procesbegrip.

Het verwijderen van resterende baculovirusverontreinigingen uit VLP-producten is een belangrijke uitdaging voor het BEVS en kan leiden tot aanzienlijk verlies van waardevol product. In **Hoofdstuk 4** onderzoeken we of de temperatuurgevoelige mutatie in het baculovirus-eiwit GP41 de basis kan vormen voor een BEVS met een induceerbare uitschakeling van BV-productie om de productie van chikungunya-virus (CHIKV) VLPs te ondersteunen. Hiervoor werd de I317T-mutatie in het GP41 gen geïmplementeerd in een baculovirus bacmid-vector op de polyhedrin-locus en onder de p10-promotor. Met behulp van een micro-bioreactor systeem werd door middel van screening van verschillende temperaturen vastgesteld dat het verhogen van de temperatuur tot 34°C kort na de infectie de BV-titers aanzienlijk verminderde, terwijl VLP-productie en de levensvatbaarheid van insectencellen behouden bleven. Deze strategie werd succesvol opgeschaald naar geroerde tank bioreactoren, waarbij een 100-voudige vermindering van de uiteindelijke BV-titers werd bereikt voor zowel hoge als lage MOI-infectiestrategieën. Voor de lage MOI-strategie bleek online monitoring van de cel diameter een effectief hulpmiddel om het optimale tijdstip van de temperatuurverandering te bepalen. Het voorgestelde nieuwe temperatuurgevoelige baculovirus-expressievector systeem met verminderde baculovirusverontreinigingen tijdens de eiwitproductiefase (BacFree) kan de vereisten voor productopwerking verlagen en het verlies van kostbaar product verminderen tijdens baculovirus verwijdering, terwijl het nog steeds schaalbaar blijft en compatibel is met bestaande productiestrategieën.

**Hoofdstuk 5** richt zich op de ontwikkeling van een schaalbaar perfusieproces om de productopbrengst en de volumetrische productiviteit van het BEVS te verbeteren. Bioreactor perfusie werd geïmplementeerd om infectie van insectencellen met hoge cel dichtheden mogelijk te maken. We gebruikten een lage MOI van 0,01 om insectencellen te infecteren met baculovirus bij celconcentraties van  $1,0\text{--}1,2 \times 10^7$  cellen/mL. Door gebruik te maken van een akoestisch perfusie systeem voor mediumuitwisseling en celretentie werden voldoende voedingsstoffen geleverd en/of giftige metabolieten verwijderd om infectie bij hoge celconcentraties mogelijk te maken. Celconcentraties van  $2,5\text{--}2,8 \times 10^7$  levensvatbare cellen/mL werden bereikt in twee perfusiekweken. De opbrengst van recombinante eiwit per cel werd gehandhaafd bij hoge cel

dichtheden en de volumetrische productiviteit van de bioreactor was tot 4,8 keer hoger in vergelijking met batchprocessen. Het implementeren van deze perfusiestrategie voor het BEVS maakt productie op kleinere schaal mogelijk. Dit vermindert de tijd die nodig is voor opschaling en kan de productiecapaciteit van bestaande productiefaciliteiten vergroten. Verdere optimalisatie om een hogere volumetrische productiviteit te bereiken is mogelijk. Bovendien kan het systeem worden gecombineerd met de in **Hoofdstuk 4** beschreven BacFree-technologie om BV-titers te verminderen.

In **Hoofdstuk 6** bespreken we de verkregen resultaten en hun implicaties voor het BEVS en overwegen we aanvullende aspecten die mogelijk voordelig zijn voor het systeem. Ten eerste, het verkennen van verdere verbeteringen van de BacFree-strategie, mogelijk in combinatie met een lage MOI perfusiestrategie, om BV-titers te verminderen en tegelijkertijd de volumetrische productiviteit te verbeteren. Ten tweede, onderzoek naar het gebruik van microbellen voor het toedienen van zuurstof aan de celkweek (microsparging) om zuurstofoverdracht te verbeteren en gasstromen in de reactor te verminderen, vooral met het oog op de hoge zuurstofbehoefte van perfusieprocessen. Ten derde, het onderzoeken van de potentiële voordelen van het toevoegen van korteketenvezuren aan de celkweek, waarbij boterzuur en 2-hydroxyboterzuur veelbelovende kandidaten zijn om de eiwit- en virusproductie te verbeteren. Ten slotte, het verkennen van methoden voor snelle en labelvrije kwantificering van baculovirus, zoals D3HM-technologie of het gebruik van elektrische parameters zoals elektrische capaciteit. Dit zou zeer nuttig zijn voor de ontwikkeling van BEVS-processen, met name voor processen met lage MOI. Als geheel kunnen deze maatregelen de positie van het BEVS als een robuuste platformtechnologie voor de efficiënte productie van therapeutische eiwitten versterken, om zo huidige en toekomstige gezondheidsuitdagingen snel en effectief aan te pakken.





## About the author



## CURRICULUM VITAE

---

Jort Jan Altenburg is the eldest of three children born to Ant and Evert Altenburg on the 14<sup>th</sup> of September 1993. He was born and raised in Grou (Friesland, the Netherlands). He attended the Stedelijk Gymnasium Leeuwarden, specializing in science, engineering, IT, and economics. He graduated in 2011 and continued his studies at the University of Groningen and obtained his bachelor's degree in industrial engineering and management, specializing in process technology. During his thesis he worked on anaerobic digestion of seaweed in bioreactors. After studying petroleum engineering at the TU Delft, he went to Wageningen to pursue his master's in biotechnology, again specializing in process technology. Here, he first encountered the field of cell culture during a course on biopharmaceutical biotechnology. He then performed his MSc thesis at Bioprocess Engineering under the supervision of Dirk Martens and Abdulaziz AlSayyari, investigating CHO cell perfusion processes for the production of monoclonal antibodies. His graduation internship was performed at MSD in Oss, where he also investigated CHO cell cultivation in bioreactors.

After obtaining his master's degree in 2017, he worked as a scientist at MSD, and as a sales engineer at Applikon Biotechnology. This led him back to Wageningen where he started his PhD research on the baculovirus expression vector system as part of a project funded by the Dutch Research Council. The work was conducted in the department of Bioprocess Engineering and in the Laboratory of Virology, and supervised by Dirk Martens and Gorben Pijlman. During his PhD he was a visiting researcher at Instituto de Biologia Experimental e Tecnológica - iBET, in Portugal, where he worked in the lab of cell-based vaccines development under the supervision of Ricardo Correia and António Roldão. Currently, he is key account manager at Securecell, where he specializes in the implementation of advanced bioprocessing tools at biotechnology companies and institutes worldwide.

## Overview of completed training activities

### DISCIPLINE SPECIFIC ACTIVITIES

<b>Courses</b>	<b>Organizing institute</b>	<b>Year</b>
Advanced Gene and Cell Therapy	European Society for Animal Cell Technology (ESACT)	2021
Cell Culture-Based Viral Vaccines	European Society for Animal Cell Technology (ESACT)	2022

### Scientific meetings

NBC 2020	Dutch Biotechnology Association (NBV)	2020
Biotechnology Symposium UTN	Universidad Técnica del Norte Ecuador (UTN)	2020
ACS Fall 2020 Meeting	American Chemical Society (ACS)	2020
Single-use Event	C2W	2021
Webinar Getinge Applikon	Getinge Applikon	2021
Thermo Fisher Research & Development Symposium	Thermo Fisher	2021
2nd BELSACT Scientific Meeting	Belgian Society for Animal Cell Technology (BELSACT)	2022
National Congress for Biotechnology & Bioengineering	Mexican Society for Biotechnology & Bioengineering (SMBB)	2022
Biopharma Symposium NBV	Dutch Biotechnology Association (NBV)	2022
ACTIP meeting Madrid	Animal Cell Technology Industrial Platform (ACTIP)	2022
Visiting researcher iBET	Institute of Experimental Biotechnology and Technology (iBET)	2023

### GENERAL COURSES

<b>Name of the course</b>	<b>Organizing institute</b>	<b>Year</b>
VLAG PhD week	Biobased, Biomolecular, Chemical, Food and Nutrition Sciences (VLAG)	2019
PhD Competence Assessment	Wageningen Graduate School (WGS)	2020
Presenting with impact	Wageningen Graduate School (WGS)	2020
Scientific writing	Wageningen in'to Languages	2021
Teaching and supervising thesis students	Wageningen Graduate School (WGS)	2021
Intercultural Communication Skills	Education and Competence Studies Group (ECS)	2022

### OTHER ACTIVITIES

	<b>Organizing institute</b>	<b>Year</b>
Research proposal	Bioprocess Engineering (BPE)	2019
BPE group meeting	Bioprocess Engineering (BPE)	2019, 2022
Interview online monitoring	Hamilton Bonaduz AG	2021
Nemo Kennislink article	Nemo Kennislink	2020

### TEACHING AND SUPERVISION

		<b>Year</b>
MSc Course Animal Cell Technology	Bioprocess Engineering (BPE)	2019-2022
MSc Course Pharmaceutical Biotechnology	Bioprocess Engineering (BPE)	2019-2022
Supervising BSc & MSc thesis students	Bioprocess Engineering (BPE)	2019-2023



# Acknowledgements

### Acknowledgments

The work presented in this thesis would have never been possible without the direct and indirect help of an exclusive group of people whom I was lucky to work with and have around me. In the coming lines, I would like to personally thank each of them.

First of all, I would like to thank my supervisors and promoters, **Rene, Gorben, Dirk,** and **Monique.** Your feedback and input formed an integral part of this thesis and gave direction when I needed it most. I am grateful for the opportunity to have worked with you and most of all to have learned from you.

**Rene,** you have created a great atmosphere and environment in BPE. The department has felt welcoming already since I first arrived here as a master's thesis student, later when I occasionally visited as an Applikon employee, and finally as a PhD candidate. In hindsight, it only makes sense that this department is where I found my place. I appreciated the regular project updates we had where you steered me in the right direction. Thank you for supporting me throughout the PhD in many different aspects.

**Gorben,** your creative way of thinking showed me new perspectives and your positivity and enthusiasm were very motivating for me. Working on the COVID-19 vaccine project with you was an experience that I will always remember. It was impossible to watch TV or read an article about COVID-19 without you featuring it. Thank you for all the great feedback and input you provided. I learned a lot from you, and I enjoyed the meetings and discussions (even on WhatsApp) that we had.

**Dirk,** already before I started the PhD people told me I was lucky to have you as a supervisor and they were right. Without you, I would not have been able to do all this work. You were always there when I or one of my students needed help. This is truly remarkable, and I am very thankful for all the help you provided. Your feedback and your clear way of explaining gave me a lot of direction that kept me going. Besides our scientific and technical discussions, I enjoyed our regular discussions about football. You even came to watch our match. It was great to see you there, I am sorry you had to witness such a mediocre game.

**Monique,** without you the BACFREE project would not be possible. It was great to have you as a project coordinator, your leadership made the consortium meetings a success and everyone benefited from your tremendous knowledge. I got to know you as a very nice person, you even gave me public transport cards to travel in Lisbon and Porto when I was working at iBET. I learned a lot from our collaboration, and it was a great experience to work on the BacFree patent application with you.

Besides my supervisors, there is one person who deserves special credit for all her work and help.

**Linda,** I could not have wished for a better project partner. It was great to collaborate with you. We had different backgrounds and we quickly found common grounds that made our

collaboration very efficient. I remember all the consortium meetings where we presented together, all the times you came to BPE or I walked to virology, and all the project reports we wrote. You are an excellent scientist, project manager, and supervisor and I am happy to see you will continue your work in virology as a postdoc.

Since I was mainly working at BPE and therefore not much around virology, I am especially thankful to the following virologists who supported me: **Els, Gwen, Corinne, Jerome, Tessy, and Sandra**. Thank you for helping me whenever necessary, I have always felt welcome in your department. I wished to have more time to spend at virology. Also because of you, the collaboration between both departments has thrived. It is good to see the collaboration and knowledge exchange between both departments continue with new promising projects.

To **Wendy, Fred, Sebastiaan, and Snezana** I want to express my greatest gratitude. It was a pleasure collaborating with you and the importance of your work for my thesis cannot be underestimated. Besides helping me and my students, you keep BPE running. **Wendy**, thank you for all the fruitful discussions we had about analysis methods, setting up the amino acid analysis method, and managing the purification of spike proteins. Also, you have been an immense help to my students. **Fred**, talking with you is great and I learned a lot from your extensive process knowledge (e.g., on sensors, *k<sub>1</sub>* determination, and PID settings). Thank you for helping me with determining the optimal PID settings of our bioreactors. It is rare to find people with the knowledge that you have on these topics. **Sebastiaan**, you have been an immense help in setting up the lab. The cell culture lab has undergone quite a metamorphosis and you have made sure everything went smoothly, and that we ended up with a lab to be proud of. Your flexibility and creative solutions have given us the possibility to perform experiments that we were previously not capable of doing. Thank you for all your problem-solving efforts and thinking along with us to produce the most efficient solutions. This really made a difference. **Snezana**, you are one of the most dependable and kind people I have ever met. You keep the department running smoothly, and whenever there is a problem, you are the first one to fix it. Another remarkable thing about you is the speed at which you order materials for the lab. Sometimes unexpected things happen and because of your quick communication and speed in ordering, we have not run into any bottlenecks during our experimental work. We are lucky to have you.

To my students I want to express my dearest gratitude for all the incredible work they contributed to this project, the interesting questions and discussion they came up with, and all the fun moments we shared. **Maarten**, I was very lucky to have you as the first student working on the project. Your critical thinking and thorough way of working made sure we laid a strong foundation for the project. Besides our work at BPE, I regularly encountered you at parties in Wageningen. It was a pleasure to work with you during your thesis and also later during the COVID-19 vaccine project. I am happy to see you continue your scientific career at the TU Delft on a very interesting topic. I hope we can continue to stay in touch. **John**, your passion for our scientific work was very motivating for me. We had countless discussions about all kinds of scientific and technical topics. Besides your peculiar interest in American politics (of which everyone in the lab eventually

became an expert through the continuous broadcasting of CNN on our lab computer), you were on top of the latest developments when the first coronavirus reports from China came out. We discussed the latest information daily, and this made us realize the implications of the coronavirus outbreak long before it became common knowledge in Europe. I am happy that we became friends afterward, and I wish you and Lorena all the best for the future. **Frederique**, you were doing your thesis at a difficult time, but you showed great flexibility and adapted quickly to the new situation. Your chemostat experiment was still running when the lockdown started, and we kept it running for some time afterward. The lockdown, unfortunately, meant that you could not work at the lab anymore, but you managed to adapt your thesis approach and worked with whatever data you already generated. This adaptability is a great skill and it is good to see you continue in this way as a scientist at Genmab. **Luuk**, due to the lockdown you had to do your thesis online. Despite that, you quickly familiarized yourself with the topic and delivered an excellent theoretical thesis, which laid the basis for later experiments on sparging and cell death in bioreactors. **Marieke**, it was great to work with you and you delivered excellent work. You combined many different topics in your thesis and by that not only contributed to the publication on online monitoring but also explored the potential of other topics that would lead to new research directions for our project. This is also resembled by the variety of methods you employed during your thesis, some of which were done for the first time in our lab. It is great to see you working as a USP scientist at Amarna where your skills will be very valuable. **Sonja**, you were the first and only student who combined both molecular and bioreactor work, two very different fields of expertise. You are a great person to work with and an excellent communicator. You constructed a dual fluorescent baculovirus that proved to be very useful for training our machine learning model and performed subsequent bioreactor runs using this virus. Your vision and original way of thinking led to you coming up with new ideas, such as a ‘window of opportunity’ strategy. Now you are working as a USP scientist at Koppert, a place where you will be able to contribute a lot. **Joshua**, you started your thesis during the lockdown, delivering some excellent and high-quality MATLAB models. Then you came to the lab and showed that you were also highly skillful in performing bioreactor experiments and analysis. You are a complete scientist with a broad interest which is also shown in the fact that you performed a second MSc thesis at the laboratory of nematology. You already stated your concerns with the environmental impact of the work being done within the biopharma sphere, which is a very relevant problem that should be improved. Currently, you have an interesting position as an advisor on environmental remediation. Thank you for searching through your stuff long after you completed your thesis and passing by to give us some raw data from an old lab journal. **Brenda**, you are a highly talented scientist who delivered a complete work during your thesis. The amount of data that you generated was incredible and has been used to write a paper on perfusion that will hopefully be published soon. I really enjoyed working with you and was lucky to have you as a student for this project at the right moment. Thank you for advising me to take an Uber instead of a regular taxi during the night in Mexico City, that proved to be a very good decision. It’s great to see that you are now pursuing your PhD at the TU Delft where you work on the development

of hematopoietic stem cell cultivation in bioreactors. I wish you a lot of good luck for that interesting project! **Danny**, you are a great person to have you around in the labs. You became an expert on many things and were always patiently explaining your findings to others helping wherever you could. Your input in the lab meetings was valuable as you were always thinking along and showed interest in what others were doing. After the thesis, you started your internship at VectorY and got hired afterward. It was nice to visit you there and see you found a great workplace with other familiar faces from BPE. **Vivian**, you came to BPE bringing with you experience from virology, which was very helpful. You performed a series of experiments, thereby contributing to work that would later be published. You were the first one who scaled up the BacFree strategy to bioreactors. It was an exciting moment in the project. Your independent way of working, excellent problem-solving skills, and great communication style made working with you very easy. It was great to see that you were asked to do an internship at Janssen, bringing with you experience on the baculovirus expression vector system. I wish you a lot of success in your current job at CellPoint Galapagos. **Jelle**, you also came with experience, as you previously performed your internship at Intravacc. Then you performed some of the most challenging experiments during this project. Your critical thinking, good planning skills, and precise way of working contributed to the success of those experiments (along with a regular weekend spent at the lab). These results will hopefully be published soon. Now you continue to work with the baculovirus expression vector system at VectorY. I am sure your experience will be highly valuable there as well. **Ganesh**, you are one of the most enthusiastic students I have ever supervised. Your enthusiasm also translated itself into the number of experiments you performed and all the weekends you spent at the lab. At times, I even had to slow you down. Your enthusiasm was very motivating for me and your energy made our discussions very engaging. I got to know you as an extremely kind person. I am happy that you found an interesting internship at VectorY and recently started as a researcher at UMC Utrecht. **Tessa**, your way of working is very organized and structured, something that made working with you very pleasurable. You quickly made yourself familiar with the topic and then went on to generate some very useful data on scaling up the BacFree system. The amount of work you did was incredible and will be used for a future publication. You continued with a thesis in virology and then went to iBET. The experience you already have along with the new experiences you are gaining will make sure you have a great career in front of you. It was great to work with you and I am curious to see your next steps. **Thomas**, you are an excellent communicator who was able to be a bridge between virology and bioprocess engineering. It was great to work with you, and have you join the BacFree consortium meetings. You generated some valuable data and performed interesting experiments to investigate the scalability of the BacFree system. You also contributed to the atmosphere in BPE. You were one of the driving forces behind organizing the Christmas dinner. Thank you for giving me a lab tour at Polpharma when you did your internship there. I wish you all the best for your future career. **Joshua**, you were the last student I supervised, which meant I was often away, writing or in even Portugal. Luckily, you were one of the most independent scientists I have ever seen, which meant you found your way quickly and did not hesitate to set up new experiments yourself and

bring your ideas into practice. This is a very important skill and it is great to see you are continuing your research at virology where you are also setting up bioreactor experiments. Besides that, you are organizing a conference in Switzerland, something that also shows your assertive character. Looking forward to seeing where you are going in the future.

A big thank you also goes out to the people from the Laboratory of Biochemistry with whom we collaborated closely during the COVID-19 vaccine project. **Dolf, Daan, Willy,** and **Adrie**, it was great to work with you on the project, thank you for your flexibility and valuable insights. I want to thank **Adrie** for all his help in coordinating and processing the bioreactor harvests. We've had many phone calls that allowed us to act quickly.

I was lucky to have some external partners that contributed greatly to this project. They not only provided their expertise but also equipment that allowed us to conduct new experiments we were previously unable to do. I want to thank the people from **Ovizio: Jan, Jérémie, Willem, Laurent, Nicolas, Thomas,** and **Damien** for all their help which was essential in publishing the paper on online monitoring, and keeping the iLine F microscope up and running. Thank you for your valuable insights, help with developing the machine learning models, and the regular meetings and visits to Wageningen. **Jan**, thank you for setting up the collaboration. **Jérémie**, it was great to work with you again, thank you for installing the iLine F and being our guide during the experiments. **Nicolas**, because of you we kept the systems running and were able to perform a huge amount of experiments with the systems. It was always nice when you came to Wageningen. **Willem** and **Thomas**, you took over from Jan and were instrumental in keeping the collaboration going. We even intensified the collaboration with the use of the Qmod and it is good to see that we continue to collaborate. **Laurent** and **Damien**, thank you so much for your work on the machine learning models and your input for the online monitoring paper. Without you, this work would not have been possible.

A huge thank you also goes to my former colleagues from **Applikon Getinge**, your contribution to this project proved to be so large that you became part of the BACFREE consortium during the project. We have performed countless bioreactor runs in the miniBio's and my-Controls, perfusion runs with the Biosep and did the temperature screening for the BacFree system in the micro-Matrix. It is clear that without you a lot of these experiments would not be possible and I am very grateful for your help. Also during the COVID-19 pandemic, you acted quickly and provided us with extra bioreactor systems to run our experiments. **Arthur**, thank you for making sure we got those bioreactor systems so quickly during the lockdown. **Tom**, I have lost count of the amount of times we have extended a demo agreement. You made all of this possible. **Timo**, thank you for your help with the Biosep experiments and your contribution to the BACFREE consortium. **Carolina**, you did incredible work in setting up and performing the insect cell cultivations in the micro-Matrix for the COVID-19 vaccine project. I still remember driving on empty highways to Delft with two flasks of insect cells on the passenger seat. Also, thank you for the installation and training on the micro-Matrix in our lab and later the installation of new my-Controls for fermentation courses. **Cris**, it was always great to have you over. We enjoyed many

nice lunches at our favorite Japanese MLGB restaurant until it went out of business. Thank you for setting up the scientific collaborations that led to some nice posters. **Erik**, you were the initiator behind the renewal of the collaboration with WUR. I have learned a lot from you and enjoyed the meetings and company visits we did together when I was at Applikon. **Martijn**, you were my guru on sensor technology. Except for Fred, I have never met a person with such profound technical knowledge as you. Thank you for advising and assisting me with all the questions I had, your answers were the solution to many problems and I learned a lot from you. ‘Professor’ **Rowin**, you have spent countless hours working on our Lucullus installation to develop a fully automated k<sub>1</sub>A determination method. This is an incredible work by itself. It is great to see we are continuing our collaboration and becoming colleagues at Securecell.

To my colleagues from BPE, I want to express my gratitude for all the help they offered. Besides that, we have shared many fun moments. I have felt at home at BPE from the first day I arrived. It was great to work in such an environment where colleagues were always willing to help. In this respect, I want to specifically thank a few colleagues.

**Pauline**, you taught me how to do ‘molecular stuff’. You were an unforgiving teacher but because of your strict regime and attention to detail, I managed to generate some recombinant plasmids without any prior molecular experience. Thank you for allowing me in the molecular lab and helping me with this, even though you had to finish writing your thesis.

**Christian**, you were always willing to help and share your expertise. Thank you for trusting my technical judgment so much that you thought I was running gel electrophoresis without a tray on purpose.

**Camilo**, like Pauline you were helping me a lot with the molecular work, sharing with me your incredible experience in genetic engineering. Besides that it was great to have you as an office mate and be your paronymph. You are a trading wizard, and Chunzhe and I learned a lot from our discussions about financial markets.

**Jin**, you were my office mate and we became good friends. We have been on many trips together and you invited me to celebrate Chinese festivities with you. I have learned a lot about Chinese culture because of you. You are a great friend, it was an honor to be your paronymph and I hope we can meet more often in the future!

**Narcis**, we know each other from many different occasions. As a teammate in GVC, as a colleague at BPE, and as a friend in Wageningen. It was a great moment to witness you becoming a PhD and be by your side as a paronymph. Let’s hope for a successful season for GVC, and I look forward to playing many nice games together.

**Chunzhe**, we have spent many lunches together, eating Chinese food from ‘Double E’ and talking about all kinds of topics. You were always staying on top of the latest Dutch news which allowed us to have some interesting discussions. You taught me many useful Chinese words and gave me new perspectives on many things I did not consider before. I loved your sense of humor and the

## Acknowledgements

---

continuous joking between you and Ruud. You are a great scientist and a very hard worker. I was proud to be your paranymph. Now you live in Groningen and I look forward to visiting you in the north.

**Ana**, you are an incredibly talented and hard-working scientist. We became good friends and you were an exceptionally well-appreciated member of our department. Everyone was sad to see you leave for Madrid but I am happy that you found your place there. Despite the distance we have been able to meet regularly and I hope we can keep doing this. Thank you for showing me Madrid, and joining me to watch an Atletico game.

**Fengzheng**, it was great to be your colleague. You have a lot of experience and you are a natural leader, stepping up when necessary. I liked to learn from your experience and listen to your point of view. You have a great career in front of you and I wish you the best of luck in your new position at ETH. I enjoyed the time we spent in Zürich together with Fabian, hopefully, there will be many more such occasions to come.

**Fabian**, I once told you the quality of life slogan of WUR should refer to you. I have never met a person who is such a good host as you are. You prepare the highest quality food and drinks for your guests. As an ambassador for Calabria, many people have enjoyed your delicacies made from only local products. I am glad to see you continue doing this in Zürich. I won't forget the gigantic piece of meat we put on the BBQ after you brought it from Italy. Besides being a great host, you are an excellent scientist and you can be proud of what you achieved in the field of mixotrophic cultivation of microalgae.

**Anna**, you were the organizer of the department. Because of you, we have enjoyed countless nice group lunches, after-work gatherings, and trips. Thank you for inviting us to your place in Germany, it was a great trip that I enjoyed. Without you, the experience at BPE would have been different.

**Marina**, it was very nice to have someone in the department with such a passion for sports. It was great to catch up with you about the latest developments in football, cycling, and Formula 1. Thank you for all your help and for your monthly reminder to fill in my hours.

**Miranda**, thank you for all the help you offered and for the many interesting conversations about all kinds of topics. You have a great sense of humor and are always up for a joke on an unsuspecting victim, which makes it a lot of fun to be around you.

**Abdulaziz**, because of you and Dirk I was introduced to the field of cell culture, and I have been working in this field ever since I performed my master's thesis under your supervision. Thank you for all your great advice, I learned a lot from you. You were a great supervisor, and it was an honor to be your paranymph. I hope we can meet again in the future.

I want to thank the staff members, current and former PhD students, visiting researchers, and thesis students for all the fun moments and great atmosphere they contributed to at BPE. I want to specifically mention **Enrico, Edgar, Rafa, Omnia, Kylie, Calvin, Sylviah, Henrik, Noor, Shirin,**

**Nuran, Mels, Marta, Mugesh, David, Enrique, Lyon, Iris, Christos, Arjen, Ruud, Michel, Marcel, Sarah, Iulian, Maria, Mark, Carlos, Antoinette, Sofia, Luca, Jenny, Claudia, Giuseppe, Egbert, Sabine, Ruoxi, Antonia, Wimar, Asad, Laura, Mariam, Isa, Ana-Maria, Cristina, Yuwei, Antoine, Pedro, Sophie, Kari, Lukas, Barbara, Julia, Nicola, Roel, Rudini, Nina, Rafa, Iago and Aamna** for all the nice conversations, their help, and the fun moments we shared in and around the department.

I want to thank my colleagues and friends at iBET in Portugal for their support and the wonderful experience they gave me there. **António, Ricardo, Raquel, Miguel, and Raquel**, thank you all for making me feel welcome and giving me the best spot in the lab with an ocean view. **Miguel**, you are an excellent scientist with a great sense of humor. Helping others comes naturally to you, which is a remarkable trait that helped me and Birhanu a lot to get familiar with the lab. **Ricardo**, thank you for finding the time to organize everything around the same time that your daughter was born. Without you, this research visit would not have been possible. It was great to learn from a scientist with your experience. I am sorry I did not manage to generate all the 1440 samples that we initially planned. **Raquel**, luckily you were already used to Dutch people, thank you for being so direct with me from day one. I enjoyed all the lunches we had at iBET, thank you for your daily reminder that it was not allowed to take both fruit and a dessert. You almost convinced me to stop taking both until I saw António do it as well. **Birhanu**, without you it would not have been the same. You are a great friend, and I enjoyed the time we spent together. Thank you for teaching me so many things about Ethiopia. **Emerson**, it was great to get to know you better while sharing our ocean view desk and during our trips to Sintra and Cascais. You are a very talented scientist and I wish you a lot of success in your future career, congratulations on your new job. Also, I want to specifically thank **Linda** for all the help she offered from Wageningen, preparing the necessary virus stocks and materials for the experiments in Portugal.

I want to thank my friends from Environmental Technology, **Carlos, Koen, Dainis, Selin, Nora, Thomas, Ilse, Ludo, and Andrea**, for all the nice times we had. You are a great group of people, and it was always nice to spend time with you, whether it was at the sports pub, playing football, participating in the Veluwe Loop, or at (Latin) parties. **Carlos**, it was an honor to be your Paranymp and I enjoyed our surf trips together. Thank you for inviting me to Mexico, it was an amazing trip, and I will never forget the incredible hospitality of your family. Other things I will never forget are getting cooked in the back of the Vocho, visiting the ancient Mayan city of Calakmul and of course, meeting your Mexican friends in Colima and Puerto Vallarta. Now you work for Wetsus and Paques and I hope to meet you many more times in Friesland or Wageningen. **Nora**, I will try to come to Wednesday football even when weather conditions are not optimal.

The Dutch saying goes ‘Football is the most important side issue in life,’ and in that regard, I want to thank all my current and former teammates of **GVC** for the great times we’ve had. I want to especially thank ‘Mr. GVC’ **Joost**. The amount of work you put in for GVC is incredible. You were not only a football coach but also an academic coach to me. I learned a lot from your original

## Acknowledgements

---

points of view on many different topics. No matter the occasion, you always manage to come up with an analogy related to wildlife ecology, football, or mating behavior, to further clarify your point. This also shows itself in your interviews with the local football journalists.

**Ben**, we got to know each other on the football pitch, and at some point, we were even working together in our start-up called ‘Gebakken Lucht’. You are a great scientist with an entrepreneurial spirit, and it’s good to see you have kept that creative spirit when you transitioned from a postdoc position into industry. Thank you for inviting me to a writing retreat to Laufenburg. I am happy that we managed to stay in touch after you moved to Switzerland with Marlotte and have you as my paranymph.

**Kostas**, we have spent a lot of time together after that first encounter on the football pitch, where you threatened to break my legs if I dribbled past you again. You were the first to visit me in the hospital when my leg was actually broken. Many trips inside the Netherlands, to Friesland, Greece, and even Emmerich have followed. I am lucky to have you as a friend and a paranymph.

**Douwe, Adria, Jurrian, Joost**, and **Narcis**, we have spent many games playing together, including our favorite win against Stroe. But next to that, we have become good friends. It is always great spending time with you, and you are great advisors. **Douwe**, I really enjoyed our trip to Sweden (and briefly Finland before the border control sent us back). It can be quite intense to spend a whole week with me and my brother, but you handled it well. At some point, we felt so comfortable that we only spoke in Frisian to you.

**Rijk, Sebas, Jouke**, and **Stan**, with you, fun is guaranteed. Your performance outside the pitch is unparalleled. **Rijk**, besides being a great captain, your command of the German language is phenomenal.

**Qing**, you are an excellent midfielder, both technically gifted and also physically strong when needed. Even a local newspaper wrote about you and Tomo’s performance, introducing the term ‘Asian tackle’ in this context. Given that the standard for tackles is quite high in the fourth class, this is quite an achievement. Soon, you will be a PhD and also a certified pilot. I wish you the best of luck in the final stretch of reaching these milestones.

**Alex, Jordi**, and **Narcis**, you are amazing football players, thank you for including me in your ‘Friday night + Jort’ WhatsApp group as the only non-Spanish speaker. Those Friday nights were an excellent preparation for our match on Saturday.

I want to thank my friends for the great moments we shared next to work. Wageningen is a place that surprised me. It’s incredible to find so many great people from all over the world in this small city.

**Baibing**, we have known each other for a very long time now. You are a great person, always willing to help other people, and the driving force behind the organization of many activities. Without you, Wageningen would be a different place. Thank you for the great times, fun events, and all the lunches at Ambacht.

To my Greek and Cypriot friends, **Kostas, Kostas** 'the teacher,' **Aris** and **Yiannis**; it is always great to spend time with you. Your renovation skills are remarkable. Bremen will never be the same!

**Lisanne**, you are an amazing friend. I can always depend on you and you are always there to help your friends. You are also one of the few people I know in Wageningen that manages to arrive on time consistently. Thank you for all the nice moments.

**Gabriel**, you are an amazing friend, and although we live far apart now, I am happy that we still manage to stay connected and update each other regularly. I hope that we soon get the opportunity to meet again.

**Irving**, you are the most flexible and spontaneous person I know. Adventures are guaranteed with you. Maybe those things are related. I am looking forward to the next adventure with you and Justé.

**Yoran**, we were always together during our studies in Groningen. I am glad we managed to stay in touch afterward, occasionally meeting in Wageningen and Hoogeveen. I hope we can see each other more often in the future!

**Menika**, ik had je bijna niet eens ontmoet als je de flowcytometer bij BPE niet nodig had gehad. Bedankt voor alles wat je voor mij gedaan hebt.

Lastly, I want to thank my family for their help and unconditional support.

**Heit** en **Mem**, jim binne der altyd foar my. Sels at ik wer ris wat fetjitten wie yn Fryslân koe ik op jim rekkenje. Jim bin faak lâns west yn Wageningen, bygelyks om oranjekoek te bringen foar myn jierdei, mar ek om in airco te ynstallearjen yn myn keamer of gewoan foar de gesellichheid. **Sido**, troch dyn help mei it ynstallearjen fan de bioreaktoren wie ús lab presys optiid klear. We ha in protte wille hân yn Wageningen en yn Sweden. **Marte**, we hawwe in soad gemien, dat blik wol at ik dy wer ris ûnferwachts tsjinkaam op in feest. At ik dyn hulp noadich ha dan bist der foar my.

The research described in this thesis was financially supported by The Dutch Research Council (NOW).

Financial support from Wageningen University for printing this thesis is gratefully acknowledged.

Cover design by Menika Paragh

Printed by ProefschriftMaken



